Analysis of Transient Liquid Slosh inside a Partly Filled Tank Subjected to Lateral and Longitudinal Acceleration Fields

Korang Modaressi-Tehrani

A Thesis

in

The Department

of

Mechanical and Industrial Engineering

Presented in Partial Fulfillment of the Requirements
for the Degree of Master of Applied Science (Mechanical Engineering) at
Concordia University
Montreal, Quebec, Canada

August 2004

Your file Votre référence
ISBN: 0-612-94732-7
Our file Notre référence
ISBN: 0-612-94732-7

ABSTRACT

The liquid motion within a partially filled moving container has been associated with reduced overturning limits and braking efficiency of highway tank trucks. While the studies using quasi-static models have evaluated the contribution of cargo displacement in degrading the stability characteristics of tank trucks, the role of transient load surges on the directional stability and safety measures has been ignored. It has been suggested that the transient fluid slosh and fluid-structure interactions may further reduce the stability limits of the vehicle. This dissertation work focuses on various dynamic response measures of the dynamic liquid slosh in a partially filled circular-cross section tank exposed to the lateral, longitudinal, a combination of lateral and longitudinal acceleration excitations. The analysis of a partially filled clean bore circular tank is performed under different magnitudes of steady as well as harmonic lateral acceleration fields using the FLUENT software. The measures include the dynamic variations in forces, moments, centre of mass coordinates and mass moments of inertia of the cargo, which could be applied to assess the direction performance of vehicles subject to transient fluid slosh. The results are compared with those derived from the quasi-static liquid slosh model and the significance of the dynamic slosh behaviors is discussed as functions of the fill level, magnitude of acceleration, physical properties of the liquid cargo. A relationship between the lateral force and the resulting roll moment is derived, which suggests that the roll moment could be defined as a function of the horizontal force and tank radius.

A general three-dimensional nonlinear model of a partly filled circular cylindrical tank with and without baffles has been developed to investigate the significance of resulting destabilizing forces and moments caused by transient fluid slosh. The influence of fluid

viscosity on the transient behavior is further investigated under time-varying lateral acceleration in terms of slosh damping rate and peak responses. The role of baffles on liquid slosh attenuation in partially filled tanks is also investigated under pure longitudinal acceleration, and lateral and longitudinal acceleration fields. The effect of lateral acceleration excitation frequency on the dynamic response measures is further investigated.

The results in general suggest that the mean responses attained from the dynamic fluid slosh analyses correlate well with those attained from the quasi-static analyses. The ratios of transient responses to the mean responses, termed as amplification factors, are defined to emphasize the significance of transient fluid-structure interactions and thus the vehicle stability. The results revealed the longitudinal and lateral slosh force, and roll moment amplifications in the order of 1.96. The dynamic viscous forces were evaluated, which showed insignificant influence on the peak responses, while the effect of fluid density was significant on both the mean and the peak responses.

TABLE OF CONTENTS

Chapter 4

Chapter 5

LIST OF FIGURES

LIST OF TABLES

NOMENCLATURE

g_x, g_y, g_z	magnitudes of the unit body forces acting along the X, Y and Z directions, respectively
ρ, ρ_f	mass density of the fluid
P	fluid pressure
G_x	ratio of the applied lateral acceleration to acceleration due to gravity
y_0	coordinate of free surface at x=0
α	slope of the liquid free surface
f	free surface height in the absence of the lateral acceleration
R	Radius of the tank
y_{st}	vertical coordinate of the c.g. measured from the origin
β	half of the central angle of the circular sector (Rad)
x_{cg}, y_{cg}, z_{cg}	X,Y and Z coordinates of the cargo c.g. with respect to the origin
m	the mass of the liquid
$\vec{D}$	the position vector of the c.g. from the reference point 'O'
$\vec{F}$	the resultant force acting on the c.g. of the fluid
M_z	the roll moment about the axis passing through the base of the tank (point 'O')
G_z	ratio of the longitudinal acceleration to acceleration due to gravity
V_l	total volume of the liquid

I_{xx}, I_{yy}, I_{zz}	mass moments of inertia of the liquid cargo about the X,Y and Z axes, respectively
F_x, F_y, F_z	resultant slosh force X- , Y- and Z-components acting on the tank, respectively
u, v	flow velocity X- and Y-components of liquid inside the domain at arbitrary points
ν	kinematic viscosity
U_T	total velocity of the liquid at arbitrary points
η	the displacement of free surface from its mean position
ρ_e	mass density of the fluid
$\vec{v}_e$	velocity vector at the cell face
$\vec{A}_e$	area of the face enclosing the cell
φ	scalar quantity representing u , v and w in the general form of steady-state momentum equation
V_c	volume of the cell
α_q, α_2	the volume fraction of target phase in cell
ρ_q	density of the target phase
ρ'	the volume-fraction-averaged density
τ, τ_c	shear stress at the tank wall
μ	dynamic viscosity of the liquid
M_x, M_y, M_Z	pitch, yaw and roll moment, due to liquid slosh, about the middle of the bottom of the tank
MV_Z	roll moment about the base of the tank due to viscous forces

FV_x, FV_y	horizontal and vertical viscous force due to shear stress in the vicinity of the wall
I_{xx}, I_{yy}, I_{zz}	pitch, yaw and mass moments of inertia about X, Y and Z axes passing through the geometric center of the tank
$(I_{zc})_i, (I_{zo})_i$	the roll mass moment of inertia due to mass m_i of cell i about the geometric center and base of the tank, respectively
r_i, r_i'	position vectors of the cell i with respect to the geometric center and base of the tank, respectively.
γ	the angle of the position vector r_i from the X axis
m_i	mass of the liquid in the cell 'i'
$\bar{y}$	the vertical coordinate of the mass center
x_{CP}, y_{CP}	the X and Y coordinates of the centroid of a cell 'c'
F_{xc}, F_{yc}	components of the forces acting on the centroid of the surface cell 'c'
$\bar{I}_{xx}, \bar{I}_{yy}, \bar{I}_{zz}$	the mean values of mass moments of inertia in the pitch, yaw and roll planes, respectively
$M_{Ixx}, M_{Iyy}, M_{Izz}$	the amplification factors of the pitch, yaw and roll mass moments of inertia, respectively
$\bar{x}, \bar{y}$	the static solution or mean value of c.g. X and Y coordinates
M_{CGx}, M_{CGy}	the amplification factors of the X and Y coordinates
$\overline{M}_x, \overline{M}_y, \overline{M}_z$	the mean values of the moments in the pitch, yaw and roll plane respectively
M_{Mx}, M_{My}, M_{Mz}	the amplification factors of the pitch, yaw and roll moments, respectively

$\overline{F}_y, \overline{F}_z$	the mean vertical and longitudinal forces
M_{Fy}, M_{Fz}	vertical and longitudinal force amplification factors

To my parents

ACKNOWLEDGEMENTS

The author wishes to thank the supervisors Professor S. Rakheja and Dr. R. Sedaghati for their guidance, encouragement and support during the course of this investigation. The author is deeply indebted to his parents and his wife and his family members for their continued support and understanding.

CHAPTER 1

INTRODUCTION

1.1 MOTIVATION AND PROBLEM STATEMENT

Heavy vehicles with their high center of mass, and large weights and dimensions, exhibit relatively lower directional stability limits, when compared to those of the other road vehicles. Such vehicles carrying liquid cargoes yield even lower limits under a partial fill condition, which has been attributed to dynamic load transfer caused by fluid slosh within the container. A few studies have concluded that partially filled tank trucks yield lower values of static rollover threshold, a direct measure of the roll stability in steady turning. The lower stability limit has also been demonstrated through analyses of reported accidents involving tank trucks. These studies have reported that vehicles carrying hazardous liquid products are more frequently involved in single vehicle accidents [1]. The same study further reported that 17% of single vehicle and 11.5% of multi vehicle accidents caused property damage in excess of 100,000 dollars. A few studies have also identified the lateral load surge as one of the contributing factors [2,3,4,5]. An analysis of Hazardous Material Incident Reports (HMIR) during the period 1983 to 1987 reported that 81.6% of actual vehicle accidents were rollovers [6]. Another recent study by Transport Canada concludes that heavy vehicles transporting hazardous liquid products are 4.8 times more likely to rollover than the conventional cargo heavy vehicles [7].

A few studies have developed analytical models defining the fluid motion and its interaction with the vehicle dynamics to assess the effect of liquid slosh on the vehicle's

roll stability and its directional responses [**8**,**9**]. These studies have clearly shown that the dynamic load shift caused by fluid slosh within a partly filled tank affects the directional dynamics and thus the roll stability in an adverse manner. A vast majority of these studies have focused on rollover threshold property of the vehicle, which describes the peak lateral acceleration encountered in a steady-turning maneuver that the vehicle can withstand without rolling over [**8**,**9**]. A few other studies have also shown that the load shift under straight-line braking and braking-in-a-turn maneuver deteriorates the braking performance and directional stability of the vehicle [**10**,**11**]. These models are mostly based upon kineto-static solutions of the invicid fluid, which do not characterize the forces and moments caused by the transient fluid slosh. Analytical models based on pendulum and spring-mass systems analogies of the fluid slosh have also been proposed to estimate the fluid slosh force and moment in the roll plane, which involve complex system identification task and do not characterize the transient phenomenon [**4**,**12**,**13**,**14**].

Only a limited number of studies have attempted to study the slosh behavior within moving containers, while the interactions with vehicle are ignored [**4**,**13**,**15**]. Moreover, the majority of the studies have considered two-dimensional liquid flow inside the tank while the free surface distortion or separation and the viscosity effects are mostly ignored. On the basis of comparisons of the model results with the road-measured data attained for a scale model tank, it was concluded that the kineto-static model yields good prediction of the steady-state slosh response, while the transient forces and moments could be relatively higher. These studies have provided significant information on the effect of tank geometry, cargo fill ratio and the intensity of lateral and longitudinal acceleration fields on the directional dynamics of partly filled tank-vehicle combinations.

This dissertation research focuses on the analysis of transient fluid slosh and associated slosh forces, and overturning and pitch moments in the roll and pitch planes. The study is carried out in two systematic phases, where the initial phase involves the roll plane analyses of a clean bore cylindrical tank. The second phase of the study includes the transient and steady-state fluid slosh analyses of a clean bore as well as baffled tanks under braking and braking-in-a-turn excitation. Two- and three-dimensional models of fluid slosh are thus developed and solved in the FLUENT environment. The analytical results are compared with those attained from quasi-static solutions to demonstrate the significance of transient slosh forces and moments.

1.2 REVIEW OF THE RELEVENT LITERATURE

The dynamics of vehicles transporting cargo have been extensively studied from different points of view. The stability and directional dynamics of such vehicles under different types of maneuvers have been the most concerned issues. Tank trucks hauling liquid cargo have been found to be more susceptible to rollover which is attributed to the dynamic load shifts encountered under partial fill conditions [**1**,**16**,**17**]. Analysis of the dynamic load shift due to a floating cargo and its effect on vehicle's directional dynamics involves consideration of the vehicle system dynamics, tank geometry, fluid properties and motion of the liquid inside the tank. The reported studies on the influence of liquid motion on the vehicle's performance have been reviewed to formulate the motivation and objectives of this dissertation research.

1.2.1 FACTORS AFFECTING DIRECTIONAL DYNAMICS OF VEHICLE

A few studies have investigated the directional dynamics and roll stability performance of heavy vehicle combinations transporting liquid goods. Vast majority of those studies consider kineto-static motion of the invicid liquid bulk, while the roles of transient slosh

and fundamental slosh frequencies are ignored [**8**,**16**]. These studies have provided considerable insight into the factors that could directly affect the directional response behavior of the vehicle, which are discussed bellow.

FILL LEVEL

The reported studies have invariably stated that the fill condition of liquid cargo affects the dynamics of the liquid motion and thus the moving container's dynamic behavior in the most significant manner. Budiansky [**18**] analyzed the liquid slosh in partly filled circular canals and spherical tanks subjected to lateral acceleration of the container. The study evaluated the Eigen frequencies and natural modes under different fill levels of the circular canal and spherical tanks using potential flow theory under small amplitude harmonic oscillations. It was shown that the first Eigen frequency of the slosh increases monotonically with increasing fill level. The higher frequencies were shown to have minima occurring slightly below half-full condition. The study further computed the forces exerted on the container wall and concluded that the fill volume is an important contributing factor.

The Budiansky's study has been followed by many investigations on the fundamental slosh frequencies and fluid slosh behavior within partly filled containers of different cross-sections [**3**,**4**,**13**,**22**]. The reported studies have suggested that the fundamental slosh frequency of a 50% full highway container lies in the 0.5-0.6 Hz range. This frequency may lie in the vicinity of steering frequency under an emergency type of maneuver and thus cause resonant oscillation and excessive dynamic load shift [**3**,**28**]. The effect of load shifts caused by dynamic fluid slosh on the directional dynamics of vehicles has been the subject of a single study which was limited to fluid slosh in the roll plane alone [**1**].

Bauer [**13**] investigated the stability of space vehicles, specifically the influence of natural frequency of the fuel inside the container. The study proposed an equivalent mechanical system on the basis of the potential flow theory to investigate the liquid slosh inside the container. Considering upright circular cylindrical tanks, the focus of his study was to identify the best geometry for the tank that would yield higher slosh frequency or diminish oscillation of the liquid inside the tank. The influence of liquid height on the hydrodynamic forces was a function of fill level, and concluded that the second modal mass could be considerable under very low fill heights. Following the similar approach Ranganathan [**12**] developed a pendulum analogy of the liquid slosh inside a partially-filled horizontal circular tank coupled with roll dynamic model of the vehicle. The roll dynamic responses of the 50% and 70% filled vehicle were evaluated under step and sinusoidal lateral accelerations. Comparison of the responses with those of an equivalent rigid cargo vehicle revealed that the mean responses of a partially-filled tank vehicle are considerably larger than those of the corresponding rigid cargo vehicle. The response frequency was found to be close to the natural frequency of the liquid. Irrespective of the fill level, the peak angle of the pendulum approached near 90 degrees repudiating the assumption of small angle of oscillation. The model formulation was thus modified to account for large angles under sinusoidal excitation

Sheu and Lee [**19**] investigated the effect of fill level under the presence of baffles on the slosh behavior in a rectangular oil tanker through formulation of a two-dimensional problem and concluded that the baffles geometry in conjunction with the fill level influences the natural frequency of the liquid. It was further demonstrated that the level of wave heights due to harmonic excitations at resonance frequencies are different for different fill levels.

Salem [17] proposed a mechanical analogy of liquid slosh inside the elliptical tank as a trammel pendulum assuming small angles of oscillations. The natural frequency of oscillation, derived from the linear analysis, was compared to those attained from numerical modeling softwares such as LS-DYNA and FLUENT. The results revealed reasonably good agreement with the frequencies obtained from LS-DYNA and FLUENT models. The forces and moments due to liquid slosh normalized with respect to the steady state values revealed monotonic decrease with increasing fill level. The results attained for a circular cross section tank revealed good agreements with those reported by Ranganathan [20], under lower levels of acceleration, which allowed for the use of the linear model. The results further showed that the peak values of roll moment and horizontal force under application of a lateral acceleration occur under a certain fill level and aspect ratio of the tank.

Abramson [4] investigated the fluid slosh within the spacecraft tanks and concluded that the fill level is one of the factors determining the natural frequency of the liquid motion. Bauer [21] investigated the liquid slosh in rectangular and upright circular containers using potential flow theory and concluded that the natural frequency of liquid in rectangular cross section increases with increase in the fill level and approaches a constant value for height ratios greater than 0.5. It was further reported that the natural frequency of slosh increases with compartmented tanks. The dynamic fluid slosh and the dynamic behavior of an elastic separating wall in a container was further investigated in a subsequent study [22]. The study concluded that the natural frequency of the liquid assuming rigid wall container is a non-linear function of the fill level considering various tank geometries.

A few studies have also investigated the effect of fill condition on the roll stability limits of the vehicles. Owing to the complexities and high computational demands associated

with dynamic fluid slosh analyses, these studies have mostly employed a simplified kineto-static fluid slosh model. Assuming steady state displacement of the fluid inside a circular tank Rakheja et al. [**8**] developed a roll plane model of the tank to study rollover threshold of a tractor-semitrailer vehicle when negotiating a steady turn. It was concluded that lower fill levels causes greater lateral load shift leading to proportionally larger overturning moment and thus lower roll stability limit. While a lower fill volume yields lower center of mass (c.g.) height, the increased lateral load shift tends to offset the stability gain from the lower c.g. height. Further studies following this investigation suggested that some cross sections are more sensitive to changes in the fill level when rollover threshold is concerned [**27**]. The analyses performed under constant payload condition but varying fill conditions revealed that the rollover limit decrease with an increase in cargo density or reduced fill level.

The above reported studies on dynamic fluid slosh have employed linear formulations assuming small amplitude slosh. Popov et al. [**23,24**] developed the model of large amplitude liquid slosh inside a circular tank subject to lateral acceleration through formulation of non-linear Navier-Stoke's and continuity equations. The studies suggested that fill level not only influences the mean values of the horizontal force and turning moment, but also the peak magnitudes of the oscillating forces and moment are considerably larger. It was further stated that the first natural frequency of the liquid slosh deviates from that predicted by linear theory of Budiansky [**18**], when different fill levels are considered. Reasonably good agreement with the Budiansky's results were observed for small input acceleration (0.1g). The non-linear slosh model was applied to determine the liquid dynamic behavior inside a rectangular tank equipped with baffles and compartments [**2,23,24**]. The results attained for long and short containers revealed the existence of a particular fill level for each configuration that would yield considerably

lower magnitude of the overturning moment, while the addition of compartments resulted in significant effect on moment reduction, specifically under higher fill ratios.

Ranganathan [**1**] considered the two-dimensional liquid slosh in partially filled container and its influence on the directional behavior of the five-axle tractor-semitrailer tank vehicle. The study considered two different slosh models; a quasi-static roll plane model assuming steady state motion of the liquid inside the tank neglecting free-surface deformation; and a dynamic non-linear slosh model developed by Popov [**24**] defining transient motion of the liquid. The slosh models were coupled with three-dimensional vehicle dynamics model, developed by the University of Michigan Transportation Research Institute (UMTRI) [**25**], to investigate the directional response of the partly-filled vehicle. The results suggested lowest static rollover threshold of the vehicle corresponding to fill levels around 40%. Considerable liquid load shift expressed in terms of lateral translation of the cargo c.g. due to lateral acceleration was observed when compared to an equivalent rigid cargo vehicle response. It was shown that the rollover limit reduces when the fill level is reduced under constant axle loads. The results revealed that the fill level strongly affects the dynamic response characteristics, irrespective of the slosh model used and the tank geometry considered. The study considered circular, modified oval, modified square and elliptical cross section tanks, while the transient directional responses of the vehicle under closed-loop maneuvers were investigated for a clean bore circular cross section tank. The results revealed that a 40% fill level can cause larger amplitudes of response compared to those due to the 70% fill.

Rakheja [**26**] proposed a simple methodology for estimating the static rollover threshold of a vehicle equipped with partially filled circular tank using the moment equilibrium of a single-degree-of-freedom model. The studied showed slight increase in the rollover

threshold of a circular tank vehicle with decrease in the fill level, which contradicted the reported results from the quasi-dynamic models. Ranganathan and Rakheja [**9**,**16**] extended this method for elliptical and modified oval tank vehicle, while incorporating the suspension and the compliance, to estimate the rollover threshold under constant payloads and variable axle loads. The results revealed that the rollover threshold of a circular cross section tank is less sensitive to fill level variations while those of the elliptical and modified oval cross-section tank vehicles are quite sensitive to fill level.

The application of quasi-static model, proposed by Rakheja et al. [**27**], was extended to B-train combinations to study their responses to steering inputs [**28**]. The study demonstrated most significant influence of the fill level on the roll dynamic responses of the vehicle, namely sprung mass roll angles, lateral acceleration and lateral load transfer. The same quasi-static model was further applied in the pitch plane to study the braking performance of compartmented truck and tractor-semitrailer tanks under straight-line braking [**10**]. The braking performance of a tractor semi-trailer equipped with a clean bore circular tank under a straight line braking input was also investigated by Ranganthan and Yang [**11**]. Comparison of the braking responses in terms of dynamic normal load factor, stopping distance, braking efficiency with those of an equivalent rigid cargo revealed significantly deteriorating effect of the liquid load shift and the fill volume.

Ibrahim et al [**29**] investigated the ride dynamic behavior of a truck loaded with two partially filled spherical tanks subject to vertical and translational accelerations simultaneously. The ride responses in terms of truck pitch and vertical accelerations were investigated under 55, 75 and 95% fill conditions. The results revealed the 55% fill condition of a low viscosity fluid causes larger peak values of the acceleration responses.

It has been reported that the liquid slosh and thus the vehicle roll stability is strongly influenced by the tank cross-section [**16,30**]. Kang et al. [**31**] proposed an optimal tank geometry that would yield lower c.g. height and reduced lateral load transfer, thereby higher roll stability. The study revealed that the optimal tank cross-section was strongly related to the fill level. Two optimal cross sections resulting in a better compromise between the load shift and fill ratio were proposed for ranges of 50-70% and 70-90%. A three-dimensional model of the optimal tank was developed to study the vehicle response under braking-in-turn maneuvers [**32**]. The results revealed the most significant effect of fill level on the dynamics of the liquid as well as the vehicle. A lower fill volume of liquid resulted in considerably larger c.g. translations in the pitch and roll planes, and considerable variation in the mass moment of inertia is more significant.

VEHICLE ACCELERATION

The magnitude of steady-state as well as transient fluid slosh and thus the vehicle responses are strongly affected by the magnitude of longitudinal and lateral acceleration encountered by the vehicle. When analyzing the motion of propellant in upright cylindrical containers, Bauer [**13**] showed that the magnitude of moment due to hydraulic forces was a function of the amplitude of excitation. The effect of level of excitation on liquid response on the tank's wall in the forms of forces and moment were also investigated and considered by NASA [**33**] in the design criteria of space vehicles under propellant slosh loads. Introducing pitch, yaw and translational excitation to the rectangular containers and pitch and translational excitation to the circular tank, Bauer [**21**] further illustrated that moment due to hydraulic forces is a function of the level of excitation. Using similar methodology, Bauer [**22**] illustrated the role of excitation on the forces and moment due to hydraulic forces acting on the wall for different tank geometries.

Assuming steady turning, Rakheja et al. [8] demonstrated that forces and moment exerted on the partially filled circular tank body are direct functions of the lateral acceleration imposed on the liquid. This observation was verified for other cross section tanks, such as ellipse, modified oval and modified square [27]. Popov et al. compared the results from non-linear slosh model with the steady state solutions and illustrated that the input level affects the peak responses. The application of increasing acceleration field tends to suppress the deviations from steady solutions [23,34], which is most likely attributed to the free surface separation and the constraint imposed by the converging cross-section near the upper boundary of the tanks. It was concluded that the steady state values of horizontal force and turning moment are proportional to the magnitude of input acceleration. The analyses performed to study the role of baffles and compartments on the liquid responses under constant acceleration also suggested the strong influence of acceleration input on the resultant overturning moment [2,24].

The direct influence of the magnitude of lateral acceleration on the static rollover threshold of circular, oval and modified tank-vehicles is also evident from the results attained from the simplified models based upon moment equilibrium [9]. The studies showed that the translation of liquid cargo in the roll plane is a direct function of the input acceleration. The analyses of three-dimensional models of different vehicle configuration, such as five-, six- and seven-axle tractor-semitrailer, and B-train combinations, coupled with a quasi-static plane-roll model of the circular cross section tank, under path change and evasive maneuvers, further demonstrated the significant effect of the excitation magnitude. The lateral load transfer caused by a larger excitation at highway speeds resulted in vehicle rollover. Similar analyses under longitudinal accelerations caused by braking revealed excessive load shifts in the pitch plane under high deceleration levels, and thus relatively higher stopping distances [10,28]. The study

proposed optimal locations of compartments to enhance the braking performance of vehicle.

The effects of magnitudes of lateral and longitudinal accelerations on the lateral and longitudinal load transfers and vehicle responses have been investigated through analysis of a three-dimensional quasi-static slosh model coupled with a comprehensive vehicle model [**32**]. The model employed the circular as well as optimal tank geometries. The results revealed that the translations of the cargo c.g. in the pitch and roll planes increased monotonically with increasing input accelerations. The results further revealed that the directional responses of the vehicle, such as sprung mass roll angles, lateral acceleration, yaw rates and load transfer ratio, increase with increasing excitation due to a steering input. Further, larger fluid slosh causes significant variations in the roll, pitch and yaw mass moments of inertia of the deflected cargo.

Employing a trammel pendulum model Salem [**17**] indicated that the level of lateral acceleration is a determining factor in liquid response characteristics in forms of horizontal force, vertical force and roll moment. The study also illustrated that the natural frequency of liquid is a function of the magnitude of lateral acceleration, increasing with increase in the latter.

TANK GEOMETRY

Budiansky [**18**] studied the behavior of liquid inside the circular and spherical containers subjected to harmonic excitation, and concluded that the natural frequency of free oscillation is influenced by the tank's radius. Bauer [**13**] also concluded that the frequency of the slosh as well as the amplitude of the forces and moments exerted on the tank wall are strongly influenced by the geometry and dimensions of the container, and design of anti-slosh devices, such as baffles and compartments. The analyses of

different cross-sections including a rectangular container with compartments and an upright cylindrical tank clearly demonstrated the influence of tank geometry on the slosh frequency and the moment exerted on the tank structure [**21**,**22**] Considering that the baffles tend to reduce the dynamic load shift and increase the slosh frequency, the baffles are commonly applied in propellant tanks and the vehicle tanks [**4**,ASME Section 8 Dev. 1, CFR 49].

Popov et al. [**2**,**24**] carried out a comprehensive investigation on liquid slosh in a rectangular tank with baffles and compartments subjected to a step acceleration representing a steady turn or braking. It was concluded that the number of compartments greatly affects the resultant overturning moment and its peak value. Role of baffles in diminishing the liquid oscillation was also illustrated in this investigation. Furthermore the damped natural frequency of liquid is strongly influenced by the number of compartments, baffle configuration and tank aspect ratio. Investigating the role of baffles and their configurations on liquid behavior, the study presented the transient solutions assuming two-dimensional flow inside a rectangular tank equipped with baffles. The results suggested strong influences of the orifice size and its location together with the number of baffles, on the overturning (or the pitch) moment. The addition of baffles also resulted in a time delay for the liquid oscillation to approach its steady-state values in terms of overturning moment and horizontal force. The size of the orifice was shown to have significant effect on peak value of moment. It was shown that an orifice size of 5% of the cross sectional area had increased the moment by 29% compared to corresponding compartmented tank while the horizontal force was practically independent of the orifice size. While an orifice area as large as 20% of the cross sectional area resulted in peak moment of 173% as larger as the steady-state moment. The results also revealed that the baffles provide relatively smaller reduction in force

when compared to that caused by compartmented tank. Increasing the number of separating walls was also shown to have desirable effect on forces and moments [**2**]. It should be mentioned that the effect of compartments on roll moment was examined by developing analytical steady state slosh model.

The effect of baffles on the free surface distortion was investigated by Sheu and Lee [**19**] considering a rectangular tank partially filled with oil subject to forced oscillation at resonance and nonresonance frequencies. Numerical techniques were used to solve the model equations and it was concluded that the baffle could significantly reduce the oscillating behavior of liquid by monitoring the wave height adjacent to the tank wall. The results revealed that the size of baffle strongly influences the liquid slosh behavior. An increase in the height of baffle plate reduced the wave heights, while a larger size of the perforation on the baffle caused larger waves.

Apart from the baffles, the addition of compartments within a tank can help reduce the partial fill conditions and limit the longitudinal fluid slosh. Rakheja et al. [**8**] investigated the rollover threshold of a tractor-semitrailer vehicle comprising a circular cross-section tank with a number of compartments. Assuming steady state turning and kineto-static motion of the liquid free surface, it was concluded that the rollover threshold could be significantly enhanced by introducing compartments and eliminating the partial fill condition. The study also proposed an optimal order of its compartments. Analyses performed using a kineto-static model of the partially filled tank have provided most significant information on the role of tank cross-section on the lateral load shift and thus the roll stability [**16**,**27**,**30**]. These studies have investigated the steady-turning rollover threshold and roll dynamics responses of heavy vehicles equipped with partly filled tanks of circular, elliptic, modified oval and modified rectangular cross section tanks. A circular cross-section tank yields higher sprung mass c.g. but lower lateral load shift in relation to

oval and rectangular cross-sections of identical cross-section areas. The wider elliptic, modified oval and rectangular tanks, on the other hand, yield lower c.g. height but higher lateral load shift under application of a lateral acceleration. The studies have thus concluded that the modified square and circular cross sections yield the lowest and highest performance in term of the rollover threshold acceleration limit respectively [16,27,30].

Ranganathan [1,16] considered the four most common cross sections say circular, modified oval, modified square and elliptical cross sections, and investigated the influence of geometry on dynamic behavior of an articulated vehicle equipped with a partially filled tank. He employed a simple method initially developed by Rakheja [9] leading to the roll plane slosh model and demonstrated the significant influence of geometry on load shift under different magnitudes of step lateral acceleration assuming constant payload. The study concluded strong influence of tank geometry on the static roll performance of the vehicle. It was further concluded that a modified oval cross section tank yields relatively poor directional performance under partial fill condition.

Reapplying the non-linear model of liquid slosh, Popov et al. [34] considered dynamic response of liquid inside a rectangular tank subjected to a step acceleration input. It was shown that the dynamic response of the liquid slosh in terms of horizontal force and overturning moment are function of the tank's aspect ratio. The lowest performance regarding overturning moment was obtained for a near square configuration under certain fill level and acceleration. Horizontal force was shown to be strongly dependent on the length of the tank with largest coefficient occurring for the longest tank configuration. The influence of aspect ratio on slosh frequency was also considered, showing deviation from linear theory for short tank.

Using a two-dimensional steady-state roll plane model of a partly-filled elliptical tank, Popov et al [**35**] proposed optimal aspect ratio of the tank. It was shown that for a low profile configuration the peak moment exceeds the overturning moment of a fully filled tank. Further investigations revealed that the height/width ratio of an optimal tank decreases with the magnitude of input acceleration. It may be quoted that elliptic tanks were found to be less stable compared to rectangular or modified rectangular cross section tanks of equal capacity.

Owing to the significant influence of tank cross-section on the rollover threshold acceleration of the tank vehicle, Kang et al. [**30**] carried out a shape optimization to realize an optimal geometry. A generic cross section of a tank comprising eight circular areas was proposed for optimization. Objective functions based on static rollover threshold and roll plane load shifts were minimized subject to constraints imposed on tank weight, tank width, tank height and tank volume. The study proposed two different optimal cross-sections for fill ranges of 50-70% and 70-90%. The results showed considerably high rollover threshold acceleration of the optimal tank when compared to those of the equivalent circular, elliptical, modified square and modified oval tanks. The application of the three-dimensional kineto-static model of the optimal tank to the three-dimensional model of the vehicle permitted the analyses under turning as well as braking [**32**,**38**]. The study concluded that the optimal tank geometry yields considerably lower responses in terms of cargo c.g. translation, trailer roll angle, liquid mass moment of inertia and load transfer ratio regardless of fill volume, deceleration and the steer angle.

TANK VEHICLE-ROAD INTERACTION

The directional dynamics of heavy vehicle combinations arising from the vehicle-driver-road interactions have been extensively investigated over the past three decades. These include the studies on the lateral and roll dynamics under steering inputs, and braking

dynamics [**36**]. While a large number of analytical models of varying complexities have been developed to study the directional response characteristics of different combinations of heavy vehicles, the interactions between the cargo and the vehicle have been addressed in only a few studies [**9,22,28**]. The tank vehicle dynamics is most strongly influenced by the moving cargo, specifically when a partial fill condition is encountered. Owing the local road laws governing the axle loads to variations in the mass density of the products, such vehicles may frequently encounter the partial fill conditions. Partial fill conditions are also realized in vehicles operating on a local delivery route. The consideration of dynamic interactions between the sloshing cargo and the vehicle are thus vital for assessing the directional dynamics and stability limits of partly filled vehicles.

The studies on the influence of moving liquid cargo on the directional dynamics have utilized the reported analytical models of commercial vehicles together with a quasi-static model of the partly-filled tanks of different cross-sections [**16**]. The earlier reported studies on the vehicle-cargo-road interactions had focused on the static roll stability analysis developed on the basis of the static roll model for the tractor-semitrailer combination [**37**]. The roll dynamics analyses of such vehicles were performed on the basis of the yaw / roll model coupled with the two-dimensional quasi-static model of the fluid motion to study the response to steering inputs [**28**]. The dynamic interaction between the vehicle and the moving cargo has also been investigated using mechanical analogue models of the fluid slosh [**12**].

Rakheja et al. [**8**] developed a static roll model of an articulated tank vehicle to investigate its rollover threshold as a function of the fill volume. The model incorporated the vertical and lateral forces acting on the tire, nonlinear suspension properties and torsional compliance of the tractor and the trailer structure. The model effectively

provided the steady-turning roll stability of the vehicle with a partly-filled circular cross-section tank. Ranganathan [**1**] incorporated the non-linear tire characteristics into the above model, when investigating the directional response characteristics of a five-axle tractor semi-trailer tank vehicle. The model integrated the yaw-roll vehicle model [**25**] and kineto-static model of the tank reported in [**8**], and permitted the analyses of directional responses under steady as well as transient steering inputs.

Assuming rigid suspension and tires with no slip on the road, Rakheja [**26**] developed a simple methodology to estimate the rollover threshold of a cylindrical tank vehicle on the basis of the overturning moment derived from a quasi-static formulation of the partly filled tank. The study demonstrated that the results are in good agreement with those attained from a more comprehensive static roll models. Subsequently, the method was extended to obtain rollover threshold for elliptical and modified oval cross section tank vehicles incorporating compliant suspension and tires and multi-degrees-of-freedom vehicle model [**16**]. The proposed model provided good agreement with the results attained from the static roll model with quasi-static fluid slosh for the circular cross-secton tanks, but revealed errors for non-circular tanks.

The dynamic interaction between the vehicle or the moving cargo under braking inputs have also been investigated through analyses of conventional vehicle models coupled with a pitch-plane quasi-static model of the tank. Zhanqi et al. [**10**] included the nonlinear function of tire-road adhesion characteristics in the analytical model for analysis of braking performance of a partly-filled but compartmented tank truck and concluded that the stopping distance is a function of the partition size. The study proposed optimum partition location to minimize the braking distance and the lag time. The proposed model was further applied to an articulated tractor-semitrailer combination subject to straight line braking. Through analysis of the braking performance as a function of the fill

condition and compartment sizes, it was concluded that the braking performance is dependent upon the tire-road adhesion coefficient, the fill level, and number and location of the compartments.

Kang et al. [**32**] developed the three-dimensional quasi-static model of a partly filled tank, which was integrated into the well-known phase-IV directional dynamic model of commercial vehicles, developed by UMTRI, to study the responses under simultaneous braking and steering inputs. The model could be applied to different vehicle configuration, such as straight trucks, tractor-semitrailers and various tractor-trailer combinations. The model incorporated nonlinear cornering and braking properties of tires, nonlinear suspension properties, and tire-road adhesion. The analyses were performed to study the effect of partial fill condition and tire-road adhesion on the vehicle responses to braking-in-a-turn maneuvers. The study concluded that a higher rollover risk exists under dry road condition.

Salem [**17**] developed two-slice roll plane model of the partially filled elliptical tank truck representing loads in rear and front axles. He considered compliant suspension and tire characteristics and exhibited that increase in suspension stiffness increases the rollover limit.

1.2.2 ANALYSIS OF FLUID SLOSH

In vehicular application, the analyses of fluid slosh within moving containers have been limited to the evaluation of dynamic load shift and the resulting overturning or pitch moments. Kineto-static models of the fluid motion in the roll and pitch planes have been applied to determine the translation of the cargo c.g. within a partly-filled tanks under application of pre-defined lateral and longitudinal acceleration fields [**8,11**]. In this method, the free surface of the liquid is assumed to be stationary under a specific

acceleration field with its gradient being proportional to the magnitude of the tank body acceleration. The coordinates of the c.g. of the fluid with arbitrary cross-sections are obtained through weighted integration over the area or volume of liquid with its free surface being a function of the acceleration, roll angle, tank geometry and fill level. This method has been utilized to investigate the liquid load shift and corresponding roll moment in circular , elliptical, modified oval, modified square, rectangular as well as optimal conical shape tanks [1,2,8,9,16,27,28,10,11,30,31,32,26,35,38]. For the two-dimensional flow in a circular tank, the trajectory of the c.g. is considered to follow a circular arc with its center lying on the center of the tank. The quasi-static assumption of the free-surface under time-varying acceleration excitations of the vehicle is considered to provide the mean load shift, while the dynamic load shift associated with oscillating free surface cannot be estimated. Moreover, a quasi-static model does not permit the consideration of the viscosity effects. Through video recording of the free surface of liquid in a transparent scale model tank vehicle, it was shown that quasi-static free surface could describe the mean slosh behaviour reasonably well [1]. The roll dynamic analyses of a tank vehicle employing quasi-static and dynamic fluid slosh model further revealed that a quasi-static model could characterize the mean slosh forces and roll moment reasonably well [1]. It has been suggested that a vehicle may encounter considerably larger magnitudes of slosh forces and moment due to transient and oscillatory nature of the free surface [1]. Moreover, the steering frequency may lie in the vicinity of the fundamental slosh frequency and cause resonant oscillation of the free surface. The analysis of the fluid slosh has thus been suggested to study the effect of transient slosh forces and moments on the vehicle responses. The development of a dynamic fluid slosh model coupled with the nonlinear vehicle model, however, poses considerable analysis challenges. The vast majority of the studies on fluid slosh have

thus been limited to the tanks alone subject to idealized forces and acceleration excitations.

A number of linear slosh models have been developed assuming irrotational inviscid flow inside a partly filled circular canal and spherical tanks. The governing equations defining the liquid motion were derived using potential flow theory [**18**]. Small amplitude harmonic excitations were assumed in deriving the model, which was solved to identify the slosh frequencies and mode shapes. The linear slosh theory has been also applied to analyze the liquid motion inside a rectangular and an upright cylindrical tank [**21**]. Using this theory, the effect of compartments on the natural frequency of liquid was illustrated. The translational, pitch, roll and yaw forced excitations were also considered for the rectangular tank.

Apart from the dynamic slosh models, a number of mechanical equivalent models have been proposed to characterize the dynamic interaction between the moving cargo and the vehicle [**4**,**12**,**13**,**21**]. The reported models may be grouped into two major types, namely: mass-spring and pendulum analogy. The model parameters are identified by tuning the model frequencies close to those obtained from the linear slosh model. The parameter identification task, however, poses many complexities when varying fill condition and tank geometries are considered.

The effect of compartmenting of a tank on the oscillating mass of liquid has also been investigated using the mechanical analogy of fluid slosh. Using the mass-spring mechanical system, the damping effect of the liquid was considered for different types of damping devices, while relying on experimental results for damping treatment [**21**]. The roll dynamic response of a tank truck equipped with a partly-filled circular clean bore tank under lateral sinusoidal as well as step acceleration inputs was investigated using a

pendulum analogy of the fluid slosh model [**12**]. Specifications of mechanical models representing the lateral sloshing inside the conical, cylindrical ring, and ellipsoidal tanks [**33**] have been defined in a design criteria for the propellant tanks. The liquid slosh inside a clean bore elliptical tank and its influence on the dynamic behaviour of a tank vehicle was studied by developing a trammel pendulum that described the slosh with small amplitudes [**17**].

Owing to the presence of large amplitude motion of the free surface and limitation of the linear fluid slosh models, a few studies have applied nonlinear slosh analysis to study the slosh forces and moments. Popov [**23,24**] developed a two-dimensional nonlinear model of fluid slosh within rectangular and circular cross section tank subject to step lateral acceleration. The Marker and Cell (MAC) numerical method was applied to solve the dynamic fluid slosh model in conjunction with the finite difference method. Sheu [**19**] used the Volume of Fluid (VOF) and finite difference numerical technique to solve for the non-linear Navier-Stoke's equations and mass conservation equation simultaneously. Subsequently the solution for liquid sloshing inside a rectangular tank containing inviscid liquid was implemented. The effect of baffles on behaviour of the liquid was also investigated using this model.

1.3 SCOPE AND OBJECTIVES OF THE PRESENT INVESTIGATION

From the review of reported investigations, it is apparent that the directional dynamics and stability limits of tank vehicles have been of major concern in view of the highway safety issues. Various investigations have been carried out to analyze the dynamics of a liquid cargo and its interaction with the moving vehicle to identify its effect on the directional performance of the vehicle. Different types of analytical models have been developed to characterize the liquid slosh within a container subject to an acceleration field. Mechanical analogies of the slosh have been developed based upon the linear

potential theory of slosh and frequently applied in studies of tank vehicle dynamics. The model development involves small amplitude of liquid oscillation, while the model identification is quite complex, when alternative tank designs and fill levels are considered.

Liquid slosh models based upon linear potential theory have also been employed to express the liquid non-viscous behavior under different acceleration excitations. The quasi-static liquid slosh model has provided a more simple method to estimate the directional performance of the vehicle under partial fill conditions. The quasi-static model does not permit the analysis of the effects of dynamic liquid slosh and the fundamental slosh frequency. The nonlinear behavior of liquid slosh has been investigated in a few studies, which clearly show the significant effect of the dynamic components of the slosh forces and the slosh frequencies.

The vast majority of the investigations focus on the two-dimensional models of liquid slosh, either in the roll or in the pitch planes, irrespective of the model used. Furthermore, the majority of the studies have utilized the quasi-static planar model, where the transient responses are ignored. A single study has applied the three-dimensional quasi-static slosh model to analyze the tank and vehicle behavior under simultaneous lateral and longitudinal acceleration fields.

Although the baffles are widely used to limit the fluid slosh within a partly filled tank, only a few attempts have been made to quantify the effectiveness of baffles in limiting the liquid slosh in the lateral and longitudinal planes.

The scope of this dissertation research is formulated upon identifying the need for analysis of three-dimensional fluid slosh within partly-filled tanks in order to develop methods for developing effective designs of baffles and tanks. The effects of fluid slosh

on the peak forces and moments imposed on the tank structure and thus the vehicles, needs to be quantified to assess their impact on the dynamic safety performance of the vehicles. Owing to the complexities associated with analyses of coupled nonlinear fluid-tank-vehicle system, the preliminary analyses of fluid slosh could be effectively performed with consideration of the tank alone.

1.3.1 OBJECTIVES

The primary objective of the dissertation research is to evaluate the dynamic forces and moments caused by the fluid slosh within a partly-filled moving container subject to lateral and longitudinal acceleration fields. The specific objectives of the study are as follows:

- Develop two- and three-dimensional nonlinear models of liquid slosh within a clean bore cylindrical horizontal tank subject to lateral and longitudinal accelerations.

- Develop the three-dimensional nonlinear slosh model of a baffled tank with baffle geometry in accordance with ASME standards.

- Formulate performance measures that directly relate to directional stability of the vehicles, such as forces, moments, and variations in mass moments of inertia, and derive methodologies to assess theses measures from the fluid slosh responses.

- Perform analyses under steady and time-varying lateral accelerations, and evaluate the transient lateral force, roll moment and load shift characteristics of the partly-filled tank.

- Investigate the influences of fill levels and magnitude of lateral acceleration on the fundamental slosh frequency, lateral force and roll moment.

- Investigate the magnitude of viscous force, and effects of fluid viscosity and density on the performance measures.

- Evaluate the forces and moments caused by three-dimensional fluid slosh under simultaneous application of lateral and longitudinal accelerations.

- Evaluate the roll of baffles in limiting the liquid slosh in both planes, and their effects on the fundamental slosh frequency.

1.4 ORGANAIZATION OF THE THESIS

Chapter 2 includes analytical formulations expressing the liquid slosh inside a partly-filled tank subject to acceleration excitation, based upon quasi-static and nonlinear models. The method of solution along with the corresponding boundary conditions applied to solve the nonlinear model is also expressed and the selected responses, characterizing the liquid slosh behavior are derived, based upon the quasi-static and nonlinear models. Chapter 3 includes the analysis of the liquid slosh in the roll plane when a partly filled circular cross-section clean bore tank is subjected to steady as well as harmonic acceleration excitations. Chapter 4 includes the analysis of the dynamic liquid slosh in a partly filled cylindrical tank with and without baffles subjected to lateral, longitudinal as well as the simultaneous lateral and longitudinal acceleration excitations, where the effect of factors such as fill level, magnitude of acceleration and presence of baffles, on the liquid behavior is investigated. And finally, chapter 5 concludes with synthesis of the major contributions and conclusions of the present study and various recommendations are put forward for the future work.

CHAPTER 2

Model Development And Methods Of Analysis

2.1 INTRODUCTION

Fluid motion inside a partially filled tank subjected to external excitation results in forces and moments which may impose high magnitude of forces and moments on the container structure and destabilize the vehicle. Considering the relatively higher frequency of involvement of tank vehicles in highway accidents, a number of investigations have been carried out to study the interaction between the sloshing and the vehicle [3,5,8]. These studies have provided significant knowledge on the mean and steady-state forces and moments caused by fluid motion within the tank under excitations arising from steering and braking of the vehicles [9,10]. It has been suggested that the vehicle may encounter considerably larger magnitues of slosh forces and moments due to transient fluid slosh. Moreover the analyses of dynamic fluid slosh have been limited to two-dimensional flows [15,17].

Owing to the complexities associated with the nonlinear fluid slosh and integration with the nonlinear directional dynamic model of a commercial vehicle, the dynamic fluid slosh effects in this study are investigated in terms of dynamic load shift, slosh forces and moments, through development and analysis of model of the tank alone. The resulting forces and moments could be applied to a vehicle model to obtain its directional response behavior under steering and braking inputs. This chapter presents the formulations of kineto-static and dynamic fluid slosh models within a clean bore circular

cross-section tank. The model equations together with the boundary conditions representing liquid motion are described.

2.2 KINETO-STATIC MODEL (ROLL-PLANE)

The free surface of the liquid inside a tank, subject to a constant acceleration assumes an inclined straight surface after the liquid has come into steady state and free surface oscillations have diminished. The steady-state motion of the free surface under vehicular excitations may be used to compute the dynamic load shift and the corresponding moment. A kineto-static model of the two-dimensional flow has been formulated for analyzing the steady flow under unidirectional lateral acceleration.

Considering equal hydrostatic pressure along the free surface, the equation of the free surface in two-dimensional Cartesian coordinate system (Figure 2.1) may be obtained.

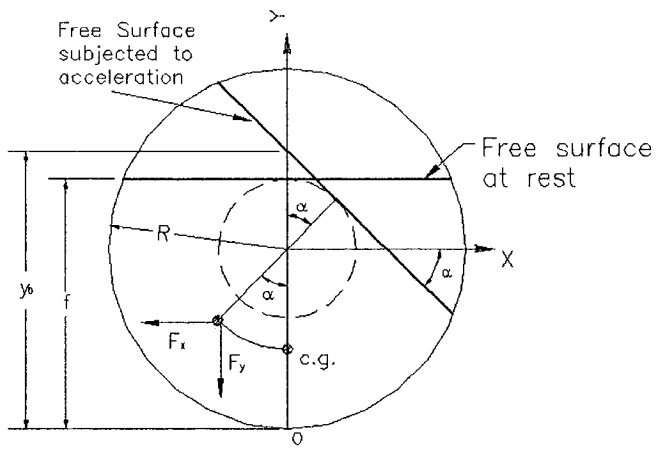

Figure 2.1: Steady-state free surface of liquid under a constant lateral acceleration

Simplified Navier-Stoke's equations for an incompressible flow are used for deriving the free surface equation at its steady state. Since these equations consider the domain

associated with the liquid mass, a constant acceleration ($a = g_x$) with its direction opposite to that of the tank has been assumed. Referring to Figure 2.1, the force equilibrium for a fluid element yields:

$$0 = -\rho g_x - \frac{\partial P}{\partial x} \qquad (2.1)$$

$$0 = -\rho g_y - \frac{\partial P}{\partial y} \qquad (2.2)$$

In which, g_x is horizontal (lateral) acceleration, g_y is the acceleration due to gravity, P is the hydrostatic pressure, and ρ is the mass density of the fluid. It has to be mentioned that the lateral acceleration field is not homogeneous, when a tank is negotiating a turn with radius of the curvature comparable with tank dimension. However, the assumption of the uniform acceleration field would be valid for curves with radius larger than the tank diameter [**24**].

From equations (2.1) and (2.2) the total pressure differential can be easily obtained as:

$$dp = \frac{\partial P}{\partial x}dx + \frac{\partial P}{\partial y}dy = -\rho g_x dx - \rho g_y dy \qquad (2.3)$$

At the free surface, the left hand side in equation (2.3) is equal to zero leading to equation of isobars indicating function of straight lines parallel to the free surface as follows.

$$y = -G_x x + y_0 \qquad (2.4)$$

where $G_x = g_x / g_y$ is the ratio of the applied lateral acceleration to acceleration due to gravity, and y_0 is the coordinate of free surface at x=0.

Assuming constant liquid volume, it may be deduced that the free surface lines at all acceleration levels are tangent to an imaginary circle concentric within the tank cross-section, as illustrated in (Figure 2.1). The constant y_0 may be obtained from Eq. (2.5).

$$y_0 = R + (f - R)/\cos\alpha \qquad (2.5)$$

where α defines the slope of the liquid free surface, which is directly related to the normalized acceleration G_x, and f is the free surface height in the absence of the lateral acceleration, measured from the origin located at the base of the tank. Applying trigonometric relationship, Eq. (2.5) may be rewritten as:

$$y_0 = R + (f - R)\sqrt{1 + G_x^2} \qquad (2.6)$$

2.2.1 CENTER OF GRAVITY AND MASS MOMENT OF INERTIA

The coordinate of the mass center (c.g.) of the deformed liquid and the corresponding roll mass moment of inertia (Izz) can be computed from the tank geometry and the equation of the free surface. The coordinate of the c.g. of the liquid in the static situation ($g_x = 0$) is computed using the tank geometry and the fill height f. The trajectory of c.g. of the liquid under different magnitudes of lateral acceleration may then be defined as a circle concentric within the tank as shown in Figure 2.1. The c.g. of the liquid volume with fill level f under static conditions is obtained assuming unit thickness for the

volume, thereby considering the cross section as a disk (Figure 2.2). The vertical coordinate of the centroid of the liquid in static situation is derived as:

$$y_{st} = -\frac{4\sin\beta(R-(f-R)\cos\beta)}{3(2\pi-2\beta+\sin 2\beta)} \qquad (2.7)$$

where y_{st} is the vertical coordinate of the c.g. measured from the origin, and with no acceleration. The angle β is related to the fill height and expressed as

$$\beta = \cos^{-1}\left(\frac{f-R}{R}\right) \qquad (2.8)$$

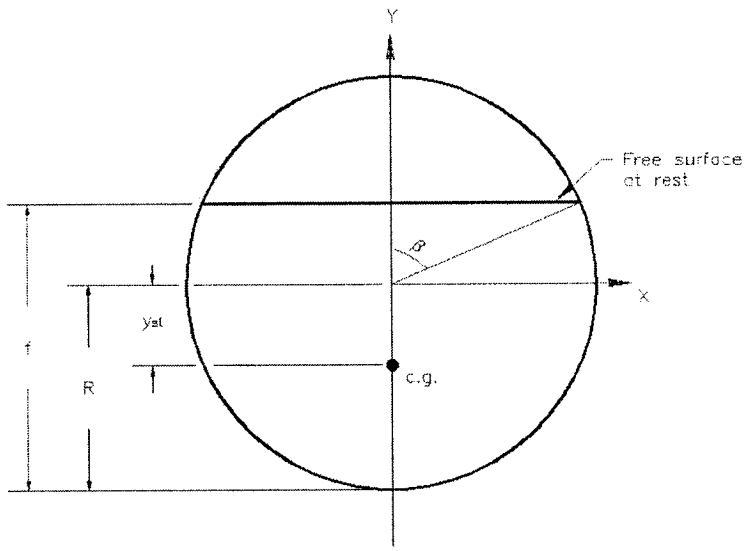

Figure 2.2: The c.g. coordinates of the liquid in a partly-filled tank

The mass moment of inertia of the liquid with an arbitrary fill level f about the center of the tank may be obtained through the moment integral, assuming unit length of the tank:

$$I_{zz} = \iint_{liquid} \rho(x^2+y^2)dA \qquad (2.9)$$

where the limit 'liquid' defined the domain of integration as:

$$\left(-R \le y \le f-R; -\sqrt{R^2-y^2} \le x \le \sqrt{R^2-y^2}\right)$$

The above integration yields following expression for the roll mass moment of inertia in static situation as a function of fill level f :

$$I_{zz} = \frac{\rho R^4}{2}\left[\left(\theta_2 + \frac{\pi}{2}\right) - \frac{1}{12}\sin 4\theta_2 + \frac{1}{6}\sin 2\theta_2\right] \qquad (2.10)$$

where $\theta_2 = \sin^{-1}\left(\frac{f-R}{R}\right)$.

Under application of a constant lateral acceleration in field, the free surface assumes steady gradient, the angle between the free surface and the "X" axis is related to the magnitude of acceleration, such that:

$$\tan\alpha = -G_x \qquad (2.11)$$

The coordinates of the liquid cargo c.g. at the steady state can be derived from the geometry, as:

$$y_{cg} = y_{st}\cos\alpha \qquad (2.12)$$

$$x_{cg} = -y_{st}\sin\alpha \qquad (2.13)$$

x_{cg} and y_{cg} define the lateral and vertical coordinates of the cargo c.g. with respect to the origin. The above equations for the coordinates may be rewritten in term of the normalized lateral acceleration G_x:

$$y_{cg} = y_{st} \Big/ \sqrt{1+G_x^2} \qquad (2.14)$$

$$x_{cg} = y_{st} G_x \Big/ \sqrt{1+G_x^2} \qquad (2.15)$$

2.2.2 ROLL MOMENT

The translation of cargo c.g. under a lateral acceleration field introduces an additional overturning roll moment on the vehicle, which does not exist in case of rigid cargo vehicles. The horizontal slosh force under steady-state condition may be directly derived from:

$$F_x = -g_x m \qquad (2.16)$$

where m is the mass of the liquid. The vertical force due to liquid cargo ($F_y = -mg_y$) also deviates from the central axis and thus contributes to the overturning moment, as illustrated in Figure 2.1. The overturning moment caused by the translation of the cargo c.g. about the origin 'O' can be derived from:

$$\vec{M} = \vec{D} \times \vec{F} \qquad (2.17)$$

where $\vec{D}$ is the position vector of the c.g. from the reference point 'O' and $\vec{F}$ is the resultant force acting on the c.g. of the fluid. The roll moment may be simplified as:

$$M_z = F_y x - F_x (y+R) \qquad (2.18)$$

where M_z is the roll moment about the axis passing through point O. Upon substituting for horizontal and vertical forces in terms of accelerations, the roll moment can be rewritten as:

$$M_z = -mg_y x + mg_x (y + R) \qquad (2.19)$$

The above equation suggests that the overturning moment caused by the cargo load shift is related to the instantaneous coordinates of the c.g. (x, y), the magnitude of lateral acceleration, tank radius and the cargo mass. The substitution for the coordinates x and y from equations (2.13) and (2.12) in (2.19), yields:

$$M_z = mg_x R \qquad (2.20)$$

The above formulation suggests that the roll moment is related to the tank radius, fluid mass and magnitude of lateral acceleration. The reported studies here invariably emphasize a major contribution of the load shift in term of the shifts in the c.g. coordinates [**26**,**28**], which is not clearly evident from the above roll moment formulation.

2.3 THREE-DIMENSIONAL QUASI-STATIC MODEL

The tank vehicles encounter longitudinal as well as lateral forces during steering and braking maneuvers. The fluid motion within a partly filled tank thus experiences load shifts in both roll and pitch planes, as illustrated in Figure 2.3.

Assuming quasi-static motion of the fluid under application of longitudinal and lateral accelerations, the total pressure differential in the three-dimensional form can be expressed as follows [**39**]:

$$dp = \frac{\partial P}{\partial x}dx + \frac{\partial P}{\partial y}dy + \frac{\partial P}{\partial z}dz \qquad (2.21)$$

Considering the force balance on a liquid element in steady state, the differential terms in Eq. (2.21) may be written as follows:

$$g_x = \frac{1}{\rho}\frac{\partial P}{\partial x}, g_y = \frac{1}{\rho}\frac{\partial P}{\partial y}, g_z = \frac{1}{\rho}\frac{\partial P}{\partial z} \qquad (2.22)$$

The total pressure differential may be thus expressed in the following form.

$$dp = \rho g_x dx + \rho g_y dy + \rho g_z dz \qquad (2.23)$$

Considering that the pressure at the free surface vanishes or is uniformly distributed ($dp = 0$), the three-dimensional equation of the free surface at the static condition may be obtained as:

$$Y(x,z) = -G_x x - G_z z + c_0 \qquad (2.24)$$

where $G_x = g_x / g_y$ and $G_z = g_z / g_y$ are the ratio of lateral and longitudinal acceleration to the acceleration due to gravity, respectively and c_0 is the constant parameter which may be determined based on the constant fluid volume.

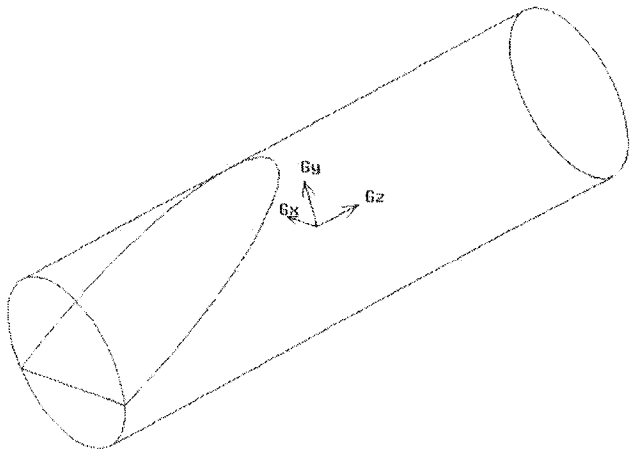

Figure 2.3: Free surface of liquid in a partly filled tank subject to longitudinal and lateral acceleration

The coordinates of the mass center of the fluid can be derived from the following volume integrals.

$$x_{cg} = \frac{1}{V_l}\iiint_V x dv \, , \, y_{cg} = \frac{1}{V_l}\iiint_V y dv \, , \, z_{cg} = \frac{1}{V_l}\iiint_V z dv \qquad (2.25)$$

where x_{cg} , y_{cg} , z_{cg} are the X,Y and Z coordinates of the cargo c.g., respectively, and V_l is the total volume of the liquid.

The mass moments of inertia of the liquid volume about the three orthogonal axes passing through the center of cylindrical tank that coincides with the origin of coordinate system (Figure 2.3) may be obtained by following moment integrals:

$$I_{xx} = \rho\iiint_V (y^2 + z^2) dv \, , I_{yy} = \rho\iiint_V (x^2 + z^2) dv \, , I_{zz} = \rho\iiint_V (y^2 + x^2) dv \qquad (2.26)$$

where I_{xx}, I_{yy}, I_{zz} are the mass moments of inertia of the liquid cargo about the X,Y and Z axes, respectively. Each of the above volume integrals has to be solved over the liquid volume, which is bounded between the tank wall and the free surface of the liquid. Different fill conditions and the magnitudes of lateral and / or longitudinal accelerations cause the liquid mass to assume various complex shapes, which need to be considered during the tedious and complex process of obtaining the response values through performing corresponding integrations. Kang [**39**], as part of his investigation on identifying the optimal shape of the tank, proposed a methodology for solving the volume and moment integrals over all possible integration limits.

The pitch, yaw and roll moments caused by the liquid load shift about a point located at the bottom of the tank directly beneath the origin (center of the tank), as shown in Figure 2.3, are computed from the liquid forces and the coordinates of the mass center, given by:

$$\vec{M} = \begin{bmatrix} i & j & k \\ x & y+R & z \\ F_x & F_y & F_z \end{bmatrix} \qquad (2.27)$$

The coordinates of this point 'O' are (0,-R,0). $\vec{M}$ is the moment vector about the point 'O', and F_x, F_y and F_z are the forces acting along the X,Y and Z axes, respectively, given by $F_y = -mg_y$, $F_x = -mg_x$, $F_x = mg_z$.

2.4 TWO-DIMENSIONAL DYNAMIC SLOSH MODEL

The kineto-static slosh model yields the steady-state positions of the load c.g. within a partly-filled tank subject to constant acceleration tank. Such models have also been

applied under time-varying acceleration fields to derive the mean values of the load shift, slosh forces and moments, while ignoring the responses associated with oscillating fluid slosh [**8**,**9**,**12**]. A few studies have suggested that magnitudes of oscillatory slosh forces and moments could be considerably larger than the mean values, while the reported analyses have been limited to two-dimensional flows [**2**,**12**,**15**]. The dynamic forces and moments caused by the fluid slosh may further reduce the overturning stability limits of the partly-filled vehicles. Furthermore, the kineto-static fluid flow models do not permit the analyses for viscous flows. In addition, the slosh natural frequency strongly affects the dynamic characteristics of the forces and moments acting on a vehicle, specifically when the slosh frequency lies in the vicinity of the steering frequency. The quasi-static model does not permit the analysis of the frequency effect of overturning moment. A dynamic fluid slosh model would thus be vital to investigate the transient slosh forces and moment, and the slosh frequency. A two-dimensional model of the fluid slosh within the circular tank is developed and analyzed to evaluate transient horizontal force, vertical force and roll moment exerted on the tank.

The motion of an incompressible liquid inside the tank as a function of time may be represented by the momentum (the Navier-Stoke's) and mass conservation equations. Assuming two-dimensional laminar flow with constant viscosity [**24**,**40**] the equations of fluid flow with respect to an inertial Cartesian coordinate system (X,Y) can be expressed as:

$$\frac{\partial u}{\partial t}+u\frac{\partial u}{\partial x}+\upsilon\frac{\partial u}{\partial y}=-g_x-\frac{1}{\rho}\frac{\partial P}{\partial x}+\nu\left(\frac{\partial^2 u}{\partial x^2}+\frac{\partial^2 u}{\partial y^2}\right) \qquad (2.28)$$

$$\frac{\partial v}{\partial t}+u\frac{\partial v}{\partial x}+v\frac{\partial v}{\partial y}=-g_y-\frac{1}{\rho}\frac{\partial P}{\partial y}+\nu\left(\frac{\partial^2 v}{\partial x^2}+\frac{\partial^2 v}{\partial y^2}\right) \quad (2.29)$$

$$\frac{\partial u}{\partial x}+\frac{\partial v}{\partial y}=0 \quad (2.30)$$

where u and v are the velocity X- and Y-components of liquid inside the domain at arbitrary points, ν is the kinematic viscosity, P is the fluid pressure, and g_x and g_y are the magnitudes of the unit body forces acting along the X and Ydirections, respectively.

A homogeneous field of body force has been assumed in the formulations. Navier-Stoke's equations are solved in conjunction with appropriate boundary conditions to compute the velocity components and pressure distribution in the flow domain as a function of time and space. It would be reasonable to assume that the tank is bounded by a rigid wall, which yields that the velocity component normal to the wall is zero at the boundary, such that:

$$\frac{\partial U_T}{\partial n}=0 \quad (2.31)$$

where U_T is the total velocity of the liquid and n is the normal direction to the boundary. It has been also assumed that the fluid flow is laminar with constant viscosity and the component of velocity of the fluid tangent to the boundary (wall) is zero implying no-slip boundary condition, such that $U_{Tan}=0$ at the boundary. The deformation of the free surface at each instant of time could be derived assuming irrotational flow with no horizontal displacement of particles at the free surface, which leads to a kinematic restriction in the following form [**41**]:

$$v = \left(\frac{\partial}{\partial t} + u \frac{\partial}{\partial x} \right) \eta \text{ ; at the free surface} \qquad (2.32)$$

where η is the displacement of free surface from its mean position. The above equation exhibits limitations in analyses when a folded free surface occurs. Computation of instantaneous free surface requires a series of rather cumbersome mathematical operations, which could be computationally demanding. The concept of tracking the volume of liquid instead of free surface has thus been widely used. The methodology known as VOF (Volume Of Fluid) permits the analysis of deformation of free surface flow through numerical solution technique.

2.4.1 METHOD OF SOLUTION

The equations of two-dimensional fluid flow, satisfying the boundary conditions are solved using the FLUENT software [42]. The VOF method, available within the FLUENT environment, is applied to solve for the transient flows involving free surface separating the liquid cargo and the air within the non-filled cross-section of the tank.

FLUENT is a general comprehensive CFD code that is developed based upon Finite Volume numerical solution technique to solve a wide range of fluid flow problems. This code can be applied in a wide range of applications capable of handling transient problems involving free surface and multiphase viscous flows. In addition, the effect of fluid material properties can be introduced to the flow model by relying on an extended material database that is provided with the software. Furthermore, a powerful data post-processing is provided through coupling the solver to an external programming language such as C++, allowing the flow data obtained from simulation be utilized for further

analysis. Moreover, the flow visualization capabilities of this software helps to observe the transient flow history.

The momentum and mass conservation equations are discretized using Finite Volume technique considering each cell as a control volume. A unit thickness of the control volume has been assumed for the two-dimensional flow. The general form of the discretized momentum equation for steady state has been derived as follows [**43**]:

$$\sum_{e}^{N_{faces}} \rho_e \vec{v}_e \varphi_e . \vec{A}_e = \sum_{e}^{N_{faces}} \Gamma_\varphi (\nabla \varphi)_n . \vec{A}_e + S_\varphi V_c \qquad (2.33)$$

where ρ_e is the mass density of the fluid, $\vec{v}_e$ is the velocity vector at the cell face, and $\vec{A}_e$ is the area of the face enclosing the cell. The product $\rho_e \vec{v}_e . \vec{A}_e$ represents the mass flow through the face of a cell. φ_e is the value of variable convected through the face e being u and v in the present simulation. $(\nabla \varphi)_n$ represents the gradient of φ ($\nabla \varphi = \frac{\partial \varphi}{\partial x}\vec{i} + \frac{\partial \varphi}{\partial y}\vec{j}$ for 2D) normal to the face, while the term $S_\varphi V_c$ represents the body forces with V_c being the volume of the cell. φ is a scalar quantity (representing u, v and w in this investigation) which its transport is considered and is formulated using integral form of conservation equation for an arbitrary control volume.

For transient simulations, the governing equations must be discretized in both space and time. The spatial discretization for the time-dependent equations is identical to the steady-state case. Temporal discretization involves the integration of every term in the differential equations over a time step Δt. A generic expression for the time evolution of a variable φ is given by

$$\frac{\partial \varphi}{\partial t} = F(\varphi) \qquad (2.34)$$

where the function F incorporates any spatial discretization. The FLUENT software applies implicit method to solve unsteady free surface flow, hence the equation may be descretized into the following form, using first order backward difference technique.

$$\varphi^{n+1} = \varphi^{n} + \Delta t F(\varphi^{n+1}) \qquad (2.35)$$

The pressure-corrector PISO [**44**] algorithm is selected for solving for the transient equations coupling pressure and velocities. The classical way of discretizing the equations of liquid motion has been handled in a customized manner to include the liquid volume tracking concept in formulation for visualizing the free surface pattern during its evolution described below.

In order to resolve the shortcomings associated with the surface-tracking method, such as failing to deal with more than one interface in the vertical direction, the concept of tracking the volume of liquid has been applied to locate the interface between the two phases [**46**]. Defining a fluid fraction step function with magnitude of zero or one representing volume of the target phase existing in a cell, the free surface would be tracked with lower CPU time consumption compare to other methods [**24**]. Volume of Fluid (VOF) technique is based upon the assumption that no interpenetration occurs between the two phases of the flow, which has been widely used to study the transient free surface problems with more than one phase in the domain.

In this method, the volume fraction transportation equation replaces the kinematic condition of the free surface as a boundary condition, which defined the evolution of the

free surface as a function of time and space. The transportation equation may be written as:

$$\frac{\partial \alpha_q}{\partial t} + \vec{v} \cdot \nabla \alpha_q = \frac{S_{\alpha q}}{\rho_q} \qquad (2.36)$$

In which α_q is the volume fraction of target phase in cell, $\vec{v}$ the fluid velocity vector, $S_{\alpha q}$ in the right hand side of the equation is the source term which is zero in the present study and ρ_q the density of the target phase. It is important to note that the step value characteristics of α_q prevents the distinct free surface to be smeared out during the simulations [**46**]. The sum of volume fractions of all phases contributing to flow is equal to unity at each cell, such that:

$$\sum_q \alpha_q = 1 \qquad (2.37)$$

The transient free surface flow problem is solved using a composite momentum equation for the entire domain comprising all phases of the flow:

$$\frac{\partial(\rho' \vec{v})}{\partial t} + \nabla \cdot (\rho' \vec{v} \vec{v}) = -\nabla P + \nabla \cdot \left[\mu\left(\vec{v} + \vec{v}^T\right)\right] + \rho' \vec{g} + \vec{F}_F \qquad (2.38)$$

where $\vec{F}_F$ is the forcing function which represents the applied forces or corresponding accelerations, superscript '*T*' designates the transpose, and ρ' is the volume-fraction-averaged density calculated as follows:

$$\rho' = \sum_q \alpha_q \rho_q \qquad (2.39)$$

For the two phases of fluid (gas and liquid) considered in a partly filled tank, the above equation can expressed as:

$$\rho' = \alpha_2 \rho_2 + (1-\alpha_2)\rho_1 \qquad (2.40)$$

where ρ_2 is the density of the liquid as the secondary phase and α_2 is the corresponding volume fraction. ρ_1 is the density of the fluid in the primary phase.

The composite momentum equation, EQ (2.38), is solved together with the continuity equation to derive the transient free surface flow by applying pressure-corrector PISO algorithm.

2.4.2 COMPUTATION OF RESPONSE CHARACTERISTICS

The distribution of instantaneous or transient fluid pressure acting on the tank wall may provide significant insight into a number of characteristic features that could severely affect the behavior of the container and the vehicle, such as stresses imposed on the container, peak slosh forces and peak overturning moment. Many studies have established that the effect of distributed pressure on the tank structure could be investigated in terms of equivalent forces and moments exerted on the wall [**3,8,17,24**]. These forces and moments associated with relative movement of the liquid cargo are apparently larger than those of an equivalent rigid cargo. The reported studies on the roll dynamic behavior of partly filled tank vehicles have invariably concluded that the load shift, often expressed in terms of deviations in the coordinates of the mass centre and thus the motion of the free surface, directly affects the magnitude of the overturning moment. The motion of the free surface of fluid is thus considered as the most significant factor affecting the vehicle roll stability. The effect of the motion of the free surface would

be far more significant when transient response characteristics due to liquid slosh and the slosh frequencies are considered. The pressure distribution responses are thus post-processed to derive the instantaneous horizontal and vertical slosh forces, overturning moment and slosh frequency. Using the instantaneous coordinates of the time varying boundaries by which the liquid mass is enclosed, the coordinates of liquid cargo c.g., and thus the load shift are also derived at each instance of simulation as well. User Defined Function (UDF) feature of the FLUENT software is used to evaluate above stated dynamic measures.

LOAD SHIFT

The instantaneous coordinates of center of gravity of the liquid have been obtained carrying out a numerical integration over the liquid phase of the domain.

$$x_{cg} = \frac{\sum_{c}^{liquid} x_c A_c}{\sum_{c}^{liquid} A_c}, \; y_{cg} = \frac{\sum_{c}^{liquid} y_c A_c}{\sum_{c}^{liquid} A_c} \qquad (2.41)$$

Using C^{++} programming language simulation data post-processing has been carried out and a comprehensive code has been developed to obtain response values in terms of forces, moments, c.g. displacement and mass moment of inertia. Thus implementing the concept shown in the form of Eq. (2.41) the instantaneous coordinates of the load c.g. is obtained. Now the load shift may be defined as the difference between the new position of the center of gravity of the liquid and its initial value.

HORIZONTAL AND VERTICAL FORCE

The resultant forces as a result of distributed pressure acting on the wall have been obtained implementing integration over the wetted area of wall cells as shown in EQ's. (2.42) and (2.43) below.

$$F_x = \sum_{c}^{wet\ area} P_c \vec{A}_c \cdot \vec{i} \qquad (2.42)$$

$$F_y = \sum_{c}^{wet\ area} P_c \vec{A}_c \cdot \vec{j} \qquad (2.43)$$

where F_x and F_y are the resultant forces acting on the tank wall due to pressure P_c acting on cell "c" with area vector $\vec{A}_c$ as shown in Figure 2.4.

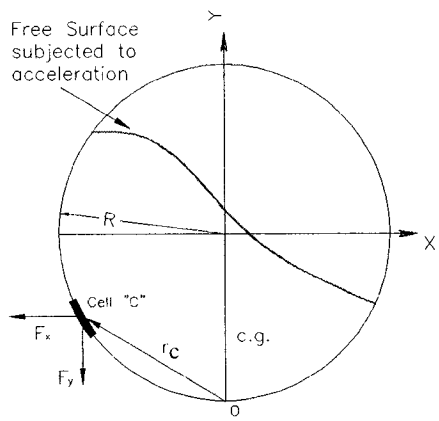

Figure 2.4: Pressure forces acting on arbitrary cell "C" on the wall

The shear stress due to viscous flow introduces a force on the tank wall that may be calculated by adding infinitesimal forces exerted on boundary cells over the wetted area. The shear stress may be defined proportional to normal derivative of the velocity tangent to the wall. For the Newtonian fluid, the shear stress can be described as:

$$\tau = \mu \frac{\partial U_{Tan}}{\partial n} \qquad (2.44)$$

in which τ is the shear stress at the wall, μ dynamic viscosity of the liquid and U_{Tan} tangential component of the velocity of liquid adjacent to the wall where "n" is the direction normal to the wall. It is worth mentioning that the viscosity has been assumed constant respecting a laminar flow at the vicinity of the tank's wall.

The corresponding resultant viscous forces acting on the wall in x and y directions may be obtained by implementing numerical integrations as follows.

$$FV_x = \sum_{c}^{wet\ area} A_c \vec{\tau}_c \cdot \vec{i} \qquad (2.45)$$

$$FV_y = \sum_{c}^{wet\ area} A_c \vec{\tau}_c \cdot \vec{j} \qquad (2.46)$$

where τ_c is the shear stress at the wall acting on the cell c, A_c area of the cell, $\vec{i}$ and $\vec{j}$ unit vectors in x and y directions.

Computation of resultant force in X and Y direction is also programmed as part of the developed computer code.

ROLL MOMENT

The roll moment about the point "O" has been obtained performing an integration of the infinitesimal moments corresponding to each cell over the wetted area (Figure 2.4). This has also been included in the code doing the data post processing.

It has been concluded that the viscous forces are very small compared to pressure (inertial) forces [47]. This has further been investigated by calculating the forces and moments due to pressure as well as the viscous stress at the wall. The roll moments corresponding to each type of force may be obtained from a single formulation by considering corresponding forces during the integration as evident in EQ's (2.47) and (2.48) respectively.

$$M_Z = \sum_{c}^{wet\ area} \left(F_{yc} x_c - F_{xc} \left(y_c + 1.016 \right) \right) \qquad (2.47)$$

In which F_{yc} and F_{xc} are pressure forces in vertical and horizontal directions acting on the boundary cell "c" with coordinates x_c and y_c.

$$MV_Z = \sum_{c}^{wet\ area} \left(FV_{yc} x_c - FV_{xc} \left(y_c + 1.016 \right) \right) \qquad (2.48)$$

where FV is the force due to shear stress in the vicinity of the wall with x and y in the suffix indicating direction of the force acting on the cell c.

ROLL MASS MOMENT OF INERTIA

The product of square of coordinate vector and the area corresponding to each cell has been numerically integrated over the liquid zone to obtain the mass moment of inertia about the center of the tank. Given constant density for the liquid and assuming two-dimensional flow with thickness of unity, the mass moment of inertia about the center of the tank is formulated as follows.

$$I_{zz} = \rho_f \sum_{c}^{liquid} \left(x_c^2 + y_c^2\right) A_c \qquad (2.49)$$

where x_c, y_c are the coordinates of the cell with volume A_c and I_{zz} is the roll mass moment of inertia

LIQUID SLOSH FREQUENCY

The Fast Fourier Transform (FFT) has been employed to obtain the first damped frequency of slosh using simulation results. The corresponding function in MATLAB platform has been employed in this regard. A Low-pass Butterworth filter with order of eight and cut-off frequency of 2 Hz has been applied for data filtering. Provided the maximum natural frequency corresponding to 80% fill level is less than 1 Hz [**18**], the 2 Hz cut-off frequency was selected to be both close to slosh frequency so as to eliminates as much of noises as possible and also to let other potential frequencies associated with large slosh amplitude be observed and investigate slosh behavior more accurately. Using parameters of Butterworth filter in the "filtfilt" function in MATLAB platform all sets of data have been filtered for further investigation. This is a built-in macro performing bidirectional filtering that eliminates phase error. The drawback would be the higher level of data error that was not considerable in this study.

2.5 THREE DIMENSIONAL DYNAMIC SLOSH MODEL

The three-dimensional version of Navier-Stoke's equations for incompressible flow may be described as:

$$\frac{\partial u}{\partial t} + u\frac{\partial u}{\partial x} + \upsilon\frac{\partial u}{\partial y} + w\frac{\partial u}{\partial z} = -g_x - \frac{1}{\rho}\frac{\partial P}{\partial x} + \nu\left(\frac{\partial^2 u}{\partial x^2} + \frac{\partial^2 u}{\partial y^2} + \frac{\partial^2 u}{\partial z^2}\right) \qquad (2.50)$$

$$\frac{\partial v}{\partial t}+u\frac{\partial v}{\partial x}+v\frac{\partial v}{\partial y}+w\frac{\partial v}{\partial z}=-g_y-\frac{1}{\rho}\frac{\partial P}{\partial y}+\nu\left(\frac{\partial^2 v}{\partial x^2}+\frac{\partial^2 v}{\partial y^2}+\frac{\partial^2 v}{\partial z^2}\right) \qquad (2.51)$$

$$\frac{\partial w}{\partial t}+u\frac{\partial w}{\partial x}+v\frac{\partial w}{\partial y}+w\frac{\partial w}{\partial z}=g_z-\frac{1}{\rho}\frac{\partial P}{\partial z}+\nu\left(\frac{\partial^2 w}{\partial x^2}+\frac{\partial^2 w}{\partial y^2}+\frac{\partial^2 w}{\partial z^2}\right) \qquad (2.52)$$

Boundary conditions similar to those considered for two-dimensional case regarding rigid wall and zero-velocity (Section 2.4) may also be applied to three-dimensional case. The free surface boundary condition considering analytical solution techniques, is the kinematic condition of the free surface generalized into the following 3D form assuming small wave amplitudes [**48**].

$$v=\left(\frac{\partial}{\partial t}+u\frac{\partial}{\partial x}+w\frac{\partial}{\partial x}\right)\eta \qquad (2.53)$$

in which η is the displacement of free surface from its mean position.

2.5.1 METHOD OF ANALYSIS

As may be observed, the formulation presented in section 2.4.1 regarding equation discretization by FLUENT is general and applies for the three-dimensional case as well thus further elaboration is not required. In order to refrain from repetition of subjects, the formulation corresponding to subject response measures are mentioned

LOAD SHIFT

The x and y coordinates of cargo c.g. can be obtained from the Eq's 2.41. In a similar manner the z coordinate of the c.g. may be obtained from EQ (2.54) below:

$$z_{cg} = \frac{\sum_{c}^{liquid} z_c A_c}{\sum_{c}^{liquid} A_c} \qquad (2.54)$$

HORIZONTAL, VERTICAL AND LONGITUDINAL FORCES

The EQ's. 2.42 and 2.43 can also be applied for a three-dimensional flow to obtain the resultant lateral and vertical forces, respectively. The resultant longitudinal force in Z direction may be expressed in terms of pressure and cell area given by:

$$F_z = \sum_{c}^{wet\ area} P_c \vec{A}_c \cdot \vec{k} \qquad (2.55)$$

where $\vec{k}$ is the unit vector in the Z direction.

PITCH, ROLL AND YAW MOMENTS

The Eq. 2.27 has also been applied to compute the moments in the pitch, roll and yaw planes.

PITCH, ROLL AND YAW MASS MOMENTS OF INERTIA

The roll mass moment of inertia has been expressed in the form of EQ. (2.49) for a two-dimensional flow, assuming unit thickness of the liquid mass. Extending the formulation over the volume of the liquid, the mass moments of inertia about the X , Y and Z axes may be obtained from the following equations representing pitch, yaw and roll mass moments of inertia respectively.

$$I_{XX} = \rho_f \sum_{c}^{liquid} \left(y_c^2 + z_c^2\right) V_c \qquad (2.56)$$

$$I_{YY} = \rho_f \sum_{c}^{liquid} \left(x_c^2 + z_c^2\right) V_c \qquad (2.57)$$

$$I_{ZZ} = \rho_f \sum_{c}^{liquid} \left(x_c^2 + y_c^2\right) V_c \qquad (2.58)$$

where I_{XX}, I_{YY}, I_{ZZ} are the mass moments of inertia in pitch, yaw and roll planes respectively, and V_c is the volume of the arbitrary cell in the liquid domain.

2.6 TWO DIMENSIONAL SIMULATIONS

2.6.1 TANK GEOMETRY AND ITS DISCRETIZATION

The circular cross-section tank of radius $R = 1.016$ meters and unit length has been assumed and three different grid sizes have been considered to investigate the effect of mesh size on accuracy of the response with number of cell indicated in Table 2.1.

Table 2.1: Comparison of computational time (sec) utilizing different grids and time steps

Grid	Number of Cells	Number of faces	Number of nodes
Grid 1	16638	33528	16891
Grid 2	3352	6857	3506
Grid 3	7996	16192	8197

The roll moment corresponding to 60% fill level and the acceleration magnitude of 0.1 g is considered to characterize the level of simulation error due to different sizes of the mesh grid and results revealed insignificant deviation with respect to that of the finer meshing 'Grid 1' for a 2 ms time step. The effect of the time step on the level of deviation for the shorter time step of 2 ms was also investigated by performing simulations with

1, 2, 5, 6 and 10 ms time steps and the results suggest small deviation of 1% with respect to the 2 ms time step, while the shorter time step could considerably elongate computational time, as shown in Table 2.2. Thus the meshing 'Grid 2' was selected to perform the two-dimensional simulations using 10 ms time step to the descritized model

Table 2.2: The effect of time step and the grid size on the computational time (in seconds for two-second flow simulation)

Grid	Time steps (S)						
	0.010	0.006	0.005	0.002	0.001	0.0005	0.0001
Grid 1		-	-	109	-	-	-
Grid 2	7	9	10	30	50	100	-
Grid 3		18	20	60	100	-	-

The structure of the mesh 'Grid 2' is illustrated in Figure 2.5.

2.6.2 ACCELERATION EXCITATIONS

It has been suggested that the transition period of steering input in a steady turning is around 0.5 sec[**37**]. This period is considered in the rounded ramp-step acceleration defined as a function of time as shown in Figure 2.6. It was further suggested that the magnitude of the lateral acceleration imposed on a tank vehicle barely exceeds 0.3 g. Thus, the range of 0.1-0.4 g lateral acceleration is considered in this present study.

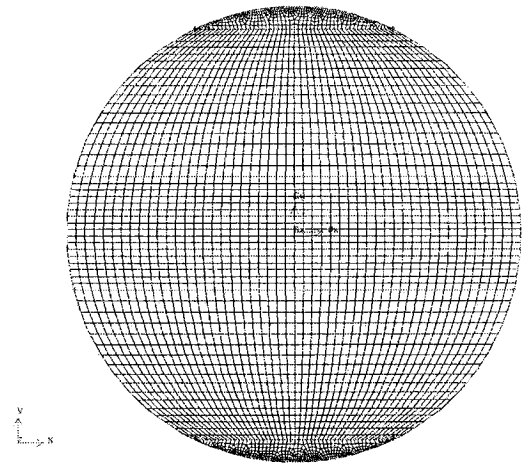

Figure 2.5 – The structure of the mesh "Grid 2"

It has also been suggested that the steering frequency of path-change maneuver, which can be idealized by a sinusoidal acceleration excitation, lies around 0.3 Hz, and can approach 0.5 Hz in case of severe maneuvers [5]. The excitation frequency range of 0.2-0.8 Hz is considered in present study to permit the liquid slosh responses in the resonance mode, be also evaluated for different fill conditions.

The rounded Ramp-step acceleration with magnitude of 0.4 g and the sinusoidal excitation with frequency of 0.2 Hz and amplitude of 0.2 g have been illustrated in Figure 2.6.

2.6.3 FILL CONDITIONS

The fill percent, as the ratio of the fill height from the bottom of the tank to the tank diameter, with the magnitudes of 40%, 60% and 80% is selected to identify the fill conditions in the present study.

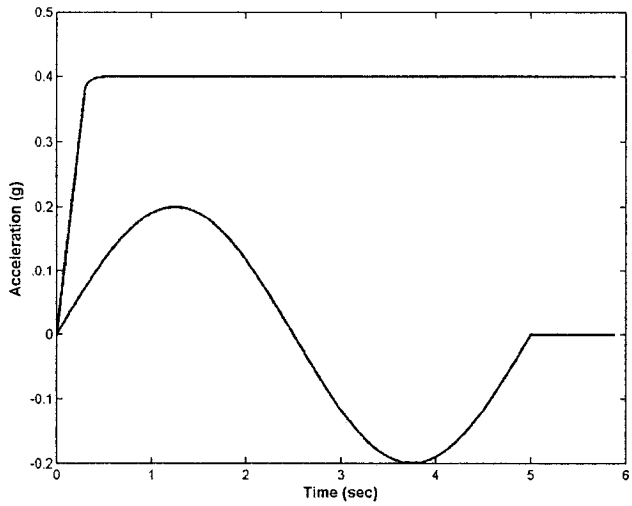

Figure 2.6: Ramp-step and sinusoidal lateral acceleration excitations

2.6.4 CARGO MATERIAL

The analyses are performed for fuel oil (μ=0.0867 kg/ms), sulfuric acid (μ=0.0255 kg/ms) and castor oil (μ=0.98 kg/ms). The weight densities for this analysis are taken as 850, 980 and 1826 kg/m^3, respectively.

2.7 THREE DIMENSIONAL SIMULATIONS

2.7.1 TANK GEOMETRY

The geometry of the cylindrical tank considered in the present study is illustrated in Figure 2.7 with the coordinate system located at the geometric center of the tank.

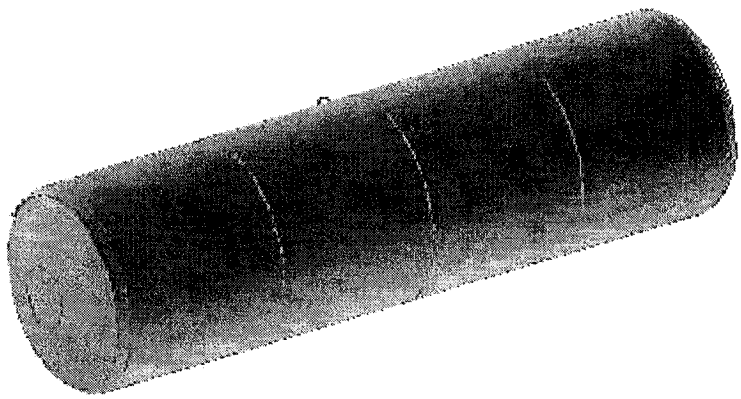

Figure 2.7: Cylindrical tank with curved bulkheads

The bulkheads are designed in accordance with CFR code 148.346-2, which addresses the instruction of ASME Section 8 Dev. 1 UG32. The CFR code also requires the same design and geometry for the baffles inside the tank. The tank with three equi-distant baffles, considered in this investigation, is shown in Figure 2.8.

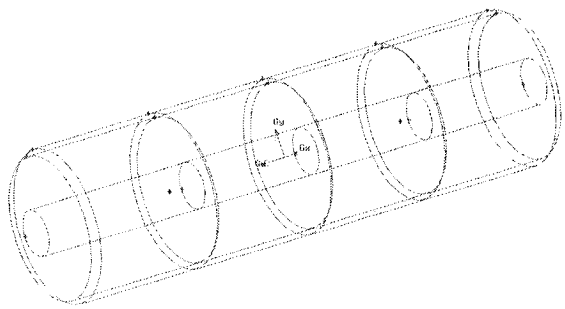

Figure 2.8: Wire frame of the tank with three baffles

The schematic of the symmetric baffle with the nozzle of 0.61 m diameter is illustrated in Figure 2.9.

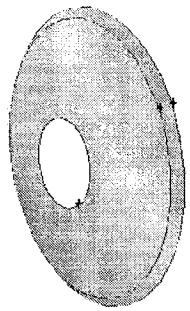

Figure 2.9: Single-nozzle baffle with the same shape as of the bulkheads

The dimensions of the tank and a typical baffle are tabulated in Table 2.3and Table 2.4 respectively.

Dimension	Meters
Diameter	2.023
Front-to-end	7.546

Table 2.3: Dimensions of the tank

Dimension	
Diameter	2.023
Bulk radius	1.016
Nozzle diameter	0.610

Table 2.4: Dimensions of a typical baffle

According to CFR code 148.346-2, the distance between bulkheads shouldn't exceed 60 in. or 5 ft. that would require four baffles within the tank. Three baffles were assumed to reduce the meshing complexity and computation demand. The three-baffle configuration yields small deviation of 6% from the standard requirement.

2.7.2 GEOMETRY DISCRETIZATION

The unstructured meshing scheme was applied using GAMBIT environment to discretize the bulkhead of the tank as is shown in Figure 2.10. The surface mesh is then swept along the length of the tank (Z axis) to generate the volume mesh as shown partially in Figure 2.10(b) that illustrates a section between to baffles. The same geometry was employed for clean bore tank by changing wall boundaries into internals [**49**].

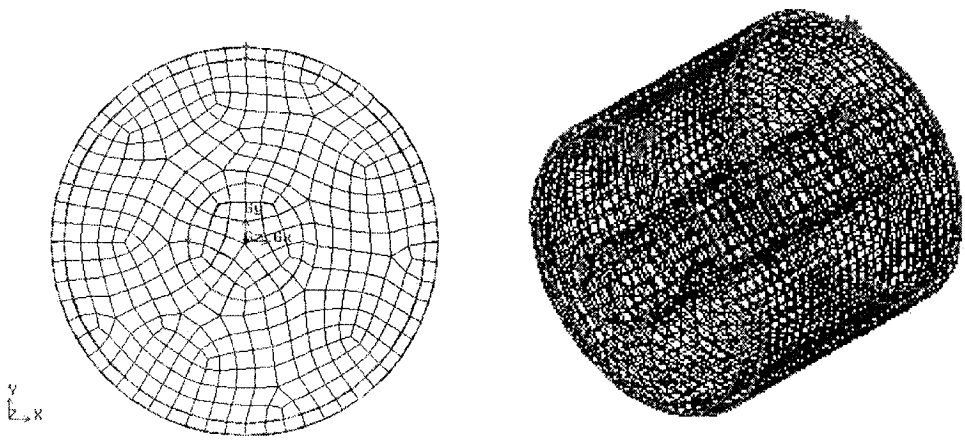

Figure 2.10: (a) Unstructured mesh applied to bulkhead surface and (b) the volume meshing between to bulk head and the adjacent baffle.

Two time steps of 0.1 and 0.25 ms were considered. The simulation results under 0.1 and 0.25 ms time steps were examined and difference values were found insignificant, thus the larger time step is selected for performing the simulations that would save the computation time.

2.7.3 ACCELERATION EXCITATIONS

The Turning, Braking and Braking-in-a-turn maneuvers have been represented by Rounded ramp-step accelerations with constant magnitudes as reflected in Table 2.5.

Acceleration		Fill level
Gx (Turning)	Gz (Braking)	
0	+0.3g	0.4
0	+0.6g	0.4
0	+0.3g	0.6
0	+0.6g	0.6
-0.25g	+0.3g	0.4
-0.25g	+0.6g	0.4
-0.25g	+0.3g	0.6
-0.25g	+0.6g	0.6
-0.4g	0	0.6

Table 2.5: Acceleration types and intensity considered for two different fill levels

The fill levels considered for each maneuver have also been illustrated in this table.

2.7.4 FILL CONDITIONS

Two fill levels of 40 and 60 percent have been considered to investigate the influence of the fill level on dynamic slosh behavior as shown in Table 2.5. The influence of the fill level has been investigated for the tank with and without baffles.

2.7.5 CARGO MATERIAL

The two-dimensional simulation results revealed that the viscous effect is negligible for the range of viscosity considered in this study. Hence the Fuel oil with the dynamic viscosity of 0.0867 kg/ms and the density of 0.85 has been considered in three-dimensional analysis.

2.8 SUMMARY

The analytical quasi-static and nonlinear liquid slosh models are formulated and the liquid responses in terms of c.g. shift, forces, moments and mass moments of inertia are derived.

The resultant moment derived from the QS solution was further simplified by eliminating simultaneous c.g. coordinates showing a relationship between the roll moment and lateral slosh force expressing the roll moment as a function of horizontal force and the radius of the tank.

The methodology of solution of non-linear liquid slosh model is presented and response values are derived from flow parameters such as pressure and flow velocity.

The meshing structure of the two- and three-dimensional models is presented

CHAPTER 3

Transient Fluid Slosh In The Roll Plane

3.1 INTRODUCTION

The roll stability characteristics of partially-filled tank vehicles are frequently evaluated under lateral accelerations representing constant velocity steady turning maneuvers [8,16]. These studies have established that the lateral force caused by the fluid motion in the roll plane imposes an additional overturning moment leading reduced roll stability limit. Furthermore, the additional overturning moment due to fluid motion under a lateral acceleration field has been strongly related to the lateral load shift expressed in terms of deviations in the coordinates of the mass centre. The dynamic slosh force, the deviations in the c.g. coordinates and the resulting roll moment, of the moving liquid cargo can be determined from the solution of the two dimensional model of dynamic liquid slosh subject to a lateral acceleration excitation. The model analysis would permit the evaluation of not only the steady-state responses but also the peak responses caused by the transient motion, which are known to be considerably larger [15]. The dynamic forces, load shift and the roll moment can be derived from the response variables, such as flow velocity and the dynamic pressure of liquid in the vicinity of the tank wall, as described in section 2.4. The analysis also permits the evaluation of the mass moment of inertia of the deformed liquid about the geometric center of the tank, which is also known to affect the roll performance of the vehicle.

In this chapter, the results attained from the solution of the two-dimensional liquid slosh model, are expressed in terms of the desired performance measures. These include the deviations in the c.g. coordinates, lateral and vertical forces due to the liquid, roll

moment and roll mass moment of inertia. The mean values of the steady-state response are compared with those derived from the quasi-static model. The influence of different parameters on the liquid slosh behavior and thus the measures of the overturning characteristics of a vehicle are investigated and discussed. These include the fill level, acceleration type and magnitude, as well as physical properties of liquid, in terms of viscosity and density. Furthermore, the fundamental frequencies of the fluid slosh are discussed as functions of the fill condition within a clean bore tank. Moreover, the coordinates of the center of pressure are obtained and the results are compared to those of cargo c.g., respectively, and the validity of assuming the c.g. as the point at which the dynamic resultant forces act, is also discussed

3.2 LOAD SHIFT RESPONSE ANALYSIS

It has been reported that the lateral load shift of the liquid cargo in a partially filled tank vehicle poses additional roll moment that leads to further reductions in the overturning threshold acceleration limit of a vehicle [21,37,50]. On the basis of the quasi-static model of the liquid slosh in a tank with different cross sections, a few studies have derived the overturning moment caused by the cargo load shift under a constant lateral acceleration [26,27]. This model, however, does not consider the load shift caused by dynamic responses, which may yield considerably larger peak magnitudes of the load shift. The transient load shift caused by liquid slosh in a partly filled circular cross-section tank is analyzed, and the results are compared with those derived from the quasi-static model in order to illustrate the significance of dynamic fluid slosh. The analyses are limited to fill height in the 40-80% range.

3.2.1 LATERAL LOAD SHIFT

The dynamic lateral load shift, attributed to fluid slosh, is the most important measure related to severity of the additional roll moment imposed on a tank and the vehicle [**26**]. The lateral load shift is often characterized in terms of the deviations of the lateral coordinate of the cargo c.g. under a specified lateral acceleration [**3**]. The analyses of the lateral load shift in terms of the cargo c.g. coordinates, however, have been limited to quasi-static analyses under steady as well as transient accelerations [**28**]. Rakheja [**9**] developed a simple method based upon the quasi-static liquid slosh model, to analyze the effect of liquid load shift on the overturning roll moment and suggested that the magnitude of the roll moment is related to the corresponding load shift. Ranganathan [**1**], applied a dynamic fluid slosh model developed by Popov [**24**] to study the transient lateral load shift within a partly filled scale model tank subject to steady as well as transient lateral acceleration. The study concluded that the quasi-static liquid slosh models provide reasonably accurate results when the mean response values under steady excitations are concerned. However, these models are incapable of predicting the transient response characteristics due to dynamic liquid slosh.

In the present study the transient response characteristics of the liquid slosh in terms of cargo displacement due to nonlinear liquid slosh behavior are derived and the effect of different parameters on dynamic response values are analyzed. The instantaneous lateral and vertical coordinates of the cargo c.g. are computed through integration of the coordinates of different cells constituting the liquid domain, as described in section 2.4.2. The transient solutions revealed significant oscillation of the lateral c.g. coordinate about its mean value. The predominant frequency of oscillation was observed to be dependant upon the fill level, as reported in earlier studies [**18,17,24**]. The transient response data in terms of the instantaneous c.g. coordinates are analyzed to identify their minimum,

maximum and mean values. Figure 3.1(a) illustrates the minimum, maximum and mean values of the lateral c.g. coordinate (X) for three different fill levels (40%, 60% and 80%). The results are attained under a 0.1 g ramp-step lateral acceleration excitation. The figure also illustrates a comparison with the c.g. coordinates derived from the QS solution under same fill conditions and lateral accelerations. The minimum and maximum values of the c.g. coordinate, corresponding to a given fill level, are identified from the time history of the response. Figure 3.1(b) illustrates the time variation in c.g. coordinate for the 40% filled tank subject to 0.1 g ramp-step lateral acceleration.

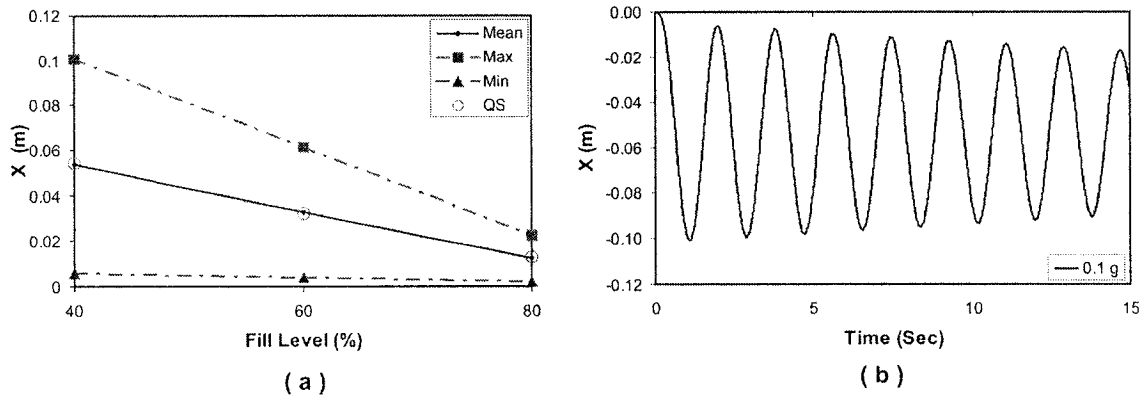

Figure 3.1: (a) Lateral load shift obtained from fluid slosh and QS analyses (b) Transient lateral load shift in a tank 40% filled with fuel oil both under 0.1 g ramp step acceleration

The results suggest that the fill level has considerable impact on the magnitude of peak values and their deviations from the respective mean responses. The mean values attained from the fluid slosh model are quite close to those derived from the QS analysis. The results thus confirm that the QS analysis would be appropriate for the mean or steady-state responses, as reported by Ranganathan [**1**]. The peak values of the load shift observed from the oscillations attributed to transient fluid slosh tend to be considerably higher, which could lead to significantly larger roll moment. The results further show that the peak as well as the mean magnitude of the coordinate decreases

with increasing fill level, while the deviation between the peak and mean values diminishes at higher fill volume.

The peak load shift expressed in terms of lateral c.g. coordinate is normalized with respect to the static solution, which represents the level of deviation from the steady solution in terms of an amplification factor, given by:

$$M_{CGx} = \frac{Max(x)}{\bar{x}} \qquad (3.1)$$

where the $\bar{x}$ is the static solution or mean value of c.g. X coordinate and M_{CGx} is the amplification factor of the X coordinate.

The amplification factors are computed on the basis of both the quasi-static and mean dynamic responses, and the results are presented in Figure 3.2(a) and Figure 3.2(b), respectively. The normalization with respect to the QS solution yields peak amplification near 60% fill condition, irrespective of the magnitude of excitation considered, as shown in Figure 3.2(a), while a monotonic declining trend of amplification factor would be expected with increase in the fill level. This would be attributed to differences between the mean values and the corresponding static solutions, which is most likely due to deformation and/or separation of the free surface. An examination of mean dynamic and the QS responses revealed differences up to 4.1% corresponding to the higher fill volume. The amplification factors based upon the mean dynamic response are thus computed for the selected fill and excitation levels, and presented in Figure 3.2(b). These results based upon the mean values of the dynamic slosh responses confirm the expected monotonically declining trend with increasing fill ratio, irrespective of the magnitude of the lateral acceleration. The results clearly show that a lower fill volume yields largest amplification of the load transfer, when dynamic fluid slosh is considered.

This amplification factor with respect to mean values can approach as high as 1.88 under low fill conditions.

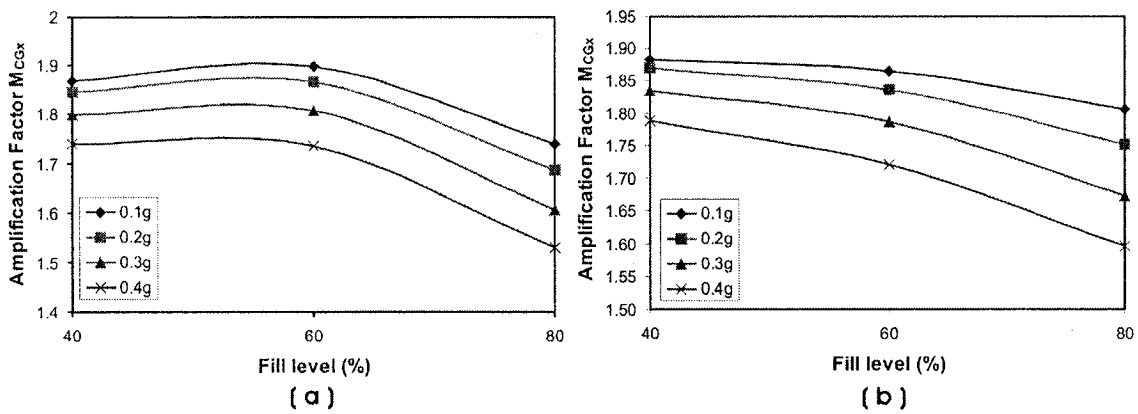

Figure 3.2: Lateral load transfer amplification factor as a function of fill level and excitation magnitude (a) based upon QS response, (b) based upon mean dynamic response

As was mentioned earlier, the amplification factor decreases with an increase in the fill level. It was further revealed that an increase in the magnitude of acceleration results in a decrease in the amplification factor (Figure 3.2(b)). This behavior was further analyzed assuming quasi-static liquid slosh in which the free surface assumes a constant gradient throughout the lateral axis of the tank cross-section, as shown in Figure 3.3. The magnitude of lateral load transfer under higher acceleration is limited due to constraints imposed by the tank walls. This has been illustrated in Figure 3.3 for two different levels of lateral accelerations, a_1 and a_2 ($a_2 > a_1$), assuming the same fill conditions. The higher level of acceleration yields higher lateral shift of the mass center, while the range of oscillation of the mass center in horizontal direction (X axis) is considerably small, when compared to that observed under the lower acceleration (a_1). This results in higher amplification factors for the lower magnitude of acceleration.

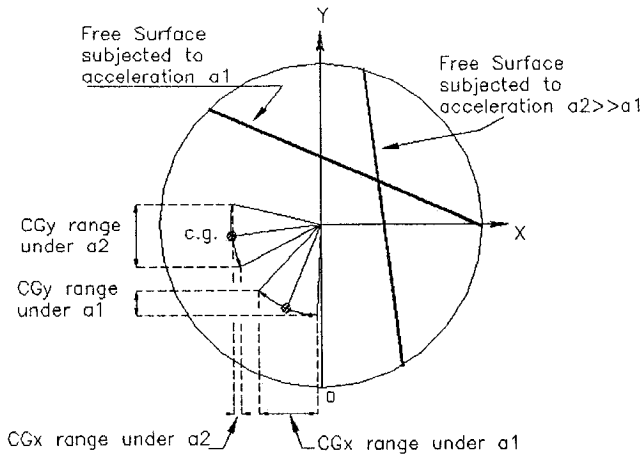

Figure 3.3: Magnitude of oscillation of the mass center as a function of the acceleration intensity

It has been reported that the rollover threshold acceleration limit of a partially filled tank vehicle is further reduced, when subject to an patch-change maneuver [**28**]. The results were obtained by applying a quasi-static slosh model into the vehicle model subjected to a sinusoidal excitation. A few studies have suggested that the frequency of lateral acceleration excitation could considerably affect the dynamic behavior of the liquid in a moving container, specifically when the excitation frequency lies close to the fundamental slosh frequency [**4,18,21**]. It has been suggested that the steering frequencies normally lie around 0.3 Hz and could approach 0.5 Hz under a rapid steering during an emergency type of directional maneuver [**5**]. The higher excitation frequency could lie in the vicinity of the fundamental slosh frequency and lead to resonant fluid oscillations. The effect of excitation frequency on the lateral load shift is thus investigated by applying 0.2 g single cycle sinusoidal lateral acceleration in the 0.2 to 0.8 Hz frequency range.

The transient load shift in a 40% filled tank (fuel oil) subject to a 0.2 g sinusoidal acceleration with frequency of 0.5 Hz is illustrated in Figure 3.4(a). The results show oscillation near 0.5 Hz, even when the lateral acceleration excitation diminishes at $t \geq 2$

s. Figure 3.4(b) illustrates the peak magnitudes of lateral load shift as functions of the excitation frequency and fill ratio. The figure also shows the results attained from the quasi-static analysis, for different fill conditions which are independent of the frequency. The results show considerably higher magnitudes of load transfer, specifically under low fill volumes, when compared to those derived from the quasi-static analysis, irrespective of the frequency of excitation. The peak values of the lateral coordinate occur in the 0.5 to 0.6 Hz for different fill conditions.

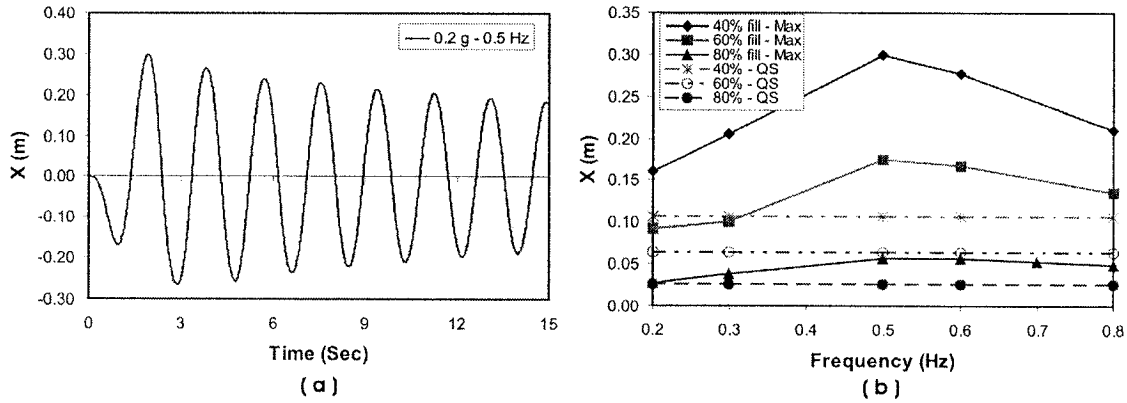

Figure 3.4: (a) Transient lateral load shift in 40% filled tank under 0.2 g sinusoidal acceleration with the frequency of 0.5 Hz. (b) Lateral load transfer as a function of excitation frequency and fill level

It should be noted that the oscillations in the fluid motion would occur near the fundamental slosh frequency when the steering input diminishes. The results show that the peak magnitudes of the lateral coordinates mostly occur in the vicinity of the slosh frequency, which varies with the fill condition. The frequencies corresponding to the peak responses, however, were observed to differ from those reported in earlier studies [**24**]. The Fast Fourier Transform (FFT) technique is further applied to identify predominant spectral component of the time-history of the lateral coordinate of the mass center, after the steering input diminishes. The identical spectral component for a given fill condition is considered to be the fundamental frequency of the fluid slosh in the absence of the

lateral excitation. The results thus attained are compared with those derived from the Budiansky's theory [**18**] as shown in Figure 3.5. Using the Budiansky's formulation, the natural frequencies of the fluid slosh corresponding to 40, 60 and 80% fill levels were estimated as 0.552, 0.608 and 0.722 Hz, respectively. The corresponding frequencies of oscillation of fluid occurring after the steering input has diminished were obtained as 0.537, 0.610 and 0.732 Hz. Figure 3.5 illustrates comparison of the identified slosh frequencies with those derived from the Budiansky's formulation. These results correlated very well with those derived from the Budiansky's formulation. It is evident that the peak magnitudes do not occur precisely near the corresponding slosh frequencies. Considering that the simulations are performed at a few discrete frequencies distant from the identified natural frequencies, the peak load shift response corresponding to 80% fill and excitation frequency of 0.7 Hz was further examined to study the effect of slosh frequency (near 0.722 Hz). The results revealed considerable deformation or separation of the free surface under large magnitudes of oscillations occurring in the vicinity of the resonant frequency, which tend to reduce the peak magnitude of the lateral c.g. coordinate.

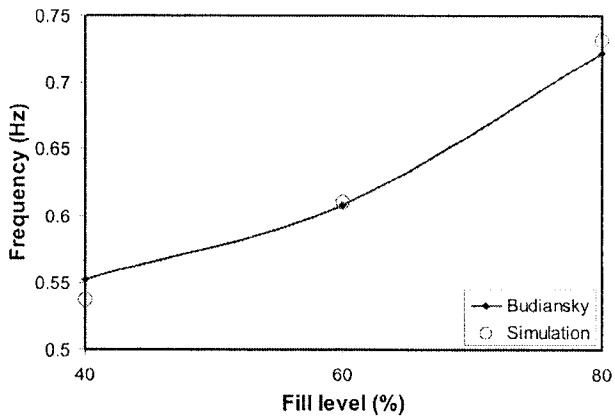

Figure 3.5: Comparisons of observed slosh frequencies from simulation and Budiansky's theory

3.2.2 VERTICAL LOAD SHIFT

The shifts in the vertical coordinate of the *c.g.* are also evaluated for different fill volumes, for both the dynamic and quasi-static slosh models. The results showed only small magnitudes of shifts in the vertical coordinate as well as the oscillations, for all fill levels. The variations in the vertical coordinate of the c.g. under 40% fill condition and 0.4 g ramp-step acceleration is illustrated in Figure 3.6(a). The figure also illustrates the corresponding variations in the lateral coordinate of the mass center. The results show relatively small magnitude of the shift in the vertical coordinate compared to that corresponding to the lateral coordinate. The deviations of the peak responses with respect to corresponding mean responses are presented in terms of amplification factors

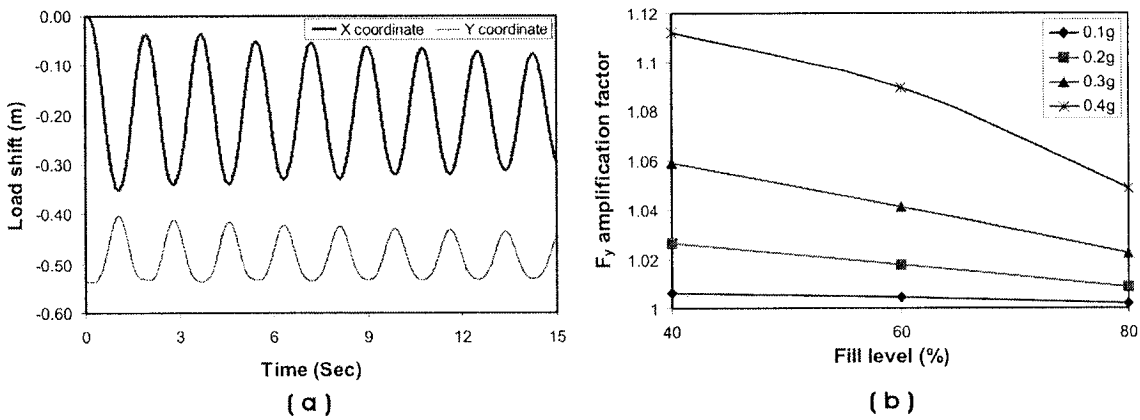

Figure 3.6: (a) Variation in the vertical and lateral coordinates of c.g. under 40% fill and 0.4 g steady acceleration (b) Amplification of vertical load shift with respect to mean values

that represent the peak values normalized with respect to mean response, given by.

$$M_{CGy} = \frac{Max(y)}{\bar{y}} \qquad (3.2)$$

where the $\bar{y}$ is the mean value of the vertical coordinate of the mass center and M_{CGy} is the amplification factor.

The results show monotonic decrease in the vertical cg coordinate as the fill level increases as shown in Figure 3.6(b). An increase in the acceleration magnitude causes the amplification to increase considerably. The amplification factor varies from 1.008 to 1.105 for steady acceleration excitation ranging from 0.1 g to 0.4 g, and it decreases with increasing fill ratio. The mean response values were also compared with those attained from the QS model. The comparison revealed identical responses from both models. It should be noted that the amplification factors for both x and y coordinates approach unity values in the steady-state, which occurs at a elapsed time in the order of a few minutes.

3.3 HORIZONTAL SLOSH FORCE

It has been reported that the magnitude of horizontal force directly increases the roll moment. An increase in the horizontal slosh force thus significantly reduces the overturning threshold of partially filled tank vehicle under a steady acceleration [8]. Owing to the oscillating fluid slosh, the peak magnitude of the horizontal slosh force causes by a lateral acceleration field would be considerably larger than that derived from the static solution used in the above study.

Equation (2.42) is solved to derive the horizontal slosh forces arising from the dynamic fluid motions under different magnitudes of lateral accelerations. Figure 3.7 illustrates, as an example, the time histories of the transient horizontal forces due to fuel oil slosh in a tank with 40% fill condition and subject to 0.1 g and 0.4 g ramp-step lateral accelerations. The figure shows the significant difference between the peak value that occurs at nearly 2 seconds of the flow and the steady-state mean value. Results also

show significant influence of the magnitude of the acceleration on the steady-state mean response as well as the peak magnitude of the response. Further analysis of the results revealed that the fill level considerably affects the deviation of the responses from the corresponding mean values. The range and mean values of the lateral slosh forces under 0.1 g ramp-step excitation are obtained as a function of the fill ratio as illustrated in Figure 3.8(a). The mean values are compared with the corresponding values derived from QS analysis and the results show that these two responses are comparable as shown in Figure 3.8(a). The maximum deviations between the two responses occurred below 2.2% for the 40% fill level, over the range of the acceleration magnitudes considered. The results show that mean and peak magnitudes of the slosh forces increase with increasing fill level, in a nearly linear manner. This increase is mostly attributed to higher mass corresponding the higher fill level.

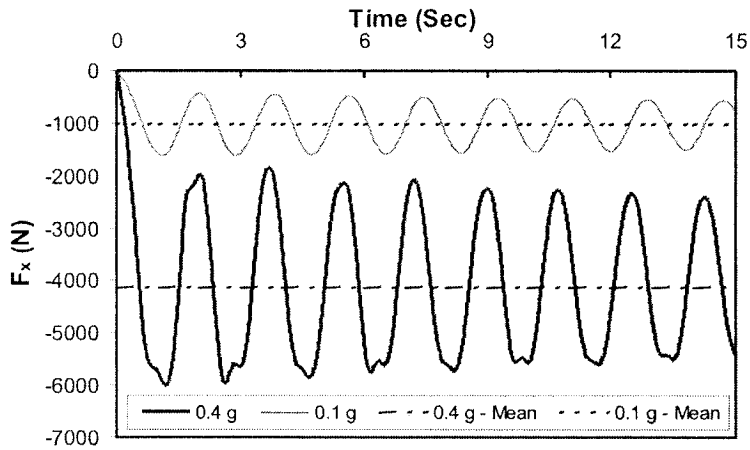

Figure 3.7: Transient horizontal force Fx in 40% fill condition and under 0.1 g and 0.4 g steady lateral accelerations

The peak slosh force is also expressed in terms of the amplification factor with respect to the mean force, representing that estimated from the QS analysis, as a function of the fill ratio and the acceleration magnitude, as shown in Figure 3.8(b). The results suggest that the peak force associated with transient slosh could attain a value 1.6 times greater than

that estimated from the QS solution, corresponding to 40% fill level. This ratio reduces to 1.57 when the dynamic value is normalized with respect to its mean value. The amplification factor approaches a unity value as the fill level increases. It was further revealed that an increase in the magnitude of ramp-step acceleration induced by a more severe maneuver tends to reduce the amplification factor due to the constraints imposed by the tank boundary, as discussed in the previous section. The magnitude of the lateral acceleration excitation strongly affects the projected wetted area, which directly relates to the magnitude of lateral force, as it is evident from EQ (2.42). A lower acceleration level causes more significant variation in the projected area due to fluid oscillations.

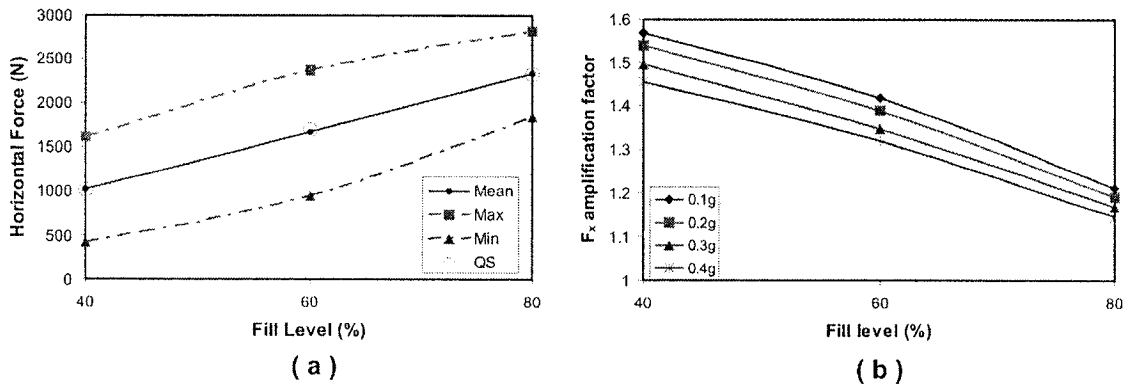

Figure 3.8: (a) Maximum, minimum and mean values of horizontal slosh forces under 0.1 g ramp-step excitation, and (b) slosh force amplification factor as a function of excitation magnitude and fill level.

As evident from the excitation frequency dependence of the lateral load shift, the frequency of acceleration also affects the magnitudes of the lateral slosh force. Figure 3.9 illustrate the variations in the transient lateral slosh forces under ramp-step and the sinusoidal accelerations of 0.2 g magnitude. The comparison between the results reveals that the lateral force attains larger peak values when the liquid is subjected to a sinusoidal acceleration field at a frequency of 0.5 Hz.

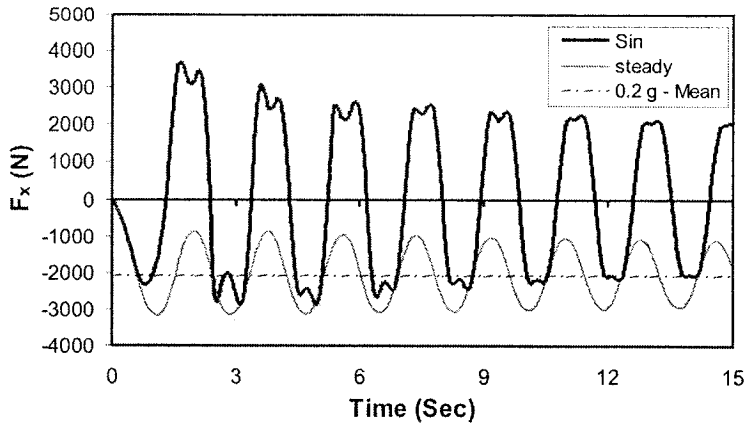

Figure 3.9: The Transient lateral slosh forces (Fx) due to slosh in the tank 40% filled with fuel oil and under 0.2 g ramp-step as well as the sinusoidal acceleration demonstrate the significant effect of excitation frequency (0.5 Hz)

The dynamic horizontal forces are further obtained under application of sinusoidal excitations in the frequency range of 0.2 to 0.8 Hz. The Results revealed that the excitation frequency in the vicinity of the slosh natural frequency yields considerably large peak values, which approach nearly 1.8 times greater than that estimated from the quasi-static model. The results further showed that the peak values occur in the vicinity of the slosh natural frequencies corresponding to each fill level. Figure 3.10(a) compares the solutions obtained from the quasi-state model with corresponding peak forces, derived from the dynamic slosh model under excitations at different frequencies. The influence of frequency of excitation is also presented in terms of amplification factors corresponding to each frequency, as shown in Figure 3.10(b). The results demonstrate that the higher fill levels cause lower amplification factors with their peak values occurring at relatively higher frequencies. As is illustrated in Figure 3.10(b), the amplification factor attains peak value of nearly 1.8 corresponding to the lower fill height of 40%. The results thus suggest that the rollover stability of the vehicle negotiating a path-change maneuver could be even lower than that estimated from a steady turning

maneuver, when the frequency of the maneuver lies in the vicinity of natural frequency of slosh. The results also show that the peak magnitudes occur in the vicinity of 0.5, 0.6 and 0.7 Hz, which are close to the fundamental slosh frequencies corresponding to 40, 60 and 80% fill conditions. The QS slosh force, however, reveals lower magnitudes independent of the excitation frequency, as shown in the figure.

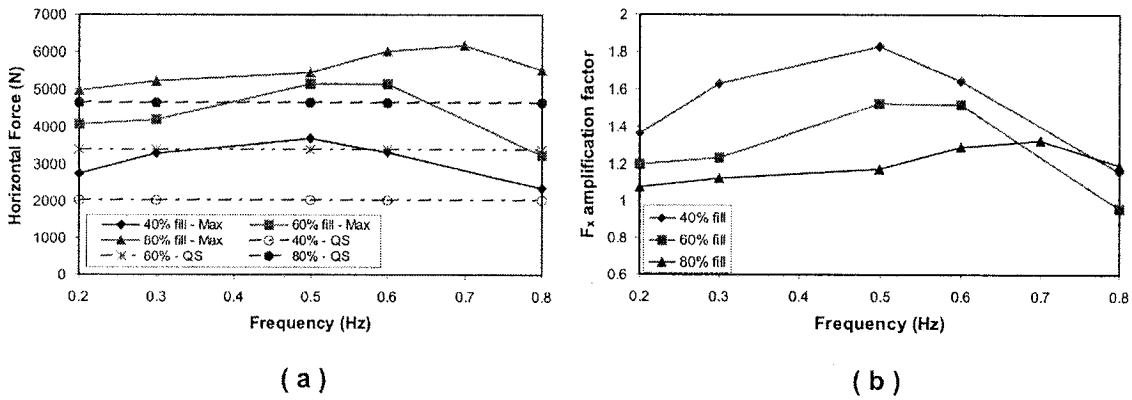

Figure 3.10: Influence of excitation frequency on the peak slosh force responses: (a) peak forces and corresponding QS solutions (b) the amplification factors as a function of the excitation frequency

Figure 3.11 illustrates the range of lateral slosh force under the application of a 0.2 g sinusoidal acceleration at a frequency of 0.5 Hz for 40% fill level. The figure also illustrates the magnitude of horizontal force derived from the QS analysis ($F_x = -mg_x$). It is obvious that the QS slosh force would diminish as soon as the excitation vanishes, while considerable magnitude of force persists due to transient fluid slosh. Moreover, the magnitudes of transient slosh forces are considerably larger than those estimated from the QS model. It can thus be concluded that the transient fluid slosh would impose considerably larger lateral force and thus the roll moment on the vehicle, which will continue even after the completion of the path-change maneuver. The influence of magnitude of lateral acceleration on the slosh frequency was also investigated by analyzing the results corresponding to the lateral slosh force and it was revealed that the

magnitude of lateral acceleration has negligible effect on the slosh natural frequency in the roll plane.

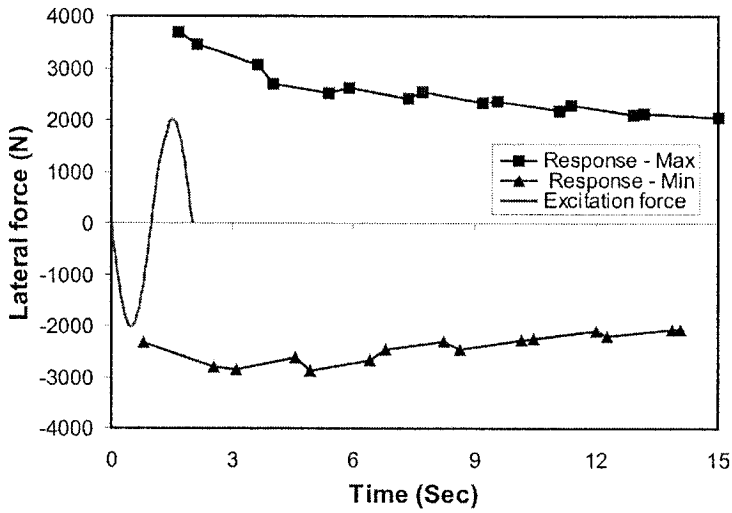

Figure 3.11: The range of transient lateral slosh force due to 40% fill level under 0.5 Hz sinusoidal excitation (0.2 g), and corresponding QS slosh force

3.4 VERTICAL SLOSH FORCE

The liquid sloshing within the tank also yields oscillatory resultant vertical force response. The variations in the vertical force amplification ratio with respect to the mean vertical force ($\approx -mg_y$) under steady acceleration excitations are relatively small as observed for the shift in the vertical mass center coordinate (Figure 3.6), and in Figure 3.12. The results show that a higher excitation yields relatively higher amplification of the vertical force, which decreases with increasing fill ratio. This decreasing trend is attributed to two factors: (i) higher fluid mass corresponding to a higher fill condition; and (ii) lower deviation in the vertical c.g. coordinate under a higher fill condtion. The peak amplification factors occur for 40% fill condition, which range from 1.006 to 1.11 under 0.1 to 0.4 g steady acceleration excitation. The corresponding factors for the 80% filled condition range from 1.002 to 1.05

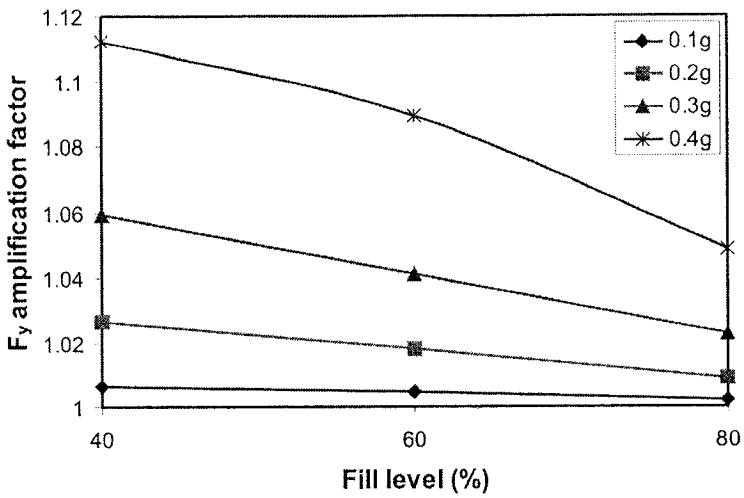

Figure 3.12: Amplification factor of the vertical slosh force as a function of fill ratio and steady acceleration level

3.5 ROLL MOMENT

The static and dynamic roll responses and roll stability limits of heavy vehicles are directly influenced by the net overturning roll moment developed due to lateral acceleration and the lateral displacement of the sprung weights. The vehicle approaches the roll instability, when the overturning moment exceeds the net restoring moment developed by the tires [**26**]. In the case of a partly filled circular tank, the overturning moment due to QS liquid motion is directly related to the horizontal slosh force and the tank radius, as evident from EQ (2.20). The transient roll moment and the corresponding lateral slosh force due to the fuel oil slosh in the 40% filled tank and subject to 0.4 g steady acceleration, is shown in Figure 3.13. This figure shows the proportionality between the lateral force and the corresponding roll moment, together with mean force and moment responses, derived from the QS analysis. It is evident that the peak roll moment is considerably larger than the corresponding mean solution, which could impose higher additional overturning moment on the moving vehicle.

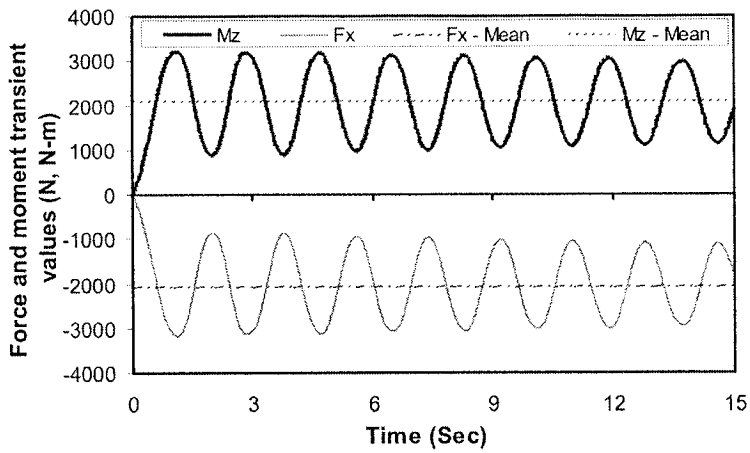

Figure 3.13: Variation in the roll moment and the lateral slosh force (40% fill and 0.2 g steady acceleration).

The roll moment developed due to transient fluid slosh is computed using EQ (2.47). Figure 3.14(a) illustrates the mean, minimum and maximum roll moment developed during transient slosh as a function of the fill height, while subject to a steady 0.1 g lateral acceleration. As observed for the lateral slosh force, the amplitude of deviation of the roll moment from its mean response decreases with an increase in the fill level. The peak values of the moments developed during transient slosh, however, are considerably larger, as shown in the figure, and the peak as well as the mean values increase with the fill volume in a nearly linear manner due to increase in the fluid mass. The dynamic peak values are normalized with respect to the mean response values representing the roll moment amplification factor given by:

$$M_{Mz} = \frac{Max(M_z)}{\overline{M}_z} \qquad (3.3)$$

where $\overline{M}_z$ is the mean roll moment and M_{Mz} is the roll moment amplification factor.

The variations in the roll moment amplification factors as a function of the fill level and magnitude of steady excitation are illustrated in Figure 3.14(b). The moment amplification factor reveals trends similar to those observed for the horizontal force amplification (Figure 3.8). The results show that the roll moment response corresponding to low fill level attains a magnitude 1.60 time greater than that estimated from the QS solution due to the transient fluid slosh, which could lead to relatively lower roll stability limits. An increase in the acceleration magnitude yields relatively lower amplification of the roll moment, as evident in Figure 3.14(b). This trend is identical to that observed from the lateral force amplification in Figure 3.8(b).

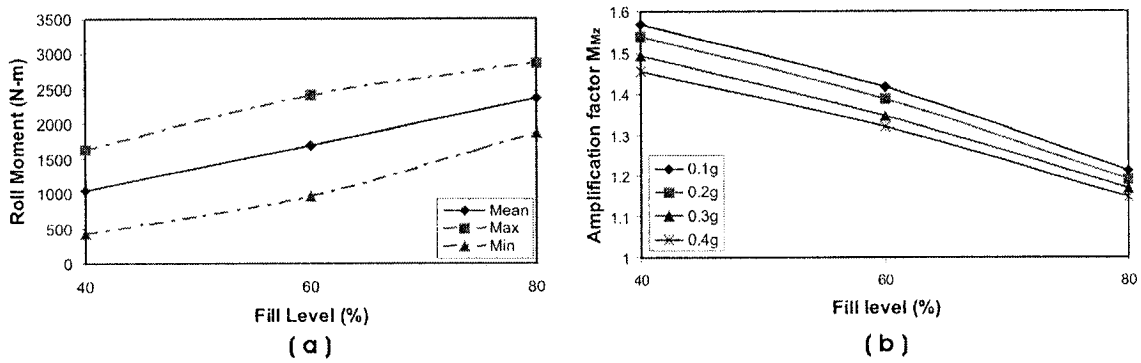

Figure 3.14: (a) Mean and range of roll moment derived from transient fluid slosh under 0.1 g steady excitation; (b) influence of fill level and excitation magnitude on the roll moment amplification

Similar to the lateral slosh force behavior, the peak roll moment due to transient fluid slosh could approach even higher values under application of a rapid directional maneuver, as observed from its variations with the lateral acceleration excitation frequency in Figure 3.15(a). The figure shows comparisons of the QS moment and the peak transient moment as functions of the fill ratio and the frequency of the sinusoidal lateral acceleration of 0.2 g amplitude. Both the peak and static values increase with the fill ratio, as observed for the horizontal slosh force, while the magnitudes of the QS roll

moments are independent of the excitation frequency. The peak moment increases gradually with increasing frequency until the excitation frequency approaches the fundamental slosh frequency. The normalized peak values with respect to the QS solution, or the roll moment amplification factor, are also presented as a function of the excitation frequency in Figure 3.15(b). The results suggest that the peak roll moments produced during the transient fluid slosh could be up to 1.8 times greater than that estimated from the QS model, when the excitation frequency approaches the fundamental slosh frequency. The frequencies corresponding to the peak values correlate well with the reported frequencies particularly for the 40 and 80% fill levels [**18**]. The similarity in behaviors of the horizontal force and the roll moment further corroborates the validity of the EQ (2.20).

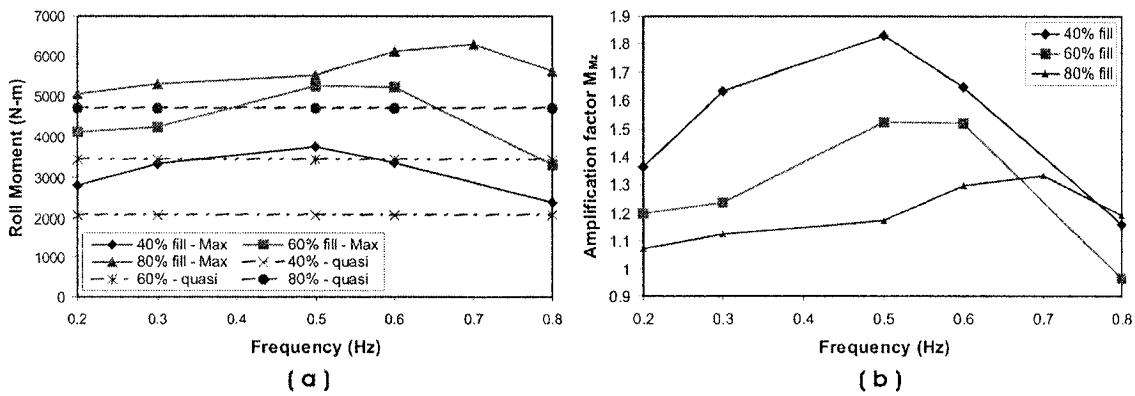

Figure 3.15: Influence of excitation frequency on: (a) the peak roll moment and the corresponding QS solutions; and (b) the roll moment amplification factors.

Figure 3.16 illustrates the peak roll moments (maximum and minimum) as well as the QS solution representing the roll moment due to the single cycle sinusoidal excitation. The results are presented for the 40% fill condition and 0.2 g sinusoidal excitation at a frequency of 0.5 Hz. The results clearly illustrate that the peak roll moment is significantly larger than corresponding QS solution. The figure also shows that the quasi-

static roll moment diminishes as soon as the excitation vanishes, while the transient roll moment persists over a considerably longer duration after the excitation is removed.

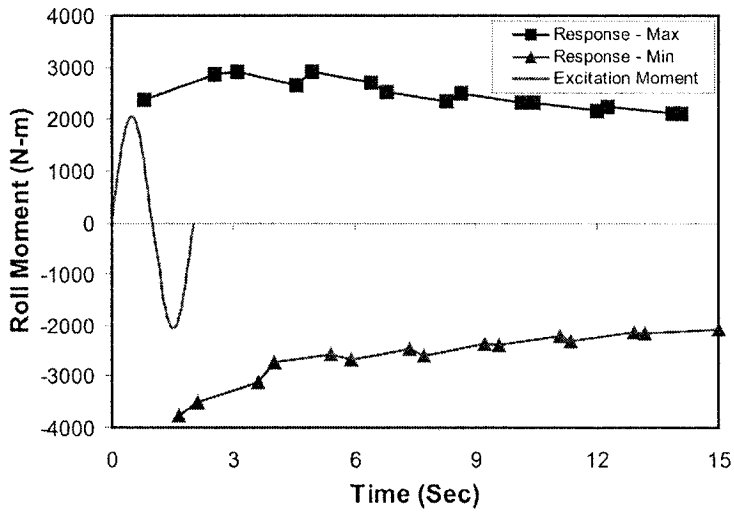

Figure 3.16: Comparison of the range of roll moment due to transient fluid slosh with the QS moment (40% fill; and 0.2 g at 0.5 Hz)

3.6 MASS MOMENT OF INERTIA

The directional response characteristics of a vehicle subject to a steering maneuver is also affected by the mass moments of inertia of the sprung and unsprung weights. In conventional rigid cargo vehicles, the roll, pitch and yaw mass moments of inertia due to the restrained cargo are considered to be constant. In case of the partly filled tank trucks, the fluid cargo undergoes deformation on a continual basis and causes significant variations in the mass moments of inertia about the three orthogonal axes. Such variations in the mass moments of inertia could affect the directional behavior of the vehicle. A few studies have investigated the variations in the mass moments of inertia as functions of the kineto-static fluid motion under pure lateral and longitudinal accelerations and combination of the two [39]. The kineto-static model yields the mean values and does not consider the transient behavior of this measure, as observed for the

slosh forces and roll moment. The dynamic slosh model formulated in the present study can be effectively applied to study the variations in the roll mass moment of inertia of the liquid cargo (I_{zz}), in a partially filled tank with a circular cross-section and subject to time varying lateral accelerations. The instantaneous values of I_{zz} are derived about the geometric center of the tank and the peak values are compared with the corresponding static solution or mean values to evaluate the deviations in the transient response. Instantaneous values of I_{zz} are computed from EQ (2.49). The analyses are performed to evaluate the deviation of the transient values from the static solutions, that may relate to degree of possible error associated with the results from the kineto-static model. Considering that the additional roll moment imposed by the deflected cargo is computed with respect to the tank base, point 'O', the roll mass moment of inertia of the liquid can be further derived about the same point (Figure 3.17).

The mass moment of inertia of the liquid mass particle 'i' with respect to the geometric center of the tank ('C') and tank base ('O') can be expressed as:

$$(I_{zc})_i = m_i r_i^2 \text{; and } (I_{zo})_i = m_i r_i'^2 \qquad (3.4)$$

where $(I_{zc})_i$ and $(I_{zo})_i$ are the roll mass moment of inertia due to mass m_i of cell i about the geometric center and base of the tank, respectively. r_i and r_i' are the corresponding position vectors of the cell i.

The position vector r_i' can be related to the vector r_i as:

$$r_i'^2 = r_i^2 + 2Rr\sin\gamma + R^2 \qquad (3.5)$$

γ is the angle of the position vector r_i from the X axis as shown in Figure 3.17 and R is the tank radius.

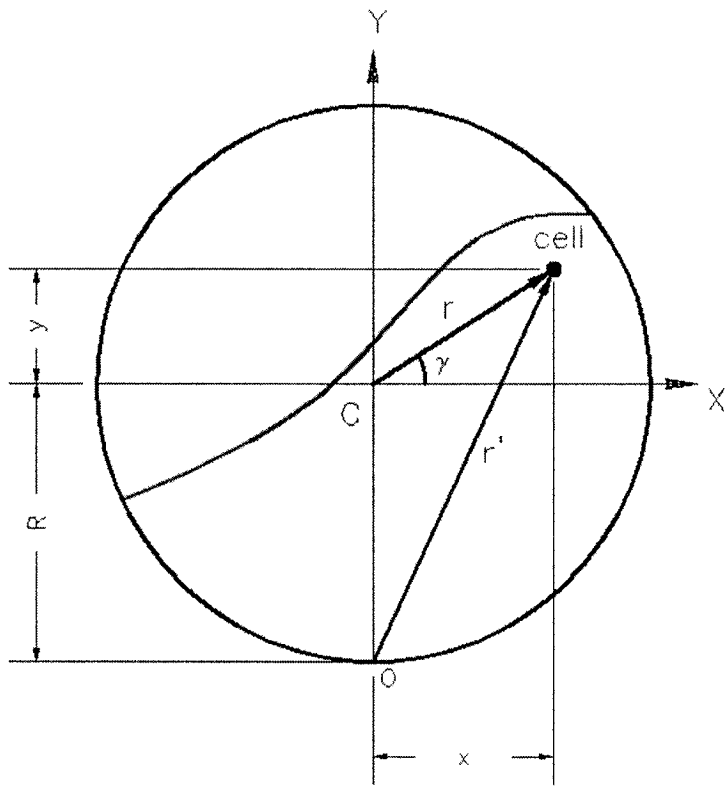

Figure 3.17: Computation of roll mass moment of inertia

Equation (3.4) and (3.5) yield following relationship between the $(I_{zo})_i$ and $(I_{zc})_i$:

$$(I_{zo})_i = (I_{zc})_i + 2m_i R\sin\gamma + m_i R^2 \qquad (3.6)$$

The total roll mass moment of inertia about the tank base can thus be derived as:.

$$(I_{zz})_O = (I_{zz})_C + 2mR\bar{y} + mR^2 \qquad (3.7)$$

where m is the toal mass and $\bar{y}$ is the vertical coordinate of the mass center.

In order to better illustrate the levels of deviations of the instantaneous roll mass moment of inertia from the respective mean values, the peak responses are normalized with respect to corresponding static values expressed in terms of the I_{zz} amplification factors. For the convenience of analysis, the amplification factors are evaluated for $(I_{zz})_c$ only, which would also relect the dynamic variations, such that

$$M_{Izz} = \frac{Max(I_{zz})_c}{(\bar{I}_{zz})_c} \qquad (3.8)$$

where $(\bar{I}_{zz})_c$ is the mean value of the roll mass moment of inertia and M_{Izz} is the corresponding amplification factor.

Figure 3.18 illustrates the roll mass moment of inertia amplification of the liquid cargo as a function of the fill level and the magnitude of the steady lateral acceleration. The results show that the amplification factor increases with an increase in the fill level. The

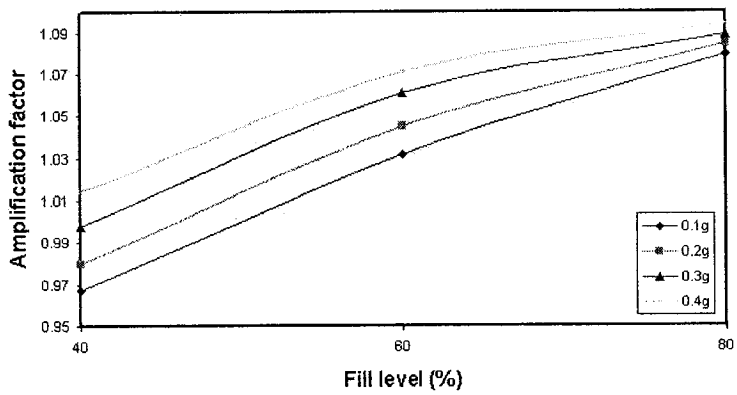

Figure 3.18: Roll mass moment of inertia on the basis of quasi-static values as a function of the fill level and steady acceleration magnitude.

results revealed a difference of up to 7% between the mean values derived from transient solution and the corresponding values derived using quasi-static solution. Therefore the amplification factors are further evaluated with respect to the corresponding mean values and the results are presented in Figure 3.19. The results show the monotonically declining trend of $(I_{zz})_c$ amplification with increase in the fill level, as was expected. The results suggest maximum amplification factor of nearly 1.04 that corresponds to the lower fill level and the higher magnitude of acceleration. From the results, it can be concluded that the deviation in the roll mass moment of inertia from the corresponding mean value is insignificant, irrespective of the fill volume and the magnitude of the steady acceleration. Furthermore, the results reveal that the amplification factor increases with increase in the acceleration and approaches a unity value for the 100% fill condition.

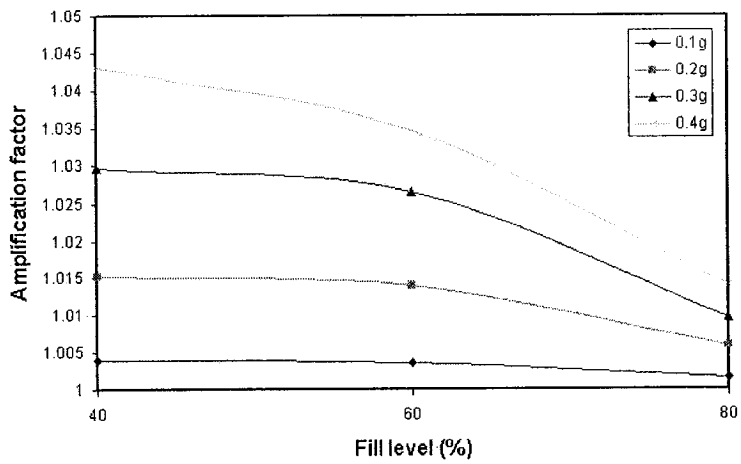

Figure 3.19: Roll mass moment of inertia amplification factor with respect to its mean value.

3.7 CENTER OF PRESSURE

The quasi-static liquid slosh model has been widely employed to analyze the effect of liquid motion on the dynamics of partially filled tank vehicles [**9**,**28**]. These studies

assume that the resultant forces act on the center of gravity of the liquid cargo (c.g.), while the analyses seem to correlate well with the mean dynamic responses. Considering that the slosh forces on the tank structure arise from the dynamic pressure distribution on the tank wall, the center of pressure may more appropriately define the coordinates at which the resultant forces act. The results obtained from analyses and experiments, considering the tank vehicle dynamics, were found comparable with those derived from the kineto-static model, which implies that the resultant forces applied at the mass center would be acceptable. In the present study, the coordinates of the center of pressure are evaluated instead of the c.g. coordinates to study the variation in the load shift. The instantaneous coordinates of the center of pressure are derived from the simulation results and are compared to corresponding c.g. coordinates. The coordinates of the center of pressure are obtained from the moment integrations over the wetted area of the tank wall, expressed as:

$$x_{CP} = \frac{\sum_{c}^{liquid} x_c F_{yc}}{\sum_{c}^{liquid} F_{yc}}, \; y_{CP} = \frac{\sum_{c}^{liquid} y_c F_{xc}}{\sum_{c}^{liquid} F_{xc}} \qquad (3.9)$$

where x_{CP} and y_{CP} are the coordinates of the centroid of a cell 'c' the tank wall; and F_{xc} and F_{yc} are the components of the forces acting on the centroid of the face of the cell 'c'.

Figure 3.20 illustrates the mean and ranges of the lateral (X) coordinates of the center of pressure of the fluid within partly filled tank as a function of the fill level. The results are evaluated for 40% fill condition and tank being exposed to 0.1 g ramp-step lateral acceleration. The results show that the mean value of the center of pressure (CP)

coordinates are nearly identical to the respective c.g. coordinates. The ranges of the CP coordinates, however, differ considerably from the ranges of the corresponding c.g. coordinates. The deviations of the CP lateral coordinate with respect to the mean values are also presented in terms of the amplification factors in Figure 3.21 as functions of the fill level and the magnitude of acceleration. The results suggest that the rate at which the amplification factors of CP converge to a unit value is higher than that observed for the corresponding c.g. coordinate. The results also show that the amplification factor is not significantly influenced by the magnitude of lateral acceleration, although some effects are evident, specifically high acceleration level (0.4 g).

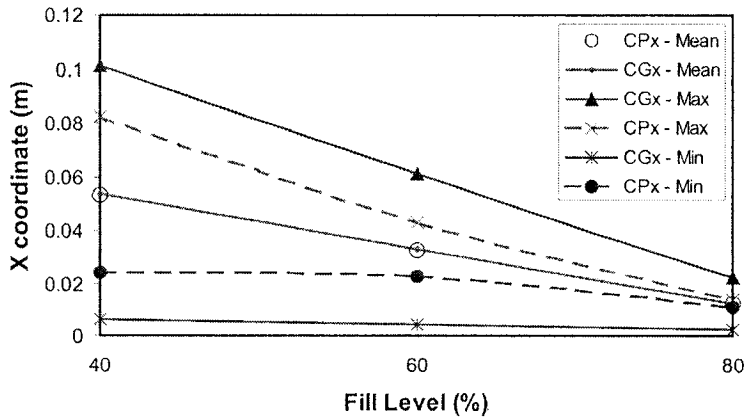

Figure 3.20: Minimum, maximum and mean magnitudes of the lateral coordinates of the center of pressure (CP) and the c.g.

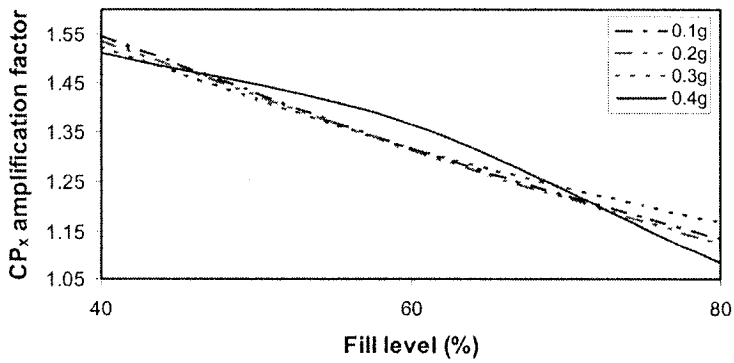

Figure 3.21: Amplification factor of the lateral coordinate of the center of pressure (CP) with respect to the corresponding mean values.

3.8 EFFECT OF DENSITY AND VISCOSITY

The results presented in the previous sections describe the slosh forces and roll moment developed due to transient slosh of a medium-viscous fluid (fuel oil, μ =0.0867 kg/ms). The influence of fluid viscosity and density on the lateral load shift and the resulting roll moment was investigated by considering two additional fluids with lower (sulfuric acid, μ =0.0255 kg/ms) and higher viscosity (castor oil, μ =0.98 kg/ms). Owing to the weight and dimensional regulations, the variation in the weight density is the primary cause of partial fill situations in the bulk transportation of liquid products. The variations in weight density of the liquid cargo would directly affect the magnitudes of horizontal slosh forces, and thus the overturning moment. The influence of variations in the fluid density on the resulting overturning moment is investigated by considering a constant fill ratio, while varying the fluid density of the cargo, which results in considerably different fluid masses. The analyses are performed for the fuel oil, castor oil and sulfuric acid, while the fill ratio is limited to 40%. The weight densities for this analysis are taken as 850, 980 and 1826 kg/m^3, respectively. It should be noted that all 3-simulation cases would yield identical *cg* height, while the total cargo weight would vary with the fluid density. The total weights per unit length of the respective cargoes under 40% fill condition were obtained as 10.28, 11.86 and 22.10 *kN/m*.

The mean and peak roll moments attained from the transient slosh analyses of the three products are compared in Figure 3.22, under a 0.1 g ramp-step lateral acceleration. The results suggest significant effect of the fluid density on the overturning moment, which would be attributed to the corresponding cargo weight. The heavier sulfuric acid yields considerably larger moment due to its high density. A heavier product not only creates a

partial-fill situation but also yields relatively higher roll moments due to transient fluid slosh, although it would yield lower *c.g.* height.

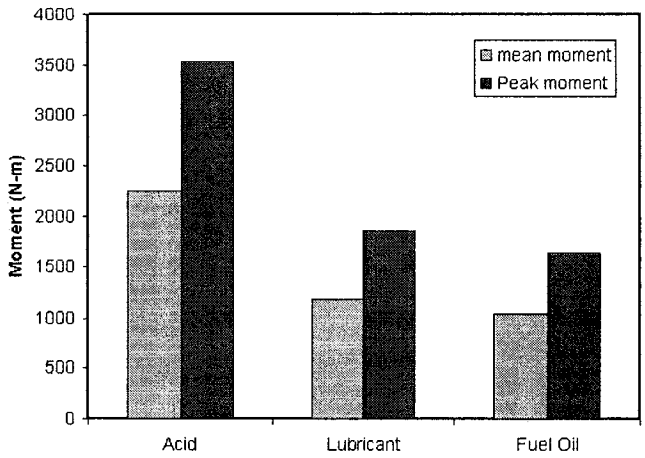

Figure 3.22: Effect of fluid density on the peak roll moment.

The simulations were performed to derive the mean and peak values of dynamic load shift, horizontal slosh force and the roll moment, while the viscous shear force was also computed using EQ's(2.45) and (2.48). The results revealed almost negligible effect of the fluid viscosity for the range of viscosity considered in this study. The proportion of the viscous horizontal force due to viscous castor oil was in the order of 3.3% of the total horizontal slosh force under 40% fill condition and 0.4g ramp-step lateral acceleration excitation. This proportion was observed to be even smaller under lower levels of excitation. It may thus be concluded that the viscous forces developed due to viscous fluids may be neglected from the fluid slosh analyses for the range of viscosity considered in this study. The fluid viscosity, however, affects the rate of decay of fluid slosh in a significant manner, as evident from Figure 3.23. The figure illustrates the peak magnitudes of the oscillations of the horizontal slosh force normalized with respect to the mean values, due to three different fluids corresponding to 40% fill volume and 0.1 g

ramp-step acceleration excitation. The peak force response of the more viscous castor oil tends to decay at a higher rate than the less viscous fuel oil. It should be noted that the three fluids yield considerably different values of the peak force due to constant fill ratio and differences in their mass density. Moreover the small differences among the initial peak values, as illustrated in Figure 3.23, may also be attributed to the viscosity effect. As evident from the figure, the largest peak value corresponds to the fluid with the lowest viscosity.

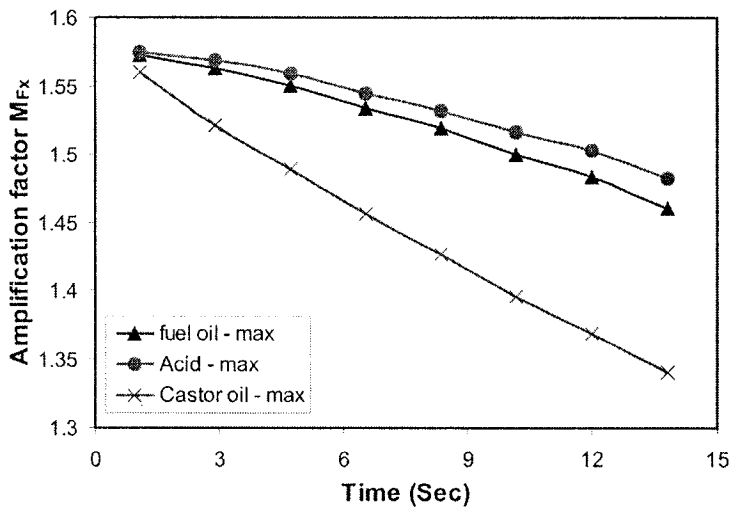

Figure 3.23: Influence of fluid viscosity on the peak slosh force (40% fill and 0.1 g acceleration).

3.9 SUMMARY

Dynamic liquid slosh in a partially filled tank under time varying accelerations was analyzed and dynamic responses were evaluated in terms of cargo displacement, forces and the roll moment. The results revealed that the mean responses derived from the transient flow analyses compare very well with those derived from the simple QS analysis. Only small deviations between the mean dynamic and QS responses could be observed, when considerable deformation or separation of the free surface occurred

under either a large acceleration excitation or low fill ratio. From the results attained in this study, it is concluded that the QS model offers an effective and efficient basis for estimating the mean dynamic load shift and the overturning moment. The response amplification factors were defined using quasi-static as well as mean response values and the effect of different parameters on the dynamic peak responses were investigated. The results revealed considerably higher magnitudes of transient values, when compared to the static solutions or the mean values. The magnitude of all response values invariably decreased with an increase in the fill level due to constraints imposed by the tank wall. An increase in the magnitude of lateral acceleration resulted in lower amplification of the lateral load shift, lateral slosh force and the roll moment. Higher magnitudes of acceleration, however, caused larger peak vertical load shift and the vertical force, while the variations in both these measures were observed to be relatively small. The influence of the excitation frequency on dynamic response values were also investigated in terms of the lateral c.g. shift, lateral force as well as the roll moment and the results revealed that these values are significantly influenced by the excitation frequency. It was demonstrated that a directional maneuver, idealized by a sinusoidal acceleration, can cause considerably larger response values when the excitation frequency is in the vicinity of the liquid slosh natural frequency. It was also observed that the maximum lateral shift of the c.g. due to a sinusoidal acceleration does not correspond with the slosh frequency, which was attributed to the large amplitude of the free surface deformation. The effect of viscosity on the response characteristics of the liquid was also investigated. The results suggested that the viscous forces due to a viscous flow are insignificant for the range of viscosity considered in this investigation. The results suggest that an increase in the density of cargo considerably increases the lateral force as well as the roll moment due to increased cargo weight. The results also

showed that the influence of magnitude of lateral acceleration on the liquid slosh natural frequency is negligible. The results also revealed that the ranges of the CP coordinates differ considerably from those of the c.g. However, the results show that the corresponding mean values are nearly identical.

CHAPTER 4

Three-Dimensional Transient Fluid Slosh

4.1 INTRODUCTION

Heavy vehicles including tank trucks are frequently subjected to simultaneous braking accelerations and steering maneuvers, resulting in simultaneous application of lateral and longitudinal forces imposed on the cargo. The fluid within a partly filled tank truck thus undergoes dynamic motion in both the pitch and roll planes. The reported studies on the fluid flow analyses in moving containers, and the influence of fluid motion on the directional dynamics of the vehicle, however, have been limited to in-plane analyses [10,11,17]. A three-dimensional kineto-static fluid flow model of a partly-filled tank subject to lateral and longitudinal acceleration fields has been reported in a recent study [32,38]. The model has been applied to demonstrate the influence of acceleration fields on the free surface motion, cargo c.g. coordinates, variations in mass moments of inertia of the liquid cargo, and the directional dynamics characteristics of a vehicle combination. The proposed kineto-static model, however, cannot be applied to study the forces and moments caused by dynamic fluid slosh and the role of baffles and separating walls.

From the review of reported studies, presented in chapter 1, it is evident that the dynamic slosh forces and moments arising from the three dimensional fluid slosh inside a partly filled tank under simultaneous lateral and longitudinal accelerations have not yet been investigated. The analysis of fluid slosh in a three dimensional domain has been severely limited mostly due to the complexities associated with the solution of the three dimensional flow problem. Amongst the contributions devoted to this issue, only a few have considered the liquid slosh analysis in a moving container, where a few response

characteristics were derived through a tedious computational process [**4**,**13**]. Furthermore, the slosh resistance offered by baffles in a circular cylindrical tank under application of longitudinal and lateral acceleration fields has not been investigated.

In the present study, the governing equations of fluid flow in the three-dimensional domain, presented in section 2.5, are solved under simultaneous lateral and longitudinal acceleration fields, using the FLUENT software. Influence of different parameters, such as magnitude of accelerations, fill condition and baffles, on the dynamic response characteristics of liquid slosh in a three-dimensional space have been investigated. The resulting pressure distributions are analyzed to derive the transient and steady-state slosh forces and moments.

4.2 RESPONSE ANALYSIS UNDER A LATERAL ACCELERATION FIELD

The Navier-Stoke's equations of fluid flow in the three-dimensional domain are initially solved under the application of a time-varying lateral acceleration field. The results attained are compared with those derived from the two-dimensional analyses, presented in chapter 3. A uniform lateral acceleration field is thus introduced simultaneously over the liquid domain [**9**,**28**,**14**]. Both the quasi-static and the dynamic slosh models in the roll plane have been developed based on this assumption. The validity of three-dimensional model is also verified by comparing the results in terms of the mean lateral force with that attained from the planar dynamic liquid slosh model under identical lateral acceleration and fill condition. This preliminary analysis is performed by considering a clean bore cylindrical tank containing fuel oil with 60% fill height and subject to ramp-step lateral acceleration of 0.4 g. The mean lateral force obtained from the three-dimensional fluid slosh analysis is normalized with respect to tank's equivalent length in order to obtain the average slosh force per unit length, as derived from the two-

dimensional analysis. For the candidate tank, with total tank volume of 23.599 m^3 and cross section area of 3.243 m^2, the three-dimensional analysis of the 60% filled condition resulted in mean lateral force per unit length of 6.724 kN/m. This compares very well with the corresponding mean lateral force of 6.713 kN/m, derived from the two-dimensional analysis. The quasi-static model, on the other hand, resulted in the lateral force magnitude of 6.776 kN/m under identical simulation conditions.

The results thus provide a verification of the three-dimensional analysis with respect to the mean lateral slosh force. The dynamic lateral slosh force responses of the three-dimensional model are further evaluated to derive the lateral force amplification factor, the ratio of the peak lateral force to the mean force. The results revealed that the resulting lateral force amplification factor of 1.297 agrees reasonably well with a factor of 1.307, derived from the planar model under 0.4 g ramp-step acceleration and 60% filled condition. The two- and three-dimensional responses suggest that the two-dimensional analyses would be adequate, when the lateral acceleration excitation alone is concerned or when the roll stability of the vehicle is the primary focus. Moreover, the reasonably good agreements in the results are considered to provide the credibility for the three-dimensional analyses performed in the study for clean bore as well as baffled tanks.

4.3 RESPONSE ANALYSIS UNDER A LONGITUDINAL ACCELERATION FIELD

It has been reported that the fill level and the magnitude of the acceleration influence the braking performance of the vehicle most significantly, due to the fluid motion in the pitch plane of the moving container [**10,11,39**]. Using the kineto-static analysis of the fluid motion, a few studies have shown that the distribution of loads on different axles of a partly-filled tank vehicle, subject to a deceleration, varies considerably due to fluid motion in the pitch plane and could thus yield poor stopping distance performance and

braking efficiency [**10,11**]. The dynamic fluid slosh caused by the time-varying deceleration could cause considerably larger peak variations in the axle loads, slosh forces and mass moment of inertia of the fluid, which may further deteriorate the transient braking performance of the vehicle. The analyses are thus performed to study the variations in peak longitudinal force, pitch moment, mass moments of inertia, under different magnitudes of longitudinal deceleration. The results are presented and discussed in the following sections.

4.3.1 SLOSH FORCES

The three-dimensional dynamic slosh model of fluid within a partly-filled clean bore cylindrical tank is solved under two different constant magnitudes of longitudinal deceleration (0.3 g and 0.6 g) and two different fill conditions (40% and 60%). The resulting pressure distributions near the tank periphery are analyzed to evaluate the resultant slosh forces along the vertical (F_y) and longitudinal (F_z) axes of the tank. The results further revealed that the mean forces correspond well with those derived from the quasi-static analyses, as observed from the two-dimensional fluid slosh analysis in the roll plane. The peak forces caused by dynamic fluid slosh are normalized with respect to the corresponding static solutions to derive the force amplification factors, which could describe the role of dynamic fluid slosh more appropriately.

For the partly filled clean bore tank subject to pure braking acceleration, the vertical and longitudinal force amplification factors are computed from:

$$M_{Fy} = \frac{Max(F_y)}{\bar{F}_y} \text{ and } M_{Fz} = \frac{Max(F_z)}{\bar{F}_z} \qquad (4.1)$$

where $\overline{F}_y$ and $\overline{F}_z$ are the mean vertical and longitudinal forces derived from the static solutions, and M_{Fy} and M_{Fz} are the vertical and longitudinal force amplification factors.

Figure 4.1(a) and (b) illustrate the $\overline{F}_z$ and $\overline{F}_y$ amplification factors, respectively, corresponding to the selected fill levels and deceleration magnitudes. The results show that an increase in the fill level reduces the response amplification and thus the peak forces along the longitudinal as well as vertical axes. These results suggest proportionally larger load shift in the pitch plane for the lower fill condition. An increase in the acceleration level causes an increase in the amplification factor, which is also attributed to higher liquid load shift in the pitch plane. As evident in Figure 4.1(a), the peak longitudinal force attains a magnitude of nearly two times greater than its corresponding mean force or the force derived from static solution under the lower fill condition (40%), which could adversely affect the braking performance of the vehicle under lower fill level and higher acceleration. Increasing the fill volume tends to limit the magnitude of fluid slosh through the constraints imposed by the container wall. The amplification of the longitudinal force, M_{Fz}, under a 0.6 g deceleration reduces from 1.96 to nearly 1.77, when the fill height increases from 0.4 to 0.6 of the tank diameter. The results suggest relatively small deviations in the vertical forces with the magnitude of acceleration and fill condition. The factor M_{Fy} approaches a peak value of 1.12 for the lower fill condition (40%) and higher longitudinal acceleration (0.6 g), considered in this study. The results show that the vertical force amplification reduces with an increase in the fill level and a decrease in the acceleration magnitude, as observed for the longitudinal force amplification.

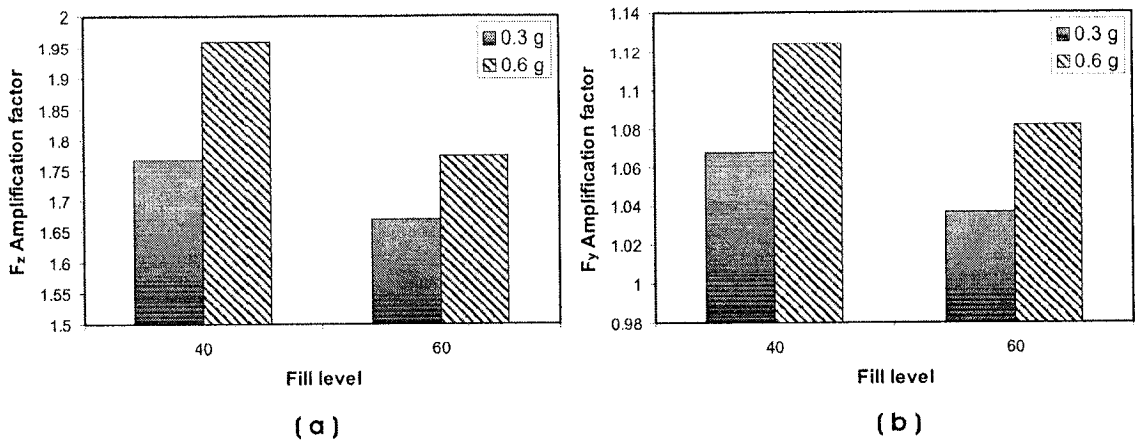

Figure 4.1: Influence of fill level and magnitude of acceleration on (a) Longitudinal and (b) vertical forces

4.3.2 PITCH MOMENT

Pressure distributions attained under different magnitudes of deceleration are applied, using EQ (2.17), to compute the pitch moment about the point 'O' at the middle of the tank bottom, as illustrated in Figure 4.2. The oscillatory pitch moment due to fluid slosh is expressed in terms of peak value of the normalized moment, referred to as the pitch moment amplification factor, given by

$$M_{Mx} = \frac{Max(M_x)}{\overline{M}_x} \qquad (4.2)$$

where $\overline{M}_x$ is the mean pitch moment and M_{Mx} is the pitch moment amplification factor.

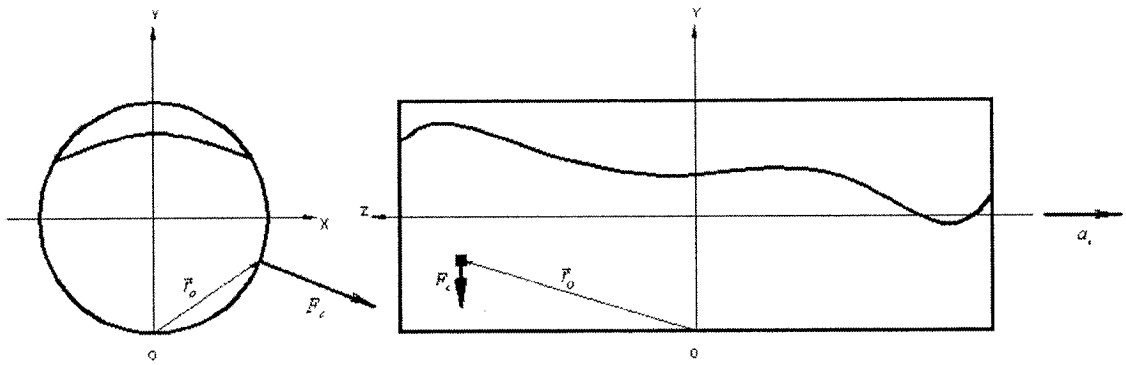

Figure 4.2: Computation of the pitch moment from the distributed pressure on the tank wall.

Figure 4.3 illustrates the pitch moment amplification factor due to dynamic slosh of the partly-filled tank for 40% and 60% fill condition, and constant deceleration magnitudes of 0.4 g and 0.6 g. The results show a peak value of the pitch moment amplification of nearly 1.2, suggesting that the peak moment could approach 1.2 times the corresponding mean value under 40% fill condition and 0.3 g braking acceleration. The normalized peak pitch moment tends to decrease with increase in the fill volume, as observed from the peak slosh forces. The moment amplification factor, unlike the peak longitudinal force, tends to decrease with increase in the deceleration magnitude.

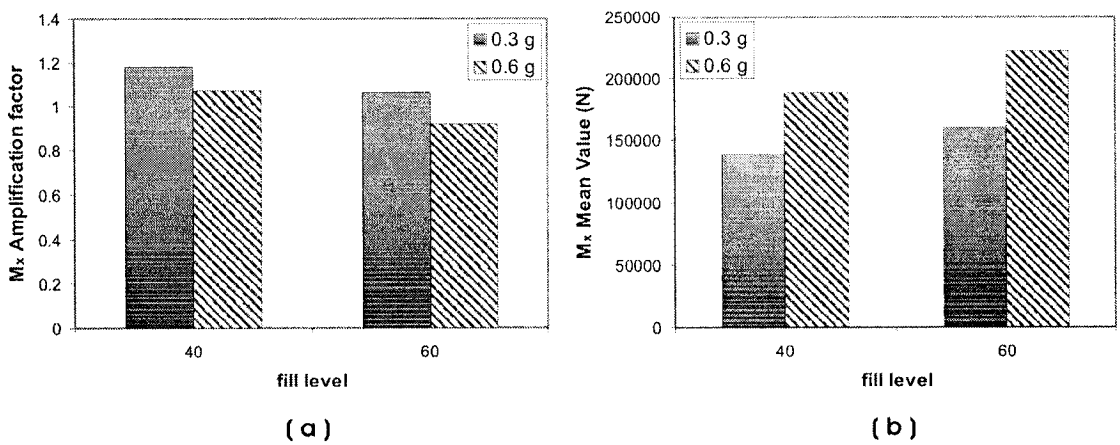

Figure 4.3: Effect of fill level and magnitude of acceleration on (a) the pitch moment amplification factor and (b) its mean value.

The relatively lower amplification of the pitch moment, in the presence of a large deceleration or longitudinal force amplification is mostly attributed to higher mean moment, as shown in Figure 4.3(b). It should be noted that the integration of the infinitesimal pitch moments over the wetted area at each instance of the time provides the transient pitch moment due to dynamic liquid slosh, as described in section 2.5.1, (Figure 4.2), which may also be expressed in the form of following equation:

$$M_x = \sum_{c}^{wet\ area} \vec{r}_o \bullet \vec{F}_C \qquad (4.3)$$

where the M_x is the pitch moment about the point 'O', as shown in Figure 4.2, $\vec{r}_o$ is the position vector introducing the distance of cell 'c' with respect to 'O' in the pitch plane, and $\vec{F}_C$ is the total force acting on cell 'c' in the pitch plane. Both the position vector and the force vector, contribute to the pitch moment. The transient pitch moment is thus a function of the behavior of the force components, and the vertical and longitudinal coordinates of the fluid cell. Figure 4.4. illustrates the magnitudes and phase relationships between the vertical and longitudinal forces and c.g. coordinates under 0.3 g and 0.6 g deceleration and 40% fill condition. The simulation results corresponding to 0.3 g acceleration indicate that, at the peak, the pitch moment does not correspond with the occurrences of peak vertical and longitudinal forces, as shown in Figure 4.4(a). On the other hand, the peak moment occurs when the c.g. coordinates approach close to their maximum values, as illustrated in Figure 4.4(c). The results thus suggest that the peak pitch moment is strongly influenced by the instantaneous coordinates of the cargo c.g. The results further show that the longitudinal c.g. coordinate is considerably larger under an acceleration field, which increases with increase in the longitudinal acceleration. The analysis of results suggests that the amplification of the longitudinal

c.g. coordinate with respect to the mean value decreases considerably, when the acceleration is increased to 0.6 g.

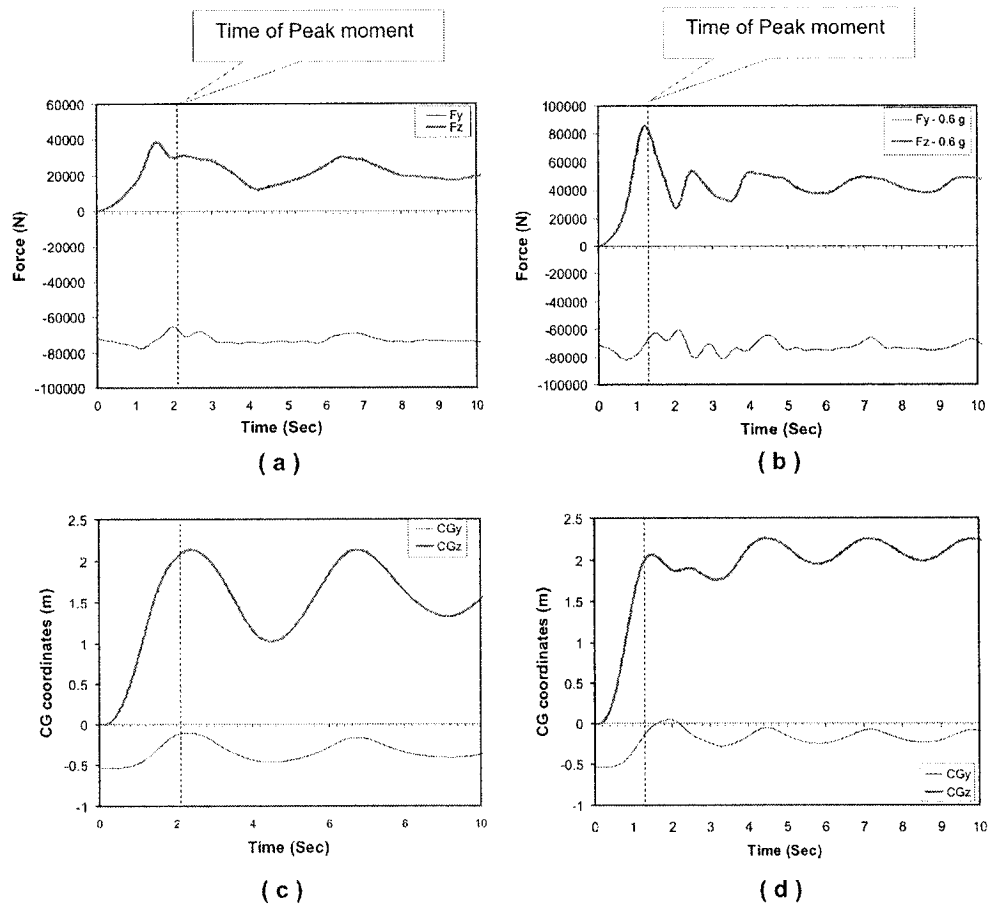

Figure 4.4: Variations in the longitudinal and vertical forces and c.g. coordinates of the 40% filled tank subject to longitudinal acceleration: (a), (c) 0.3 g and (b), (d) 0.6 g.

The peak pitch moment tends to correspond closely with the peak longitudinal force, specifically under 0.6 g deceleration, as seen in Figure 4.4(c). This would imply peak longitudinal force and the peak load shift towards the front axles would occur at the same time, which could significantly alter the distribution of braking forces developed at the different axles. The oscillating response of the c.g. coordinates show that the

fundamental frequency of longitudinal slosh under 0.3 g deceleration is 0.23 Hz, which increases to nearly 0.35 Hz under 0.6 g deceleration.

4.3.3 PITCH MASS MOMENT OF INERTIA

The directional dynamic responses of a freight vehicle are also influenced by the mass moment of inertia of the cargo, which are invariably considered to be time invariant. The mass moments of inertia of the floating cargo within a partly-filled tank, however vary considerably and would strongly affect the steering and braking responses [**1**,**39**]. The application of a pure longitudinal acceleration would not only alter the pitch mass moment of inertia (I_{xx}), but also the roll and yaw mass moments of inertia (I_{zz} and I_{yy}). In the present study, the transient pitch mass moment of inertia of the liquid cargo about the geometrical center of a cylindrical tank in a partial fill condition, when subject to pure longitudinal deceleration, is analyzed considering the fuel oil as the liquid with constant density. The effects of fill condition and the magnitudes of acceleration on the response amplification are also investigated. Deviations of the I_{xx} with respect to its mean values due to oscillatory liquid slosh behavior is presented in terms of peak response values normalized with respect to the mean value, given by:

$$M_{I_{xx}} = \frac{Max(I_{xx})}{\bar{I}_{xx}} \qquad (4.4)$$

where $\bar{I}_{xx}$ is the mean pitch mass moment of inertia and $M_{I_{xx}}$ is the amplification factor.

The peak pitch mass moment of inertia amplification factor appears near 1.18 corresponding to 40% fill condition and 0.3 g braking acceleration, as shown in Figure 4.5(a). The amplification factor tends to vary in a nonlinear manner with increasing fill volume and longitudinal deceleration. For the 40% fill condition, the mean value

of I_{xx} increases with increasing deceleration, but the trend is opposite for the 60% fill condition, as illustrated in Figure 4.5(b). Such trends have also been reported in a study on the braking dynamics characteristic of a tank vehicle [**39**]. On the other hand, the results corresponding to both 0.3 g and 0.6 g longitudinal accelerations suggest small differences between the peak pitch mass moments of inertia for the same fill conditions with the lower values corresponding to the higher magnitude of acceleration. The occurrence of lower peak values at higher accelerations may be attributed to highly nonlinear free surface deformation and flow separation that occurs during the transient liquid motion, which was also observed during the visualization of the flow. The lower fill level thus yields considerably lower amplification factor under higher acceleration, while a higher fill level causes higher amplification of I_{xx} under the same increase in acceleration.

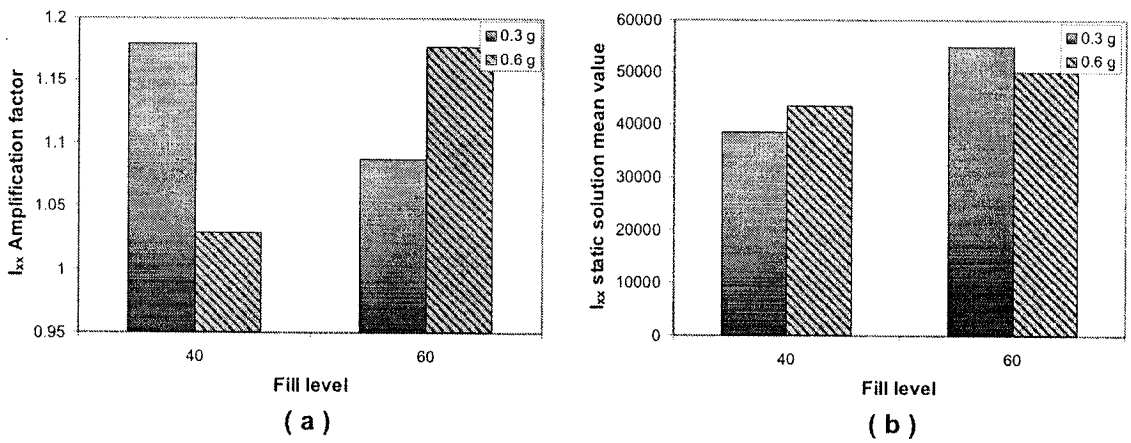

Figure 4.5: Influence of fill level and magnitude of acceleration on (a) amplification factor of the pitch mass moment of inertia and (b) the static solution mean values

4.3.4 INFLUENCE OF BAFFLES

The transient fluid slosh and its adverse effect on the response characteristics of moving containers have encouraged use of antislosh devices. Lateral baffles are frequently

employed to limit the longitudinal fluid slosh under braking and acceleration maneuvers. A few studies have investigated the effectiveness of different designs of baffles to eliminate or diminish the oscillatory behavior of the liquid slosh in the containers subjected to acceleration [**4,51**]. The majority of studies have explored the role of baffles and separating wall via experimental measurements, only a few studies have attemped to develop and analyze analytical models to demonstrate the effectiveness of lateral baffles [**2,19**]. The effects of separating walls on the dynamic load shifts in either the roll and on the pitch planes have been investigated using the kineto-static analyses [**10,39**]. In the present study, the transient liquid slosh behavior in a partially filled tank with and without baffles has been analyzed, when the tank is subjected to a longitudinal acceleration. A three-dimensional model of the liquid slosh in a cylindrical tank equipped with three single-nozzle baffles with configurations reflected in section 2.7.1, has been solved and the simulation results are analyzed to evaluate the effect of baffles on the liquid slosh in terms of vertical (F_y) and longitudinal (F_z) forces, the pitch moment (M_x) about the point 'O' (Figure 4.2), as well as the pitch mass moment of inertia (I_{xx}) about the X axis through the geometric center of the clean bore tank. The simulations were performed for a duration of forty seconds, and the steady-state response values, obtained from the transient responses are compared to the static solutions corresponding to a clean bore tank under identical conditions to evaluate the effects of baffles. The transient results are normalized with respect to corresponding static solution to characterize the amplification factors, expressed in EQ's (4.1), (4.2) and (4.4).

Figure 4.6 illustrates the transient pitch moment caused by the fluid movement within the baffled tank with 60% fill condition and exposed to 0.6 g longitudinal acceleration. The results show that the baffles effectively attenuate the flow oscillation preventing the pitch

moment to attain values larger than corresponding values derived from the quasi-static solution (QS). It should be noted that the QS solution is attained for the clean bore tank. On the other hand the baffles impose a considerable delay for the pitch moment to attain its steady value. The results further reveal that the response oscillations are damped significantly, when compared to the oscillatory response observed for the unbaffled tank.

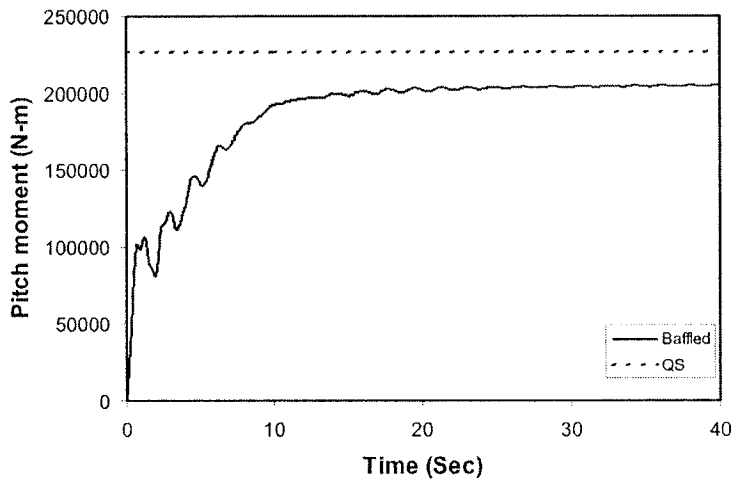

Figure 4.6: Comparison between transient pitch moment and corresponding quasi-static (QS) solution of a clean bore tank. (60% fill level and -0.6 g longitudinal acceleration)

The effects of fill level and magnitude of acceleration on transient longitudinal force (F_z) due to fluid slosh within a tank with and without baffles are illustrated in Figure 4.7. The results reveal that the baffles reduce intensity of the force amplification from 1.96 that occurs in a clean bore tank to nearly 1.32 for a 40% filled tank subject to 0.3 g longitudinal acceleration. The results also suggest that the force amplification factor increases with an increase in acceleration when a clean bore tank is considered. This trend, however, is reversed for a baffled tank showing a decrease in the amplification factor when the acceleration is increased, as illustrated in Figure 4.7(a). The results further show that the pitch moment amplification factor behaves in a trend opposite to

that of the longitudinal force, as evident in Figure 4.7(b). The pitch moment amplification thus decreases with an increase in the magnitude of acceleration for a clean bore tank, while the peak values in a baffled tank show an increase, when the acceleration is increased (Figure 4.7(b)).

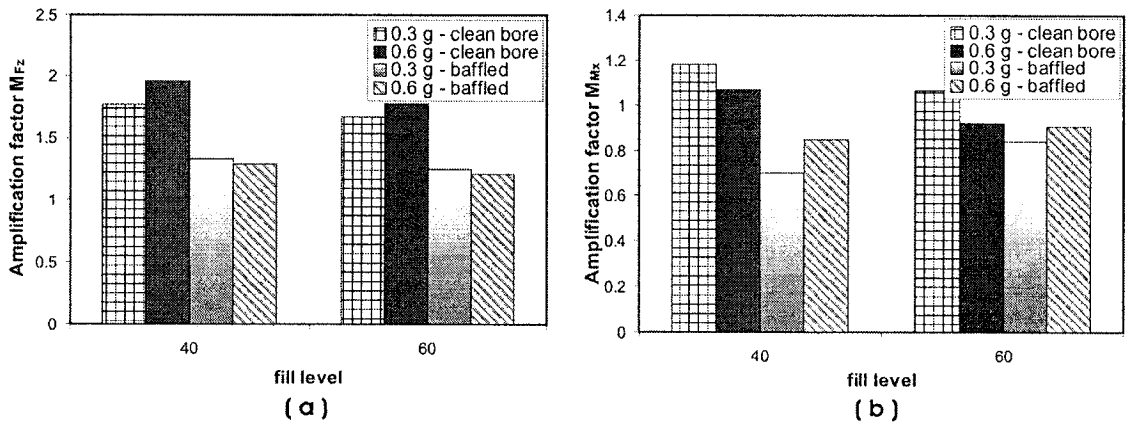

Figure 4.7: Influence of baffles on (a) the longitudinal force amplification and (b) the pitch moment amplification, under different fill levels and magnitudes of longitudinal accelerations

It has been reported that the natural slosh frequency has a crucial effect on the dynamics of a moving tank, particularly for the space-craft [4]. The considerable effect of slosh frequency in a partially filled moving tank vehicle has also been emphasized [13]. Moreover, the indispensable influence of slosh frequency on roll dynamics of the moving tank during a path-change maneuver was discussed in chapter 3.

The transient longitudinal force response exerted on the wall of the tank, with or without baffles considering different fill levels and magnitudes of acceleration, was analyzed using the FFT technique to determine fundamental slosh frequency in the pitch plane. The fundamental frequency of liquid slosh in a clean bore tank in the pitch plane was observed quite low near of 0.23 Hz corresponding to the 40% fill condition and 0.3 g longitudinal acceleration. Addition of baffles increased the natural frequency to 0.55 Hz,

under the same conditions. The fundamental frequency of slosh increases with an increase in the fill level or magnitude of acceleration, as shown in Figure 4.8. The slosh frequency in the pitch plane attained maximum of 0.63 Hz that corresponds to 60% filled clean bore tank. The influence of magnitude of longitudinal acceleration on the natural frequency of slosh in baffled tank however is negligible. The influence of lateral acceleration on the slosh frequency was also observed to be insignificant in chapter 2, irrespective of the fill level. These trends suggest that the fundamental frequency of slosh is more significantly influenced by the geometry of the tank.

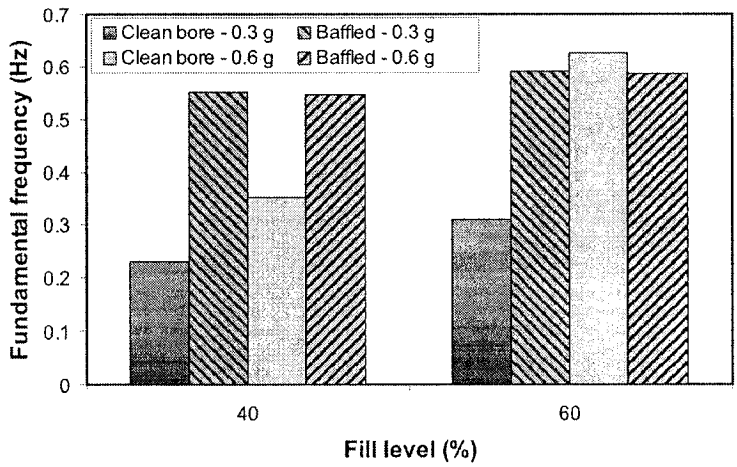

Figure 4.8: Influence of fill level, acceleration magnitude and baffles on the fundamental frequency of slosh in the pitch plane.

The results suggest that the larger response amplifications are associated with lower slosh frequency, and both correspond to a lower fill condition. The baffles could suppress the amplification in the forces and pitch moment considerably.

4.4 BRAKING-IN-A-TURN MANEUVER

As was mentioned earlier in chapter 1, the fluid slosh analysis under simultaneous braking and turning maneuver has been addressed in a single study [**39**]. The directional

stability characteristics of a partially filled tank vehicle subject to simultaneous lateral as well as longitudinal accelerations representing the braking-in-a-turn maneuver, was investigated using a kineto-static model of the fluid, which concluded that the overturning threshold of a vehicle is further reduced due to presence of a longitudinal acceleration. The dynamic behavior of liquid slosh under simultaneous application of lateral and longitudinal accelerations has not yet been analyzed. Needless to mention that effect of baffles on the transient liquid response on a moving tank subjected to such accelerations has not been investigated either. In the present study the non-linear three-dimensional liquid slosh model for a cylindrical tank with and without baffles, is solved to determine the response in terms of lateral, longitudinal and vertical forces; the pitch, roll and yaw moments; the corresponding mass moments of inertia; and the frequency response of the liquid motion. The influence of different selected dynamic parameters, such as the fill level, the magnitude of acceleration and the baffles, on the dynamic responses are evaluated.

4.4.1 SLOSH FORCES

The dynamic lateral, vertical and longitudinal forces due to liquid slosh in the tank have been normalized with respect to the corresponding mean values attributed to the clean bore tank and are presented in terms of amplification factors, M_{Fx}, M_{Fy} and M_{Fz}.

Figure 4.9 illustrates the lateral force amplification factor for the 60% filled clean bore tank subject to pure lateral acceleration as well as simultaneous lateral and longitudinal accelerations. The figure also shows the influence of magnitude of longitudinal acceleration on the amplification factor. The results suggest that the lateral force amplification increases considerably with an increase in the longitudinal acceleration. This trend is not evident from the results reported on the basis of the quasi-static

solution [39], and can be entirely attributed to dynamic fluid slosh in the three-dimensional domain. The simultaneous application of lateral and longitudinal accelerations would thus most likely deteriorate both the braking and turning performance of the vehicle.

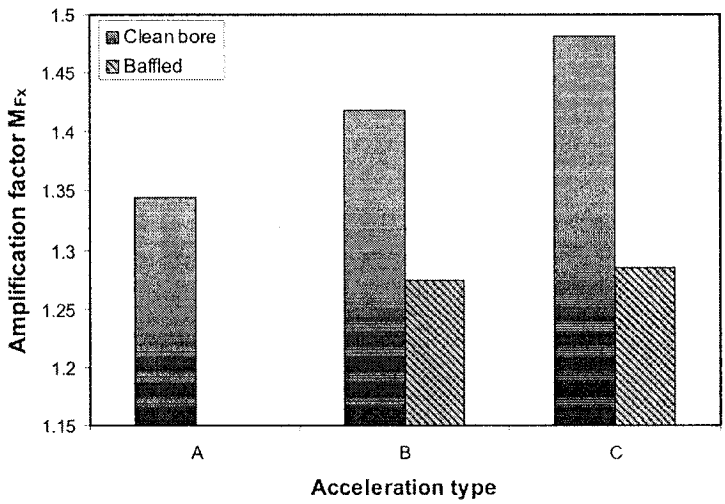

Figure 4.9: The lateral force amplification of fluid in a 60% filled clean bore tank subject to: A – 0.25 g lateral acceleration, B- 0.3g longitudinal and 0.25g lateral accelerations, and, C- 0.6 g longitudinal and 0.25g lateral accelerations.

Figure 4.10 illustrates the influence of fill level on the lateral force amplification factor, apart from the magnitude of longitudinal acceleration, when subject to a constant level of lateral acceleration (0.25 g). The results are derived for the clean bore tank with 40% and 60% fill condition and subject to 0.25 lateral acceleration coupled with 0.3 g and 0.6 g magnitudes of longitudinal accelerations, respectively. The resultant force amplification factors approach a value near 1.85 corresponding to lower fill condition and higher longitudinal acceleration, as shown in Figure 4.10. An increase in the magnitude of longitudinal acceleration leads to an increase in the amplification factor, irrespective of the fill level, although the increase is relatively small under higher fill condition. The

results further show that that the amplification factor decreases, when the fill level is increased.

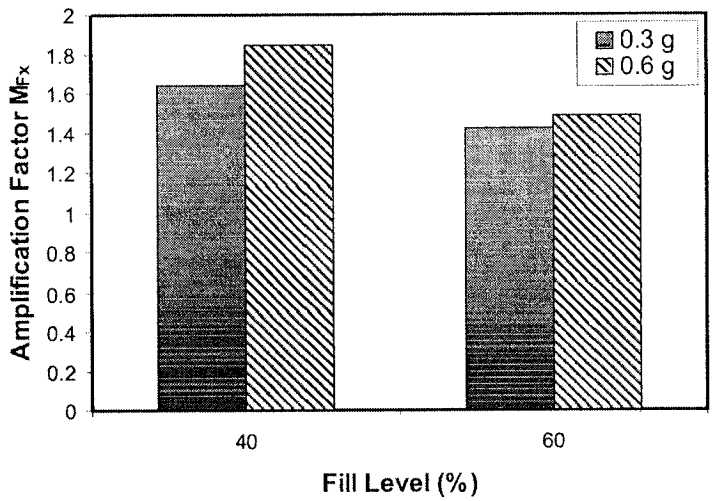

Figure 4.10: Effect of fill level and magnitude of longitudinal acceleration on lateral force (Fx) under 0.25 lateral ramp step acceleration

The corresponding vertical and longitudinal forces amplification factors are illustrated in Figure 4.11, as a function of the fill level and magnitude of longitudinal acceleration, while the magnitude of lateral acceleration is held constant (0.25 g). Both the vertical and longitudinal amplification factors show similar trends, namely, the amplification factors decrease with an increase in the fill level and increase when the longitudinal acceleration magnitude is increased. The results suggest that the amplification of longitudinal force increases significantly with the magnitude, while the dynamic vertical force deviation is not significant as observed earlier under pure longitudinal acceleration (Figure 4.4). The peak magnification factors for both responses occur under lower fill level and higher longitudinal acceleration.

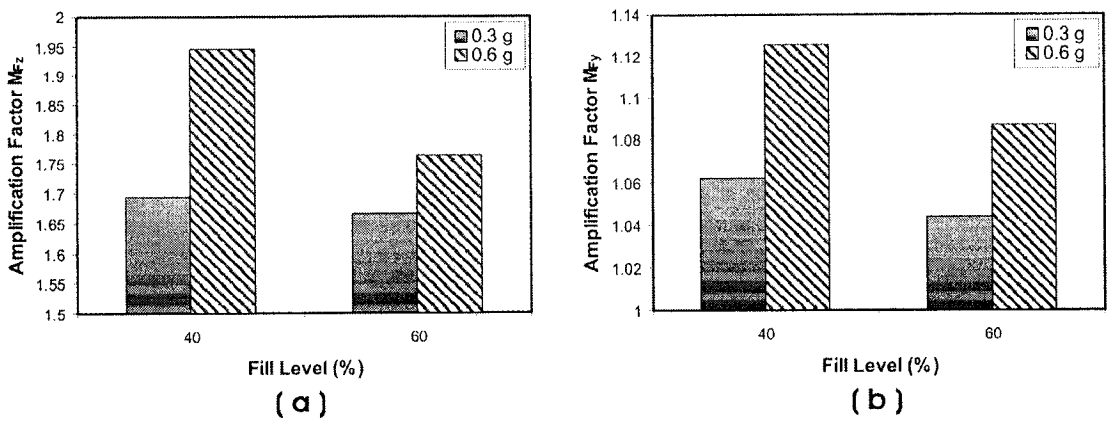

Figure 4.11: Longitudinal (a) and vertical force (b) amplification factors in a clean bore tank under different fill conditions and magnitudes of longitudinal acceleration.

4.4.2 MOMENTS

The slosh forces caused by the liquid motion under longitudinal and lateral accelerations are applied together with the geometric coordinates of each cell at which the slosh forces act, to compute the yaw, pitch and roll moments about the middle of the bottom of the tank (Point 'O'). The transient variations in the moments are expressed in terms of amplification factors by normalizing the peak moment, with respect to the corresponding mean values, such that:

$$M_{Mx} = \frac{Max(M_x)}{\overline{M}_x} \quad , \quad M_{My} = \frac{Max(M_y)}{\overline{M}_y} \quad , \quad M_{Mz} = \frac{Max(M_z)}{\overline{M}_z} \qquad (4.5)$$

where $\overline{M}_x, \overline{M}_y, \overline{M}_z$ are the mean values of the moments in the pitch, yaw and roll plane respectively, and M_{Mx}, M_{My}, M_{Mz} are the corresponding amplification factors.

The analyses are performed for both clean bore and baffled tanks with 40% and 60% fill condition and subject to constant level of lateral acceleration (0.25 g), and two different magnitudes of longitudinal acceleration. Figure 4.12 illustrates the roll moment amplification (M_{Mz}) of the 60% filled tank subject to lateral acceleration alone, and different magnitudes of longitudinal and lateral acceleration. The results show that the

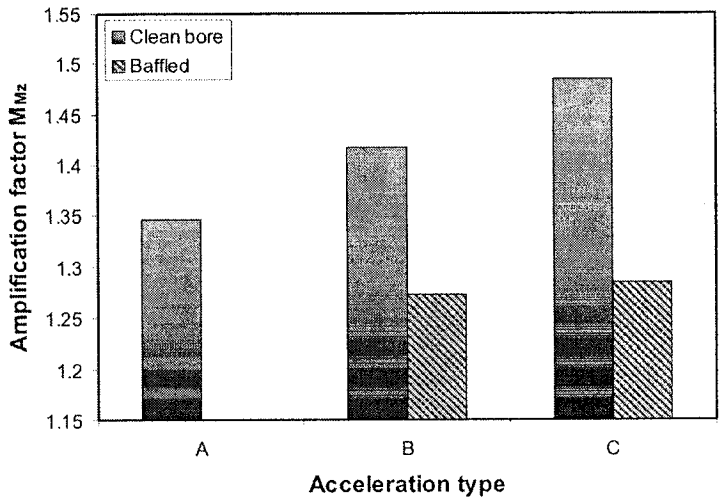

Figure 4.12: The roll moment amplification of fluid in a clean bore tank: A – 0.25 g lateral acceleration, B- 0.3g longitudinal and 0.25g lateral acceleration, and C- 0.6 g longitudinal and 0.25g lateral acceleration

roll moment of the clean bore tank increases with an increase in the magnitude of longitudinal acceleration. Evidently the most significant response amplification is attributed to the higher longitudinal acceleration. The presence of baffles tends to limit the roll moment significantly. An earlier field study conducted by Fruehauf [**51**] had concluded that baffles help to suppress the longitudinal slosh but do not affect the lateral slosh. The results derived from the present study contradict the conclusions reported by Fruehauf. The results further show that the magnitude of the peak roll moment varies only slightly, when longitudinal acceleration is increased from 0.3 g to 0.6 g.

The influences of fill condition and longitudinal acceleration magnitude on the roll moments are further are shown in Figure 4.13, for the clean bore tank. The results show that the peak roll moment amplification factor approaches nearly 1.8 for with the lower fill level and higher longitudinal acceleration. An increase in the magnitude of acceleration causes the roll moment amplification factor to increase. The higher fill level, however,

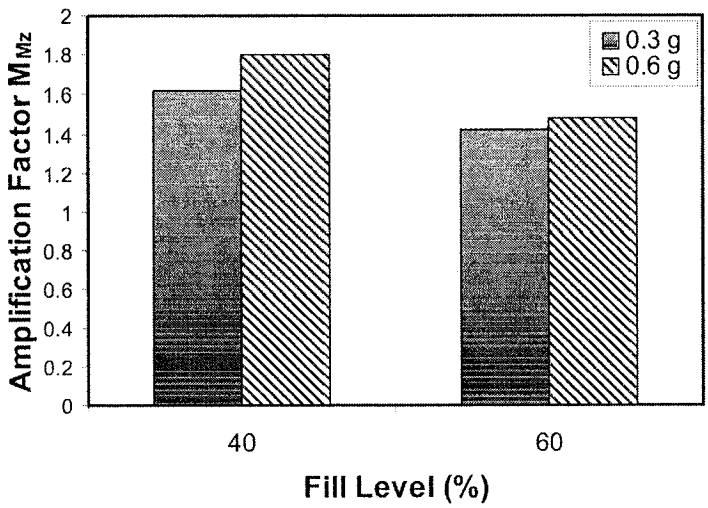

Figure 4.13: Influence of fill level and longitudinal acceleration on the roll moment amplification (M_{Mz})

causes the roll moment amplification factor to decrease. This particular trend in the roll moment amplification factor was also observed from the two-dimensional analysis under a lateral acceleration.

Figure 4.14 illustrates the pitch and yaw moment amplification response as function of the fill level and deceleration magnitude under simultaneous applications of lateral and longitudinal accelerations. The results shown are attained for the clean bore tank with 40% and 60% fill levels. The results exhibit that an increase in the fill level or the magnitude of longitudinal acceleration reduces the amplification factors of the pitch and yaw moments as it was observed from the pitch moment under a pure longitudinal acceleration. The yaw moment amplification corresponding to 60% fill, however, forms an exception to this trend, i.e. the moment amplification factor increases with increase in the acceleration under higher fill level. The results further revealed that the peak as well as the corresponding mean values of the moments increase with an increase in the

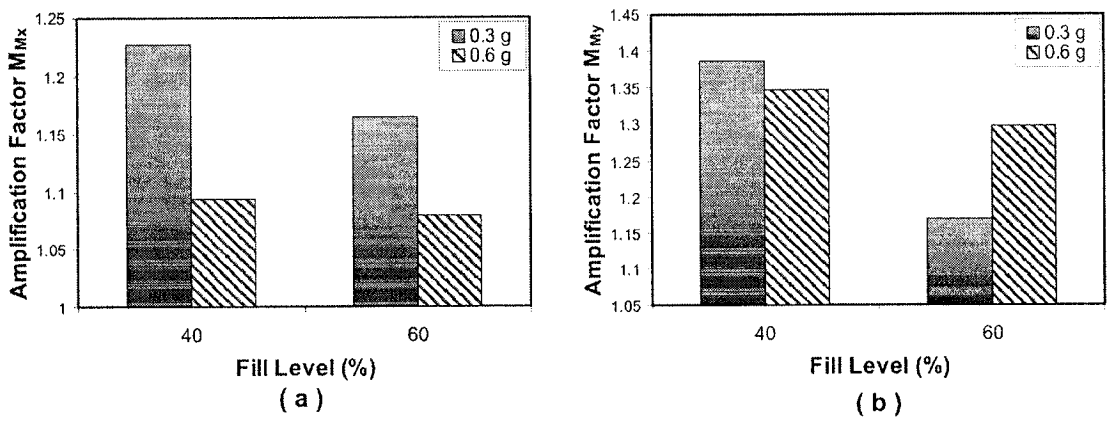

Figure 4.14: Influence of fill level and deceleration magnitude on the (a) Pitch (a) and (b) Yaw amplification factors in a clean bore tank subject to lateral and longitudinal accelerations.

acceleration magnitude irrespective of the fill level. The variations in these moments are strongly influenced by longitudinal coordinate of the liquid cargo c.g., which is further affected by the geometry of the tank as well as the magnitude of the longitudinal acceleration, as discussed earlier in section 4.3.2. A lower fill level yields a higher ratio

of the peak c.g. coordinate to its corresponding mean value for lower acceleration, while the higher magnitude of the longitudinal acceleration yields further deviation in the c.g. coordinates with respect to the mean value under the higher fill level, when compared to that attained under a lower acceleration level.

4.4.3 MASS MOMENTS OF INERTIA

The variations in the mass moments of inertia about the geometrical center of tank in the three orthogonal planes are also derived in terms of the amplification factors, indicating the normalized peak values with respect to corresponding mean values given by:

$$M_{Ixx} = \frac{Max(I_{xx})}{\bar{I}_{xx}},\ M_{Iyy} = \frac{Max(I_{yy})}{\bar{I}_{yy}},\ M_{Izz} = \frac{Max(I_{zz})}{\bar{I}_{zz}} \qquad (4.6)$$

where $\bar{I}_{xx}, \bar{I}_{yy}, \bar{I}_{zz}$ are the mean values of mass moments of inertia in the pitch, yaw and roll planes, respectively, and $M_{Ixx}, M_{Iyy}, M_{Izz}$ are the corresponding amplification factors.

The effects of fill level as well as the type of excitation, including the magnitude of the longitudinal acceleration, on the roll mass moment of inertia amplification for a clean bore tank are shown in Figure 4.15. The results show significant effect of the fill level on roll mass moment of inertia amplification with the normalized value being considerably larger under the lower fill level. An increase in the longitudinal acceleration yields higher amplification factor M_{Izz}, irrespective of the fill level. The simultaneous application of a lateral acceleration (0.25 g) alters the amplification factor, only slightly. The largest response amplification in the order of 1.17 occurs for the lower fill level under 0.25 g lateral acceleration and 0.6 g longitudinal acceleration, as shown in Figure 4.15. The addition of the lateral acceleration to the higher deceleration (0.6 g) causes higher

response amplification, while the variation is quite small under lower longitudinal acceleration.

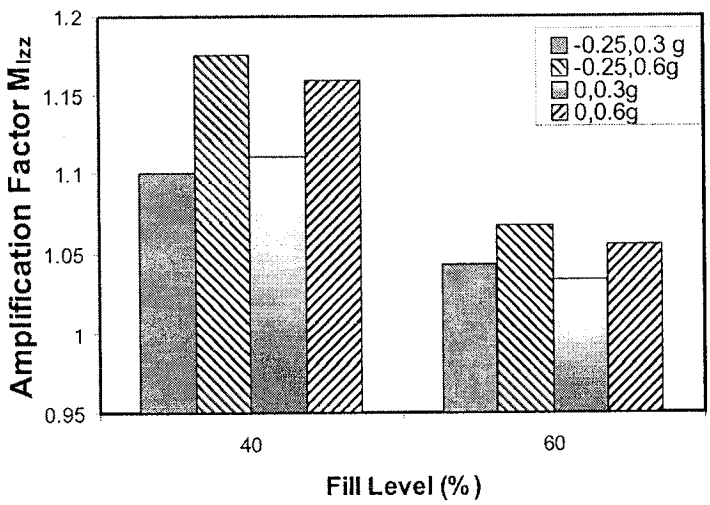

Figure 4.15: Roll mass moment of inertia (I_{zz}) in a clean bore tank under different fill levels and acceleration magnitudes

The amplification factors for the pitch and yaw mass moments of inertia under different fill levels and accelerations are shown in Figure 4.16. Both the responses reveal similar trends for the fill levels and acceleration excitations considered. The pitch and yaw mass moments of inertia increase slightly when a lateral acceleration (0.25 g) is applied in addition to the longitudinal accelerations. Furthermore, both the amplification factors tend to be lower under higher deceleration for the low fill level, but higher for the higher fill level.

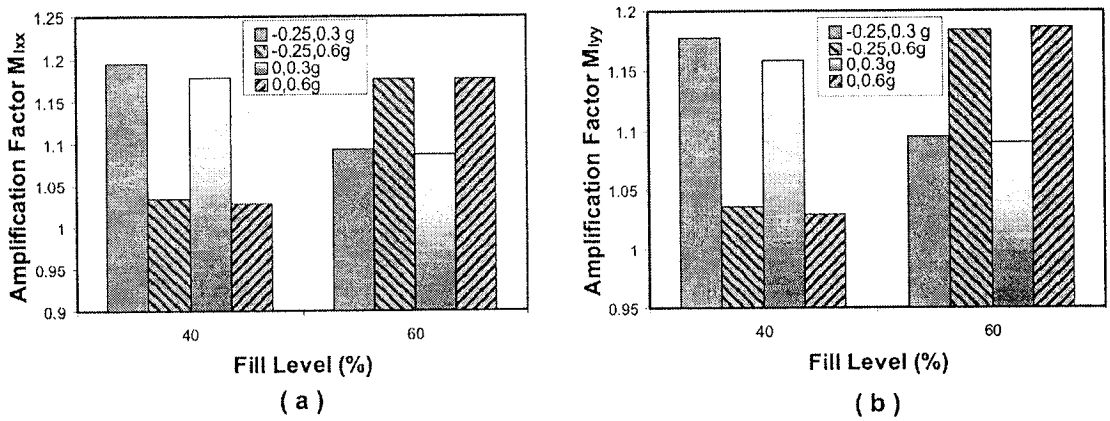

Figure 4.16: : Influence of fill level and deceleration magnitude on the Pitch (a) and (b) Yaw amplification factors in a clean bore tank subject to lateral and longitudinal accelerations.

4.4.4 EFFECT OF BAFFLES

A cylindrical tank equipped with three baffles as described in chapter 2.7.1, is assumed and the influence of baffles on the transient responses in terms of resultant forces and moments, and the mass moments of inertia are investigated under simultaneous lateral and longitudinal accelerations. Figure 4.17 illustrates the time-history of the pitch moment as an illustrative example, for the 60% fill condition, and 0.25 g lateral and 0.6 g longitudinal accelerations. The results are composed with those attained from the quasi-static solution for the clean bore tank. The results are similar to those attained under a pure longitudinal acceleration, shown in Figure 4.6. The presence of baffles tends to limit the steady-state pitch moment magnitude. The presence of baffles also tends to suppress the roll moment amplification factor, as illustrated in Figure 4.12.

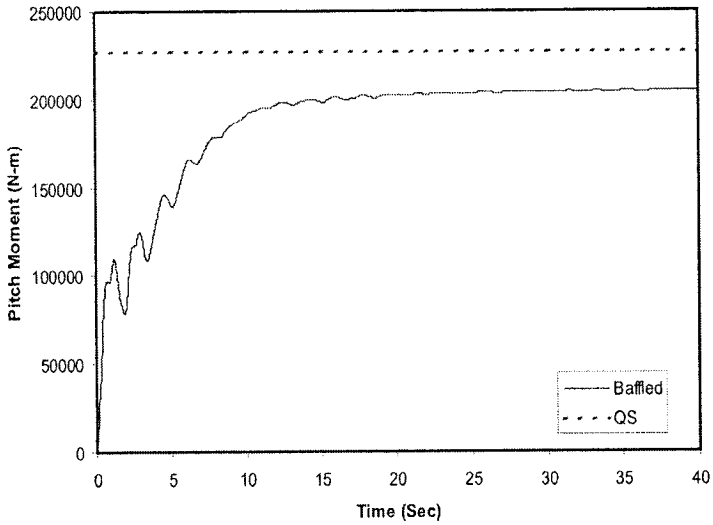

Figure 4.17: Comparison of the pitch moment derived from dynamic slosh and quasi-static solution. (60% filled, and -0.25 g lateral and 0.6 g longitudinal accelerations).

The effect of lateral baffles on the transient longitudinal force as well as the pitch moment has also been investigated. The results suggest that the baffles desirably diminish the peak values but introduce a delay for the response to approach its steady-state value. This has been illustrated for the pitch moment in a 60% filled baffled tank under simultaneous lateral and longitudinal acceleration in Figure 4.17. The influences of magnitude of longitudinal acceleration as well as the fill level on the peak longitudinal force and pitch moment are illustrated in Figure 4.18. The presence of the baffles suppresses the longitudinal force and pitch moment amplification, considerably. An increase in the fill level yields lower force and moment amplification factors for a clean bore tank. This reduction in M_{Fz} is negligible for the baffled tank, as shown in Figure 4.18(a). Furthermore, the effect of variation in the magnitude of longitudinal acceleration is negligible for the baffled tank. The pitch moment of the baffled tank, however, is more sensitive to changes in the magnitude of the longitudinal acceleration and the fill level, as shown in Figure 4.18(b). The peak values of the longitudinal force in a baffled tank, in

general, are smaller than those derived for the clean bore tank, while the magnitudes of the pitch moment were observed to be smaller than their corresponding mean values for a clean bore tank.

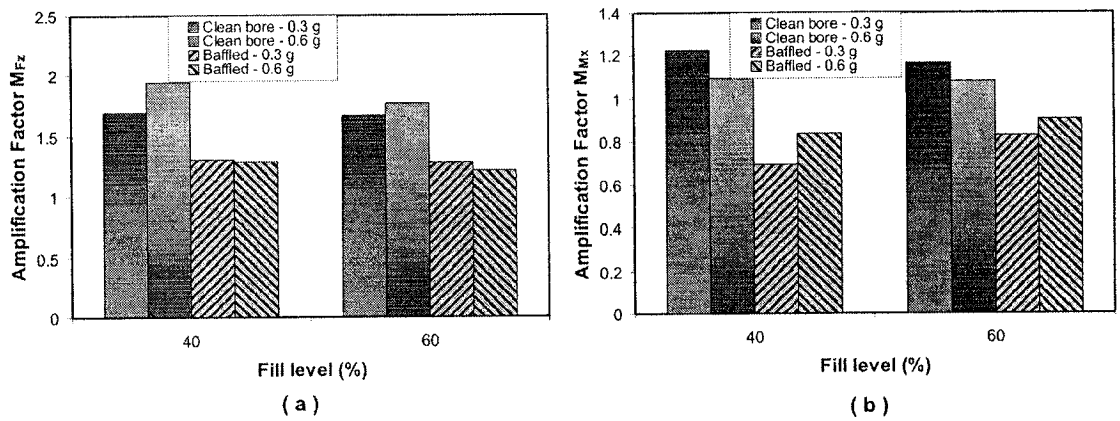

Figure 4.18: (a) Longitudinal force (Fz) and (b) pitch moment (Mx) amplification factors in a baffled tank under lateral as well as simultaneous lateral and longitudinal accelerations

The frequency response of the liquid slosh in the tank with and without baffles was also derived in the roll plane from the FFT analysis of the transient roll moment response under simultaneous lateral and longitudinal accelerations. Figure 4.19 illustrates the frequency-power spectra of the roll moment imposed by the 60% filled tank with and without baffles under 0.25 g lateral acceleration and 0.6 g longitudinal acceleration. The results suggest that the lateral frequency of fluid slosh in a clean bore tank is considerably higher than that attained under a pure lateral acceleration. The application of pure lateral acceleration revealed the fundamental frequency near 0.6 Hz (Figure 3.5), which increases to nearly 1.5 Hz under additional longitudinal acceleration. This increase is attributed to accumulation of the fluid towards the end of the tank resulting in relatively higher fill condition in the portions of the tank. The addition of baffles results in slightly higher frequency of the fundamental slosh in the roll plane.

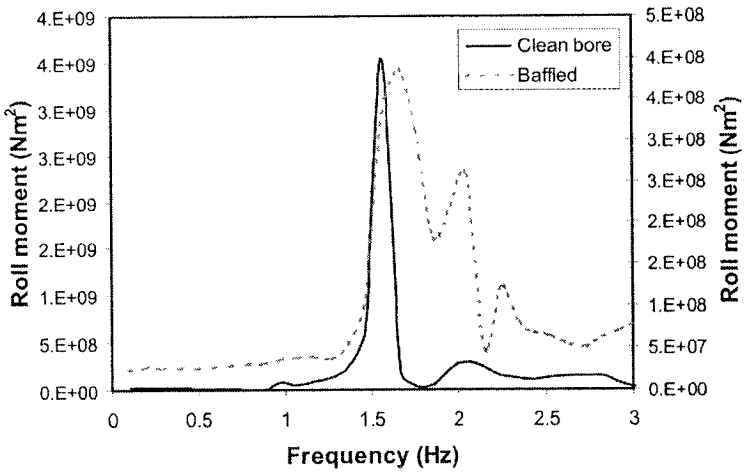

Figure 4.19: Spectra of the roll moment responses of the 60% filled tank with and without baffles subject to 0.25 g lateral acceleration and 0.3 g longitudinal acceleration

4.5 SUMMARY

The dynamic liquid slosh in a tank with and without baffles has been analyzed under longitudinal as well as simultaneous lateral and longitudinal accelerations representing the pure breaking and braking-in-a-turn maneuvers respectively. The transient response characteristics are evaluated in terms of the amplification factors with respect to the corresponding mean response of the liquid slosh in a clean bore tank. The results revealed that the peak longitudinal slosh force, and pitch and roll moments could be considerably suppressed through addition of the lateral baffles. It was also shown that the simultaneous application of lateral and longitudinal acceleration yields higher peak forces and moments, which may further degrade the roll stability characteristics of a partly-filled tank vehicle. The relatively large tank length yields considerably lower frequency of slosh in the pitch plane of a clean bore tank, in the order of 0.23 Hz. The addition of internal baffles increases this natural frequency of slosh considerably to 0.55 Hz. The natural frequency of slosh in the roll plane also increases, when the tank is

subjected to lateral and longitudinal accelerations as compared to that attained under a pure lateral acceleration.

CHAPTER 5

CONCLUSIONS AND RECOMMENDATIONS

5.1 MAJOR CONTRIBUTIONS

The major contributions of this study are summarized below:

- The quasi-static liquid slosh model in the roll plane is further simplified for a circular cross-section tank by eliminating the instantaneous coordinates of the mass center. A relationship between the lateral force and the resulting roll moment is derived, which suggests that the roll moment could be defined as a function of the horizontal force and tank radius, irrespective of the translation of the center of mass coordinates.

- The effect of excitation frequency on the roll moment imposed on a tank vehicle is presented as a function of the fill level.

- The instantaneous coordinates of the center of pressure of the liquid are computed under lateral acceleration, which are observed to be different from those of the mass center.

- The peak forces and moments induced by the liquid slosh under simultaneous applications of longitudinal and lateral accelerations are evaluated as functions of the fill level and magnitudes of accelerations.

- The variations in mass moments of inertia of the sloshing cargo are evaluated under three-dimensional nonlinear fluid slosh induced by lateral and longitudinal accelerations.

- The influence of lateral baffles in limiting the lateral as well as longitudinal slosh, and the corresponding frequency is presented.

- The slosh frequency responses in the pitch and roll planes are derived, using transient solutions, and the influences of fill level and the magnitudes of accelerations are investigated.

5.2 MAJOR CONCLUSIONS OF THE STUDY

Based on the analyses carried out in this study, the following major conclusions are attained:

- The mean responses derived from the transient flow analyses compare very well with those derived from the simple QS analysis. Only small deviations between the mean dynamic and QS responses could be observed, when separation of the free surface occurred under either a large acceleration excitation or low fill ratio. It is thus concluded that the QS model offers an effective and efficient basis for estimating the mean dynamic load shift and the overturning moment.

- The amplification factors of the lateral force and roll moment, as the ratios of the peak responses to the corresponding QS solution, could approach as high as 1.9. It is thus concluded that the dynamic fluid slosh imposes considerably larger magnitudes of forces and moments than those derived from the QS analyses.

- The magnitude of lateral force and roll moment in the roll plane invariably decreased with an increase in the fill level due to constraints imposed by the tank wall. An increase in the magnitude of lateral acceleration also resulted in lower amplification of the lateral load shift, lateral slosh force and the roll moment. Higher magnitudes of acceleration, however, caused larger peak vertical load

shift and the vertical force, while the variations in both these measures were observed to be relatively small.

- The magnitudes dynamic response values in the roll plane, such as lateral c.g. shift, lateral force and roll moment, are significantly influenced by the excitation frequency. A directional maneuver, idealized by a sinusoidal acceleration, can cause considerably larger response values, when the excitation frequency is in the vicinity of the liquid slosh natural frequency.

- The fundamental frequency of slosh in the roll plane increases with increase in the fill level. A 40% filled tank yields fundamental frequency in the order of 0.55 Hz, which increases to 0.72 Hz under 80% fill condition. The influence of acceleration magnitude on the slosh frequency is negligible.

- The results suggested that the viscous forces due to a viscous flow are insignificant for the range of Raynold's Number considered in this investigation. An increase in the density of cargo, however, considerably increases the lateral force as well as the roll moment due to increased cargo weight.

- The results of the two-dimensional analysis suggest that the coordinates of the CP differ considerably from the ranges of the c.g. coordinates. However, the results show that the corresponding mean values are nearly identical.

- Analysis of the three-dimensional liquid slosh under lateral and longitudinal acceleration excitations revealed that the peak longitudinal forces are considerably larger than those estimated from the QS analyses, irrespective of the fill level and excitation magnitude.

- The results show that the simultaneous application of lateral and longitudinal acceleration yields higher peak forces and moments, which may further degrade the roll stability and braking characteristics of a partly-filled tank vehicle.

- It is concluded that the peak longitudinal slosh force and pitch and roll moment could be considerably suppressed through addition of the lateral baffles, while the amplification ratios of these responses are significantly high for a clean bore tank.

- The results suggested that the relatively large tank length yields considerably lower frequency of slosh in the pitch plane of a clean bore tank. The addition of internal baffles increases this natural frequency of slosh considerably. The natural frequency of slosh in the roll plane also increases, when the tank is subjected to lateral and longitudinal accelerations as compared to that attained under a pure lateral acceleration

- The addition of lateral baffles also helps to reduce the magnitudes of roll moment imposed on the tank.

5.3 RECOMMENDATIONS FOR FUTURE WORKS

The present study is considered as preliminary attempt to evaluate the effects of dynamic fluid slosh in a three-dimensional field for tanks with and without baffles. The methodology developed in this dissertation could be applied to further investigate the designs of anti-slosh devices, such as lateral, longitudinal and oblique baffles to realize tank vehicles with enhanced stability limits. Considerably more efforts are needed to assess the effectiveness of the model and the methodology, some of which are outlined below:

- This study has been limited to the dynamics of the liquid slosh in a moving container, subject to lateral, longitudinal as well as the simultaneous lateral and longitudinal accelerations, while the results may be applied to study the vehicle directional characteristics, further efforts in integrating the fluid slosh model to the vehicle model are desirable to investigate the coupled tank-vehicle system.

- The analyses should be extended to include alternate tank cross-sections that are frequently used in bulk liquid cargo transportation. This would permit the characterization of the role of the tank geometry and identifications of more desirable tank cross-sections.

- The model used in this study may be applied to evaluate the performance of alternate designs of baffles. Moreover, further analyses are desirable to identify optimal number and location of baffles.

- This study has assumed uniform field of acceleration for the liquid. More accurate results could be obtained if the non-uniform field of acceleration arising from turning or simultaneous turning and acceleration / deceleration are considred.

- It is vital to validate the model and the results, which could be carried out in the laboratory using a scale model tank.

REFERENCES

1 R. Ranganathan, "Stability analysis and directional response characteristics of heavy vehicles carrying liquid cargo", 1990, Dissertation, Concordia University

2 G. Popov, S. Sankar, S.T. Sankar, "Dynamics of liquid sloshing in baffled and compartmented road containers", 1993, Journal of Fluids and Structures, 7, 803-821

3 L. Strandberg, "Lateral Stability of Road Containers", 1978, VTI (The Swedish National Road and Traffic Research Institute) Report No. 138A, Sweden.

4 Abramson, "The dynamic behavior of liquids in moving containers", 1966, NASA, NASA SP-106

5 C. P. Lam "Comparison of Simulation and Test Results for Various Truck Combination Configurations", 1986, Proc. of Int. Symp. on Heavy Vehicle Weights & Dimensions, pp 315-335.

6 Murnane, Timothy J., "Vehicle Accident Statistics Producing Rollover and Spills involving tan Semi-Trailers", Nov. 1989, SAE Truck and Bus Meet, Charlotte, NC,

7 J. Woodrooffe, "Evaluation of Dangerous Goods Vehicle Safety Performance", 2000, Transport Canada Report, TP 13678 E

8 S. Rakheja, S. Sankar, and R. Ranganathan, "Roll plane analysis of articulated tank vehicles during steady turning", 1988, Vehicle system dynamics, 17, pp. 81-104

9 S. Rakheja, R. Ranganathan, "Estimation of the rollover threshold of heavy vehicles carrying liquid cargo: a simplified approach", 1993, Int. J. of Vehicle Design, vol. 1, no. 1

10 Wang Zhanqi, S. Rakheja, "Influence of partition location on the braking performance of a partially-filled tank truck", 1995, SAE

11 R. Ranganathan and Y.S. Yang, "Impact of liquid load shift on the braking characteristics of partially filled tank vehicles", 1996, Vehicle system dynamics, vol. 26, pp 223-240

12 R. Ranganathan, "Development of a roll dynamics model of a liquid tank vehicle", 1997, Transactions of the CSME, vol. 21, no. 4, pp 357-369

13 F. Bauer, "Fluid oscillations in the containers of a space vehicle and their influence upon stability", 1964, NASA, NASA TR R-187

14 A. Slibar, H. Troger, "The steady state behaviour of tank trailer system carrying rigid or liquid cargo", 1977, VSD-IUTAM Symposim on Dynamics of Vehicles on Roads and Tracks, Vienna

15 G Popov, S. Sankar, T.S. Sankar and G.H Vatistas , "Dynamics of liquid sloshing in horizontal cylindrical road containers", 1993, Proc Instn Mech Engrs, Vol 207, Part C: Journal of Mechanical Engineering Science.

16 R. Ranganathan, "Rollover threshold of partially filled tank vehicles with arbitrary tank geometry", 1993, Proc Instn Mech Engrs, Vol 207, Part D: Journal of Automotive Engineering

17 M. I. Salem, "Rollover Stability of Partially Filled Heavy-Duty Elliptical Tankers Using Trammel Pendulums to Simulate Fluid Sloshing", 2000, PhD dissertation, West Virginia University

18 B. Budiansky, "Sloshing of liquids in circular canals and spherical tanks", 1960, Journal of the Aero/space sciences, vol. 27, no. 3 pp 161-173

19 T. W. H. Sheu, S. M. Lee, "Large-amplitude sloshing in an oil tanker with baffle-plate / drilled holes", 1998, IJCFD, vol. 10, pp 45-60

20 R. Ranganathan, Y. Ying, J. B. Miles , "Analysis of Fluid Slosh in Partially filled Tanks and Their Impact on the Directional Response of Tank Vehicles" 1993, SAE paper 932942.

21 H.F. Bauer "On the destabilizing effect of liquids in various vehicles (part 1)", 1972, Vehicle system dynamics, 1, pp 227 - 260

22 F. Bauer, "Dynamic behaviour of an elastic separating wall in vehicle containers: Part 1", 1981, International journal of vehicle design, vol. 2, no. 1

23 G. Popov, G. H. Vatistas, S. Sankar, T.S. Sankar, "Liquid sloshing in a horizontal cylindrical container", 1989, ASME Computers in engineering conference and exhibition.

24 G. Popov, "Dynamics of liquid sloshing in road containers", 1991, Dissertation, Concordia University

25 R.D. Ervin, Y. Guy, "The influence of Weights and Dimensions on the stability and control of heavy-duty trucks in Canada", July 1986, UMTRI, Report No. 86-35

26 S. Rakheja, "Estimation of rollover threshold of partially filled tank trucks", 1991, Proc Instn Mech Engrs, vol. 205

27 S. Rakheja, S Sankar and R. Ranganathan, "Influence of tank design factors on the rollover threahold of partially filled tank vehicles", 1989, SAE Technical Paper Series, Truck and Bus Meeting and Exposition

28 R. Ranganathan, S. Rakheja, S. Sankar "Dirctional response of a B-Train vehicle combination carrying liquid cargo", 1993, Journal of Dynamic systems, Measurement, and control, Vol. 115

29 I. M. Ibrahim, M. A. El-Nashar, Y.K. Younes, "Ride behaviour of trucks transporting liquids", 1998, Int. J. of Vehicle Design, vol. 5, nos. 3 / 4

30 X. Kang, S. Rakheja, I. Stiharu, "Effects of tank shape on the roll dynamic response of a partly filled tank vehicle", 2000, Vehicle system dynamics, Vol. 35, No. 2, pp 75-102

31 X. Kang, S. Rakheja, I. Stiharu, "Optimal tank geometry to enhance static roll stability of partially filled tank vehicles", 1999, SAE Technical paper series, SP-1486

32 X. Kang, S. Rakheja, and I. Stiharu, "Cargo load shift and its influence on tank vehicle dynamics under braking and turning", 2002, Int. J. of Vehicle Design, Vol. 9. No. 3

33 NASA, "Propellant slosh loads", 1968, NASA SP-8009

34 G. Popov, G. H. Vatistas, S. Sankar, T.S. Sankar, "Numerical simulation of viscous liquid sloshing in arbitrarily shaped reservoirs", 1993, AIAA Journal, vol. 31, no. 1, pp 10-11

35 G. Popov, S. Sankar, T.S. Sankar, "Shape optimization of elliptical road containers due to liquid load in steady-state turning", 1996, Vehicle system dynamics, vol. 25, pp203-221

36 M. I. Salem, V. H. Mucino, M. Gautam and M. Aquaro, "Review of Parameters Affecting Stability of Partially Filled Heavy-Duty Tankers", 1999, SAE TECH. PAPER SERIES 1999-01-3709

37 R. Ranganathan, S. Rakheja, S. Sankar, "Influence of Liquid Load Shift on the Dynamic Response of Articulated Tank Vehicles", 1990, Int. J of Vehicle System Dynamics, 19, pp. 177-200

38 S. Rakheja, I. Stiharu, X Kang, J. A. Romero ,"Influence of tank cross-section and road adhesion on dynamic response of partly-filled tank trucks under braking-in-a-turn", 2002, International Journal of Heavy Vehicle Systems, v. 9 , n. 3 , p. 223 , 18 p

39 X. Kang, "Optimal Tank Design and Directional Dynamic Analysis of Liquid Cargo Vehicles under Steering and Braking", 2001, Dissertation, Concordia University

40 T.W.H. Sheu, S-M Lee, "Large-Amplitude Sloshing in an Oil Tanker with Baffle-Plat/Drilled Holes", 1998, IJCFD, Vol 10, pp. 45-60

41 Yih Shia-shun, "Fluid mechanics; a concise introduction to the theory", 1969, McGraw-Hill

42 FLUENT 6.0 User's Guide – Section 8

43 Fluent 6.0 Documentation-Section 22

44 R. I. Issa, "Solution of Implicitly Discretized Fluid Flow Equations by Operator Splitting", 1986, Journal of computational physics, 62, pp 40-65

45 Fluent User's Guide – Section 22.3.1

46 C. W. Hirt, B. D. Nichols, "Volume of fluid (VOF) method for the dynamics of free boundaries", 1981, Journal of computational physics, 39, 201-225

47 G. Popov, "Dynamics of liquid sloshing in road containers", 1991, Dissertation, Concordia University

48 B. D. Nichols, C. W. Hirt, "Calculating Three-Dimensional Free Surface Flows in the Vicinity of Submerged and Exposed Structures",1973, Journal of Computational Physics, 12, 234-246

49 Gambit documentation

50 H. Isermann, "Overturning Limits of Articulated Vehicle with Solid and Liquid Loads", 1976, Motor Industry Research Assoc., Translation No. 22/76.

51 Fruehauf Inc., Fruehauf Tank Test, Fruehauf Report, 1962